Lagrangian approach to three-dimensional azimuthal magnetorotational instability with and without resistivity

鄒, 蓉

https://doi.org/10.15017/1470521

出版情報：九州大学, 2014, 博士（機能数理学）, 課程博士
バージョン：

Lagrangian approach to three-dimensional azimuthal magnetorotational instability with and without resistivity

Rong Zou

Abstract

Magnetorotational instability (MRI) is a plausible mechanism to trigger turbulence in the accretion disk, to excite the outward transportation of the angular momentum while the mass accretes to the center. We use the Lagrangian approach to obtain Hain-Lüst equation, which is a second-order ordinary differential equation for the radial component of the Lagrangian displacement. The WKB approximation is applied to this equation. It is a lengthy work to deduce the Hain-Lüst equation but avoids the ignorance of terms in the traditional WKB treatment. The traditional WKB treatment deals with a group of equations rather than a single one and is liable to fail in keeping important terms for studying non-axisymmetric disturbances.

In chapter 2 short-wavelength stability analysis is made of axisymmetric rotating flows of a perfectly conducting fluid (MHD), subjected to external azimuthal magnetic field B_θ to non-axisymmetric as well as axisymmetric perturbations. Our WKB approximation is applied to the Hain-Lüst equation which is deduced here in a slightly different way from the traditional derivation from the well known Frieman-Rotenberg equation. When the magnetic field is sufficiently weak, the instability occurs for $Ro = r\Omega'/(2\Omega) < Ro_c$ with Ro_c close to zero and the maximum growth rate close to the Oort A-value $|Ro|$, where $\Omega(r)$ is the angular velocity of the rotating flow as a function only of r, the distance from the axis of symmetry, and the prime designates the derivative in r. As the magnetic field is increased, the flow becomes unstable to waves of very short axial wavelengths for the whole range of Ro when $Rb = r^2(B_\theta/r)'/(2B_\theta) > -3/4$, and to waves of very long axial wavelengths for a finite range of $|Ro|$ when $Rb < -1/4$. For the both waves, the maximum growth rate increases, beyond the Oort A-value, without bound in proportion to the square of $|B_\theta|$.

Chapter 3 is concerned with the three-dimensional short-wavelength analysis of the AMRI, but in the inductionless limit. As opposed to chapter 2, the viscosity and the electrical resistivity are considered. The extended Hain-Lüst equation for the radial La-

grangian displacement is obtained. We apply the WKB approximation to the extended Hain-Lüst equation, whereby we can retain all the terms, being otherwise liable to be missed for non-axisymmetric disturbances. Envisioning a liquid metal, the magnetic resistivity is assumed much larger than viscosity, which is called inductionless limit. Unlike the case of a perfectly conducting fluid, no instability occurs for sufficiently weak magnetic field. When the magnetic field is sufficiently strong, there are mainly two instability modes depending on Rb. A Keplerian flow is unstable for arbitrary Rb. For non-axisymmetric disturbances, the growth rate is found to increase with B_θ without bound in proportion to the square of the magnetic field strength which is faster than the AMRI in strong magnetic field regime for the ideal MHD in chapter 2.

In chapter 4, the energy of the ideal MHD is calculated by means of the Lagrangian displacement. The ideal MHD is a Hamiltonian system. Krein's theorem states that when two real eigenvalues corresponding to wave energy of opposite-sign (positive and negative) collide, the real eigenvalues could bifurcate to complex ones which have imaginary part and signifying instability. Starting from the energy formula deducible from the Frieman-Rotenberg equation, we obtain two simply energy formulas expressible by the Lagrangian displacement and an induced variable which describes the magnetic field 'displacement'. Using one of the formulas, we calculate the energy of a rigid-rotation flow subject to azimuthal magnetic field which is linear in radius r and an axial constant component. We find the bifurcation in accordance with Krein's theorem of Hamiltonian spectra.

Acknowledgements

I am very grateful to my supervisor Prof. Y. Fukumoto for his every support in research and life for four years in Japan. He inspired me to do the study and research on MRI for this thesis. I learned precious knowledge and research attitudes from him.

I would like to thank Prof. Chyba for giving me the chance to experience biology

mathematical research with her and her student.

I would like to thank Prof. Kawasaki for his support on my internships.

I would like to thank my family who give me encouragement and support in my life.

I would like to thank my friends in Japan for helping and accompanying me for four years. They make my life happy and colorful.

In addition, I would like to thank my homeland for giving me the economic support for studying abroad. My four years doctoral study in Japan is supported by Chinese Scholarship Council.

Contents

Chapter 1

Introduction

1.1 Magnetorotational instability (MRI)

1.1.1 Background

Magnetorotational instability (MRI) studies the instability of an electrically conducting rotating flow subject to external magnetic field. From the name *magneto+rotational* we can catch an intuitive idea that both $magnetic field$ and $rotation$ are necessary for MRI. When there is no magnetic field, for Taylor-Couette flow, there is hydrodynamic instability of centrifugal force origin by the differential rotation. Rayleigh's criterion gives a necessary condition on the velocity for stability. When there is magnetic field and flow is static, there are different instability modes for different magnetic-field configuration [1, 2, 3]. For instance, if there is a purely toroidal (azimuthal) magnetic field, instability known as the Tayler instability occurs, e.g. sausage (varicose) mode (m=0) and kink mode (m=1), where m is the azimuthal wavenumber in the cylindrical coordinates (r, θ, z). Since the rediscovery of Velikhov and Chandrasekhar's result [4, 5] by Balbus and Hawley in 1991 [6], the MRI has attracted great attention as a plausible mechanism for triggering turbulence in the flow of an accretion disk, for promoting outward transport of angular momentum, while the matter accretes the center.

The ideal MHD refers to the dynamics of an inviscid and perfect electrically conducting flow. When there is no magnetic field, Rayleigh's criterion determines the condition for stability of a rotating flow [7]. Given the angular velocity $\Omega(r)$ as a function only of r, define the local Rossby number by $Ro = \frac{1}{2}\mathrm{d}\log\Omega/\mathrm{d}\log r = r\Omega'/(2\Omega)$ [8, 9]. Here the prime designates the derivative with respect to r. In terms of the epicyclic frequency $\kappa^2 = (\Omega^2 r^4)'/r^3$, it is expressed as $Ro = \kappa^2/(4\Omega^2) - 1$. For the absence of magnetic field, if $\kappa^2 \geq 0$ or equivalently $Ro \geq -1$ everywhere, such a rotating flow is linearly stable against axisymmetric disturbances [7, 9]. For an accretion disk, the angular velocity could satisfy the Keplerian law $\Omega(r)^2 r = -\nabla\Phi$; $\Phi = 1/r$, and as a consequence $\Omega \propto r^{-3/2}$ for which $Ro = -3/4$. Rayleigh's criterion may imply that Keplerian rotation is hydrodynamically stable. The magnetic field parallel to the rotation axis drastically alters the stability characteristics. If the axial magnetic field is applied, no matter how weak it is, a rotating flow suffers from instability if $Ro < 0$ [4, 5], implying that an accretion disk with Keplerian flow is unstable. This is the magnetorotational instability. To be specific, we refer to this instability caused by the axial magnetic field as the standard magnetorotational instability (SMRI).

In a protoplanatory disk surrounding a young star, the ionization depends on the radiation from the X-ray and cosmic rays [10], and the temperature of the disk. It tends to be that the mid-plane of the accretion disk receives fewer radiation and the cold region of the disk is only weakly ionized. In those places, the magnetic diffusion is not negligible. Laboratory experiments, for instance the Madison plasma couette flow experiment (MPCX) [11], Potsdam Rossendorf Magnetic Instability Experiment (PROMISE) [8] and the other Taylor-Couette container filled with liquid metals like sodium and gallium [13], are designated to study MRI. In astrophysics, for the cold part and less radiated part of the protoplanatory disk and for liquid metal experiments, both the effect of the viscosity ν and the electrical resistivity η should be taken into consideration. Because of comparably high electrical resistivity and low viscosity, the ratio ν/η is considered to be much small

than unity or of the order unity [13]. We focus on the former case ($\nu/\eta \ll 1$), which is known as the inductionless limit [14, 8]. Before the study of MRI, we would like to talk about the rotating flow and the magnetic field.

1.1.2 Motion of accretion disk

An accretion disk is a mass disk where the mass in a differential rotation accretes into the massive center body which is typically a star (or a black hole). The center body grows heavier and heavier by the feeding of the mass from the outer disk. The accretion disk looks like a short cylinder, with very large radius. The cylindrical coordinates ($r,\ \theta,\ z$) is introduced. The ($r,\ \theta$) plane is parallel to the top and bottom surfaces of the accretion disk, and the z axis penetrates through the center of the accretion disk. The accretion disk is usually set in a differential rotation around the symmetry axis (z axis) with velocity $U_\theta = r\Omega(r)$ in the azimuthal direction $\boldsymbol{e}_\theta$ and so $\Omega\boldsymbol{e}_z$ is the angular velocity. Newton's second law requests:

$$\frac{U_\theta^2}{r} = \Omega^2 r = \frac{\mathrm{d}}{\mathrm{d}r}\Phi, \tag{1.1}$$

where the Φ is the gravitational potential and $-\mathrm{d}\Phi/\mathrm{d}r$ is the centripetal force. The potential has different radial dependence, e.g. $\Phi \propto 1/r$ characterizes a Keplerian flow so $\Omega \propto r^{-3/2}$ by the Kepler's third law, while $\Omega \propto r^{-1}$ is characteristic of the galaxy disk. [15] For our research, the Keplerian flow is exclusively considered.

For a rotating particle, the angular momentum about the origin is defined by.

$$\boldsymbol{L} = \boldsymbol{r} \times (mr\Omega\boldsymbol{e}_z), \tag{1.2}$$

with $r\boldsymbol{e}_r$ the vector from the origin to the particle and m the mass of the particle. Here we take the relative origin to be the coordinate origin so that $\boldsymbol{r} = r\boldsymbol{e}_r$. For a Keplerian flow, $|L| \propto r^{1/2}$ so that the angular momentum increases outward. When matter accretes towards the center, the angular momentum would be lost. However, if there is no external

torque acting on it, this contradicts with the law of conservation of angular momentum; the lost momentum has to be transferred outward. As a means for realizing the outward huge momentum transformation, the turbulence is needed. The large turbulence viscosity helps to efficiently transport the angular momentum outwards to place far away from the center.For this, some instability should be invited on a rotating flow to generate the turbulence. But within hydrodynamics, Rayleigh's stability criterion implies that the Keplerian flow is linearly stable to small disturbance.

1.1.3 Hydrodynamic instability

In 1917 Lord Rayleigh found stability criterion, which states:

For a rotating inviscid flow between two rotating coaxial cylinders, the sufficient condition for stability of axisymmetric disturbance is that the circulation (angular momentum) increases outward [16], i.e.

$$\frac{\mathrm{d}(\Omega^2 r)}{\mathrm{d}r} > 0. \tag{1.3}$$

Assume that the inner and outer cylinders have radius and angular velocity as R_1 and R_2 and Ω_1 and Ω_2 respectively. (1.3) is translated into

$$\Omega_2^2 R_2 > \Omega_1^2 R_1. \tag{1.4}$$

Define the Rossby number

$$Ro = \frac{1}{2}\frac{r}{\Omega}\frac{\mathrm{d}\Omega}{\mathrm{d}r}. \tag{1.5}$$

Then (1.3) is translated into $Ro > -1$, so that the critical Rossby number for instability is $Ro_c = -1$. For the velocity profile of Keplerian flow, $\Omega \approx r^{-3/2}$, the Rossby number can be calculated as $Ro_K = -3/4$. Accordingly, an inviscid Keplerian flow is stable with respect to the hydrodynamical mechanism of centrifugal origin. It is also true for a viscous Keplerian flow as will be discussed in chapter 3 and be shown in Fig. 1.1 [17].

In 1923, Taylor considered the effect of viscosity and published his cornerstone theo-

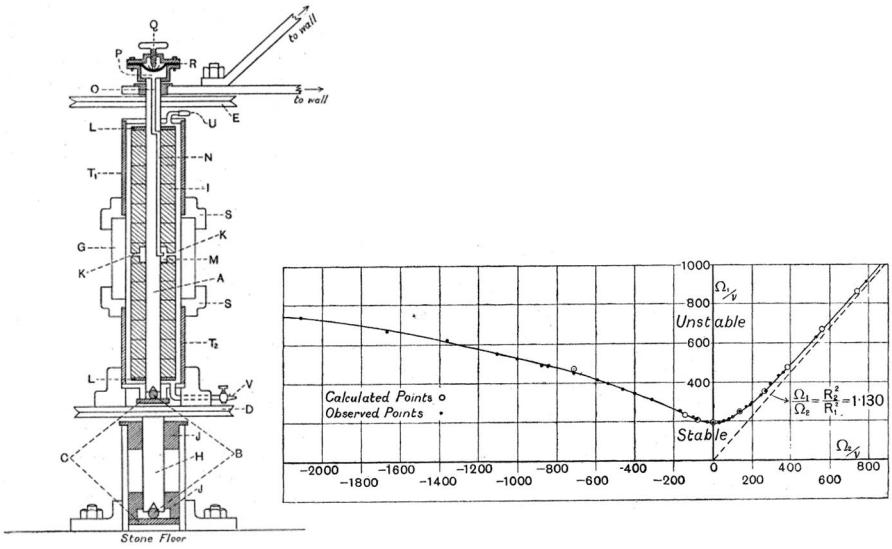

Figure 1.1: The left one is Taylor's apparatus [17] to study the Taylor-Couette flow in coaxial cylinders; the right one describes the experiment results (the dots) which coincides with the analytic result (the curve). The dashed line a little bit below the curve is the Reyleigh's stability boundary for an invisid flow. [17]

retical and experimental results on the stability boundary. He designated a new apparatus as shown in Fig. 1.1 [17]. This apparatus constitutes two coaxial cylinders with large height in order to to get rid of the end effect from the top and bottom of the cylinders. His theoretical and experimental results successfully coincided as shown in the right panel of Fig. 1.1. The curved line is the theoretical stability boundary with the instability region above it and the stability region below it. The dots are the experiment data. The curve and the dots well coincides with each other. The dashed line stands for the Rayleigh's stability boundary for the inviscid flow which is slightly lower than solid line. We see from Fig. 1.1 that the viscosity stabilizes the flow and contracts the instability region.

Hydrodynamics of neutral fluid fails to provide instability for the Keplerian flow. We have to search for other possible mechanisms. And then the magnetic field prevails in the universe and MRI comes to our view.

1.1.4 Magnetohydrodynamics

Maxwell equations, Lorentz force and induction equation

In the electrodynamics,the electric field and the magnetic field interact with each other. Their relation is determined by the Maxwell equations [35]

$$\begin{aligned}
&\frac{\partial \boldsymbol{B}}{\partial t} = -\boldsymbol{\nabla} \times \boldsymbol{E} \quad \text{(Faraday)},\\
&\frac{1}{c^2}\frac{\partial \boldsymbol{E}}{\partial t} = \boldsymbol{\nabla} \times \boldsymbol{B} - \mu_0 \boldsymbol{J} \quad \text{(Ampére)},\\
&\nabla \cdot \boldsymbol{E} = \frac{\tau}{\varepsilon_0} \qquad \text{(Poisson)},\\
&\nabla \cdot \boldsymbol{B} = 0 \qquad \text{(no magnetic monopoles)}
\end{aligned} \tag{1.6}$$

where $\boldsymbol{E}$, $\boldsymbol{B}$, $\boldsymbol{J}$ are the electric field, the magnetic field, and the current density respectively and $\mu_0, c, \tau, \varepsilon_0$ are the permeability of free space, the light speed, total charge density, permittivity of the vacuum, respectively. Faraday's law describes the generation of electric field from the magnetic field. Conversely, the magnetic field can also be generated by the electric field by Ampére's law. Because the speed of light c is very large, in Ampére's law, the left-hand side is in many cases negligible and gives the relation between J and B as

$$J = \frac{1}{\mu_0}\boldsymbol{\nabla} \times \boldsymbol{B}. \tag{1.7}$$

Assume that the accretion disk consists of the plasma being made up of particles with positive and negative charges. If a charged particle with electric charge q and moves in electric field and magnetic field with velocity u, the force exerted on it by the electric and magnetic field

$$\boldsymbol{f}_L = q(\boldsymbol{E} + \boldsymbol{u} \times \boldsymbol{B}), \tag{1.8}$$

which is a combination of the electric force $q\boldsymbol{E}$ and the Lorenz force $q\boldsymbol{v} \times \boldsymbol{B}$.

For a fluid consisting of positive and negative charged particles, the total force acting on it is the summation of the force acting on charged particles. By the assumption that

the fluid is everywhere quasi neutral, the total electric force of $q\boldsymbol{E}$ might be considered as zero and the Lorentz force on the fluid becomes

$$\boldsymbol{F}_L = \boldsymbol{J} \times \boldsymbol{B}, \text{ where } \boldsymbol{J} = \sum q\boldsymbol{u}. \tag{1.9}$$

By the relation between $\boldsymbol{J}$ and $\boldsymbol{B}$ presumed by (1.7), it can be further written as

$$\boldsymbol{F_L} = \frac{1}{\mu_0}(\nabla \times \boldsymbol{B}) \times \boldsymbol{B}. \tag{1.10}$$

The Lorentz force is added into Navier-stokes equation as an external force. Distinct from the pressure and the gravity force, Lorentz Force is not a potential force anymore. This will make a big difference on the hydrodynamical theory about the instability. Lorentz Force can destabilize the flow and bring in magnetorotational instability.

By Ohm's law,

$$\boldsymbol{J} = \sigma(\boldsymbol{E} + \boldsymbol{u} \times \boldsymbol{B}), \tag{1.11}$$

where σ is the electrical conductivity. Ohm's law connects electric field $\boldsymbol{E}$ with magnetic field $\boldsymbol{B}$.

If we replace E in Faraday's law in (1.6) by $-\boldsymbol{u} \times \boldsymbol{B} + J/\sigma$, we reach at the induction equation with electrical resistivity $\eta = 1/(\sigma\mu_0)$

$$\frac{\partial \boldsymbol{B}}{\partial t} = \nabla \times (\boldsymbol{u} \times \boldsymbol{B}) - \sigma\nabla \times \boldsymbol{J} = \nabla \times (\boldsymbol{u} \times \boldsymbol{B}) + \eta\nabla^2\boldsymbol{B}, \tag{1.12}$$

where (1.6) has been used in the second equality.

1.1.5 Spring-like Lorentz Force and MRI

The Lorentz Force comes from the Maxwell stress and can be modeled as the tension brought by the spring [18] as shown in Fig. 1.2. Consider two particles m_o and m_i set in steady state, are moving along concentric circle near each other. And consider that as

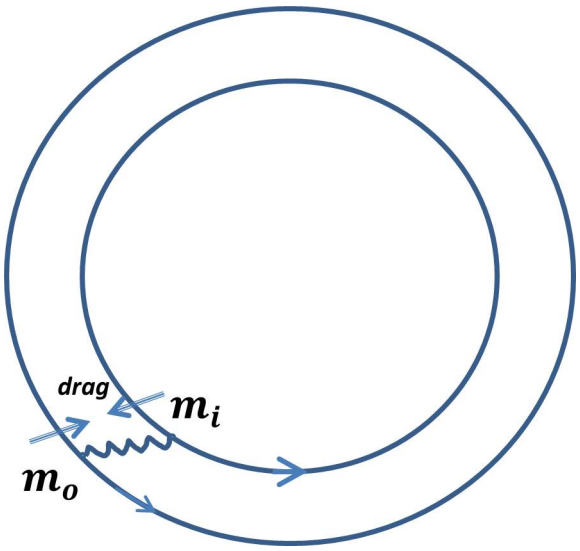

Figure 1.2: Lorentz Force acts like a spring between two particles m_o, m_i. Assume that at the beginning m_i and m_o are in the small circle of same radius and near each other. After a disturbance shifted m_i inward a little bit because the inner circle rotates faster, it will obtain a pulling back force and lose angular momentum by the pulling back from m_o and go further inward because the inner cirle has lower angular momentum. At the same time m_o will obtain the angular momentum that m_i lost and go outward. Consequently, flow becomes unstable.

would be like in the Keplerian flow, the angular velocity decreases outward. Therefore the inner orbit rotates faster. Then at a time, a tiny disturbanc makes m_i displace inward a little bit, by the spring-like Lorentz force the particle m_o will act a pull-back drug on m_i. Therefore m_i get a retarding torque. This torque makes m_i lose angular velocity. By losing angular velocity the centrifugal force becomes weaker than the inward force attracted by the mass sitting at the center, and it will further fall inward to inner orbit which corresponding to smaller angular momentum. Oppositely m_o will increase angular velocity by being pulled forward by m_i and will go further outward to the outer orbit. As a result, m_i and m_o will go further and further away from each other, signifying the instability.

In 1959, Velikhov studied the stability of the inviscid and perfectly conducting rotating flow subject to the axial direction uniform magnetic field $\boldsymbol{B} = B_z \boldsymbol{e}_z$. He first found the magnetorotational instability and obtained the stability criterion for MRI. It states that when there is a uniform axial magnetic field, the neccesary condition for a flow to be stable is

$$\frac{\mathrm{d}\Omega^2}{\mathrm{d}r} > 0. \tag{1.13}$$

It means for any flow with outwards increasing $|\Omega|$ is stable. Compared with the Rayleigh's criterion (1.3), the stability parameter region shrinks. For a Keplerian flow, $\Omega_K \propto r^{-3/2}$, so $\mathrm{d}\Omega_K^2/\mathrm{d}r < 0$, and Keplerian flow is unstable to MRI! In terms of the Rossby number, the critical Rossby number for the MRI is determined to be $Ro_c = 0$ and it is higher than the Keplerian Rossby number $Ro_K = -3/4$. As a result, MRI raises the critical Rossby number, which turns the Keplerian flow to be unstable.

Over 30 years of quietness after this discovery, the silence was broken in the year 1991. Balbus & Hawley made linear analysis of a rotating flow for ideal MHD flow (inviscid and perfectly conducting). The flow is subjected to magnetic field with both poloidal component (corresponding to axial and radial components). Later they included toroidal component (corresponding to azimuthal component). They published their redis-

covering result about the magnetorotational instability of axisymmetric disturbance [6]. A very astonishing feature of MRI is that instability occurs as long as the poloidal magnetic field exists, no matter how weak the magnetic field is . From Balbus & Hawley's rediscovery, the MRI exited a huge research group, and established its status as the desired mechanism to trigger the turbulence in the accretion disk. Later, non-axisymmetric disturbance was also studied mostly numerically and the analytical stability criterion and growth rate were yet to be examined [15].

Most of local analyses explored the Eulerian treatment is used. For non-axisymmetric disturbance, the traditional local analysis or the WKB analysis is liable to miss certain terms. We save this difficulty by appealing to the Lagrangian approach and obtain the equations retaining all the important terms.

1.2 Lagrangian approach

1.2.1 Resistive MHD and ideal MHD equations

The Basic equations for magnetohydrodynamics (MHD) include Navier-stokes equation, induction equation, continuous equation and the no-monopole equation as

$$\frac{\partial \boldsymbol{u}}{\partial t} + (\boldsymbol{u}\cdot\nabla)\boldsymbol{u} = -\frac{1}{\rho}\nabla p_0 + \boldsymbol{j}\times\boldsymbol{b} + \nu\nabla^2\boldsymbol{u} \quad \text{Navier-stokes equation,} \tag{1.14}$$

$$\frac{\partial \boldsymbol{b}}{\partial t} = \nabla\times(\boldsymbol{u}\times\boldsymbol{b}) + \eta\nabla^2\boldsymbol{b} \quad \text{induction equation,} \tag{1.15}$$

$$\nabla\cdot\boldsymbol{u} = 0 \quad \text{incompressibility (continuous equation),} \tag{1.16}$$

$$\nabla\cdot\boldsymbol{b} = 0 \quad \text{no magnetic monopole.} \tag{1.17}$$

where $\boldsymbol{u} = u_r\boldsymbol{e}_r + u_\theta\boldsymbol{e}_\theta + u_z\boldsymbol{e}_z$ is the velocity field, $\boldsymbol{b} = b_r\boldsymbol{e}_r + b_\theta\boldsymbol{e}_\theta + b_z\boldsymbol{e}_z$ the magnetic field, $\boldsymbol{j} = \nabla\times\boldsymbol{b}/\mu_0$ the current density, ρ the density, p_0 the hydrodynamic pressure and $\mu_0,\ \nu,\ \eta$ the magnetic permeability, the kinematic viscosity, the electrical resistivity respectively. We assume that $\rho,\ \mu_0,\ \nu,\ \eta$ are all constant [26]. We use lower case $\boldsymbol{u}$, $\boldsymbol{b}$,

$\boldsymbol{j}$ rather than the capital letters because the capital forms are used to describe the steady flow here.

Including the electrical resistivity η, the relation among the electric field $\boldsymbol{E}$, the magnetic field $\boldsymbol{B}$ and the current density $\boldsymbol{J}$ is provided by Ohm's law as

$$\boldsymbol{E} + \boldsymbol{u} \times \boldsymbol{B} = \eta \boldsymbol{j}. \tag{1.18}$$

By (1.18), the Faraday's law and Ampére's law in (1.6), the induction equation (1.15) is obtained. The induction equation decides how magnetic field develops influenced by the velocity field governed by the Navier-Stokes equation augmented by the Lorenz force.

For the ideal MHD where the viscosity ν and electrical resistivity η are both zero, equations (1.14)-(1.17) become

$$\frac{\partial \boldsymbol{u}}{\partial t} + (\boldsymbol{u} \cdot \nabla)\boldsymbol{u} = -\frac{1}{\rho}\nabla p_0 + \boldsymbol{j} \times \boldsymbol{b} \quad \text{Navier-stokes equation,} \tag{1.19}$$

$$\frac{\partial \boldsymbol{b}}{\partial t} = \nabla \times (\boldsymbol{u} \times \boldsymbol{b}) \quad \text{induction equation,} \tag{1.20}$$

$$\nabla \cdot \boldsymbol{u} = 0 \quad \text{incompressibility (continuous equation),} \tag{1.21}$$

$$\nabla \cdot \boldsymbol{b} = 0 \quad \text{no magnetic monopole.} \tag{1.22}$$

with the last two unchanged from (1.16) and (1.17).

1.2.2 Lagrangian displacement

There are two different viewpoints to characterize fluid. One is the Eulerian approach, which describes fluid fields in the way that we are observing the fluid motion i.e. the velocity field at specific locations as time passes by. In the Eulerian approach, we are not interested in where a particular particle comes from and goes. The velocity field is the essential variable and correspondingly we usually study the streamlines. Differently, the Lagrangian approach follows every particle and describes every particle's position. The

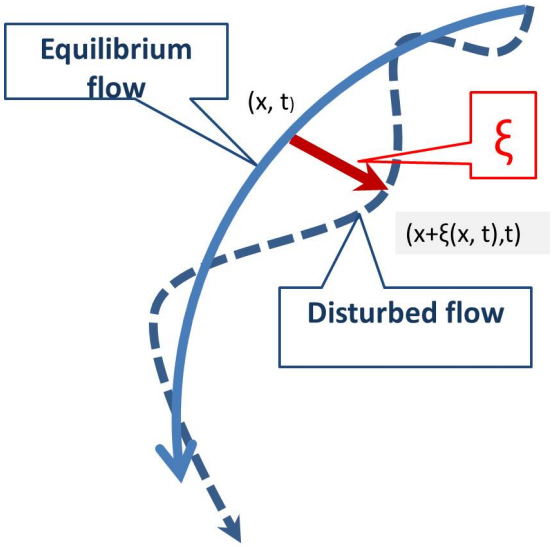

Figure 1.3: The solid line is the original path, e.g. the Keplerian rotation. After a small external disturbance added to how a fluid partical shifts away to move in the dashed line rather than the solid line. The displacement of a particle position is called the Lagrangian displacement and denoted by ξ.

position in place of the velocity becomes the essential variable and the path line can be considered correspondingly.

After tiny disturbance, the velocity, magnetic field and the total pressure are assumed to consist of two parts (steady field + disturbance)

$$\boldsymbol{u} = \boldsymbol{U} + \tilde{\boldsymbol{u}},\ \boldsymbol{b} = \boldsymbol{B} + \tilde{\boldsymbol{b}},\ p_0 = P_0 + \tilde{p_0}, \tag{1.23}$$

where $\boldsymbol{U}$, $\boldsymbol{B}$, $\boldsymbol{P}$ are the velocity, magnetic field and pressure of the badsic steady state while $\tilde{\boldsymbol{u}}$, $\tilde{\boldsymbol{b}}$, $\tilde{p_0}$ denote the small disturbance fields of them.

In the Lagrangian approach, to study the disturbance, the Lagrangian displacement is viewed as the basic variable which describes how a particle moves away from the original path of the steady state. In Fig. 1.3, the solid line is the original path, e.g. the Keplerian rotation. After a small external disturbance added to the particle, it obtains or loses energy and will shift away to move along the dashed line rather than the solid line. From the mathematical description $\boldsymbol{\xi} = \xi_r \boldsymbol{e}_r + \xi_\theta \boldsymbol{e}_\theta + \xi_z \boldsymbol{e}_z$ is used to denote the displacement from

the original path. We are interested in whether the disturbance grows or not. If it grows, the particles will be conveyed further and further away from the original path as time marches.

There are three disturbance fields in (1.23), $\tilde{\boldsymbol{u}}$, $\tilde{\boldsymbol{b}}$, $\tilde{p}$, and we will see that they can all be represented by $\boldsymbol{\xi}$ if we restrict the flow to the so-called isomagnetovortical surfaces in §1.2.4.

Let $\boldsymbol{x_0}(t)$ denote the the steady path of a fluid particle at time t, and after disturbance, the path shifts to $\boldsymbol{x_0}(t)+\boldsymbol{\xi}(\boldsymbol{x}_0(t),t)$ at time t by the Lagrangian displacement $\boldsymbol{\xi}$. Introduce the Lagrangian derivative which is also known as the material derivative

$$\frac{D}{Dt} = \frac{\partial}{\partial t} + \boldsymbol{u}\cdot\nabla. \tag{1.24}$$

The velocity is defined as

$$\boldsymbol{u}(\boldsymbol{x},t) = \frac{D\boldsymbol{x}}{Dt}. \tag{1.25}$$

Similarly the velocity of the particle at $\boldsymbol{x_0}(t)+\boldsymbol{\xi}(\boldsymbol{x}_0(t),t)$ after disturbance can be obtained by taking material derivative of $\boldsymbol{x_0}(t)+\boldsymbol{\xi}(\boldsymbol{x}_0(t),t)$ and it becomes

$$\boldsymbol{u}(\boldsymbol{x}_0+\boldsymbol{\xi},t) = \frac{D\boldsymbol{x}_0}{Dt} + \frac{D\boldsymbol{\xi}}{Dt} = \boldsymbol{U} + \frac{\partial\boldsymbol{\xi}}{\partial t} + \boldsymbol{U}\cdot\nabla\boldsymbol{\xi}, \tag{1.26}$$

where $\boldsymbol{U} = \boldsymbol{U}(\boldsymbol{x}_0,t)$ denotes the velocity of the steady flow at position x_0 and time t. By Taylor expansion, the left hand side of (1.26) can be expanded around the $\boldsymbol{x}_0$ to the first order of the small disturbance $\boldsymbol{\xi}$ as

$$\boldsymbol{u}(\boldsymbol{x}_0+\boldsymbol{\xi},t) = \boldsymbol{u}(\boldsymbol{x}_0,t) + \boldsymbol{\xi}\cdot\nabla\boldsymbol{U}. \tag{1.27}$$

Distinguish that $\boldsymbol{u}(\boldsymbol{x}_0,t)$ is the velocity at $(\boldsymbol{x}_0,t)$ after disturbance and therefore $\boldsymbol{u}(\boldsymbol{x}_0,t) = \boldsymbol{U}+\tilde{\boldsymbol{u}}(\boldsymbol{x}_0,t)$. So if we substitute (1.27) into (1.26), we see immediately that the Eulerian

variable $\tilde{\boldsymbol{u}}$ and the Lagrangian variable $\boldsymbol{\xi}$ are related as

$$\tilde{\boldsymbol{u}}(\boldsymbol{x_0},t) = \frac{\partial \boldsymbol{\xi}}{\partial t} + \boldsymbol{U}\cdot\nabla\boldsymbol{\xi} - \boldsymbol{\xi}\cdot\nabla\boldsymbol{U}. \tag{1.28}$$

To get the relation between $\boldsymbol{b}(\tilde{\boldsymbol{x_0}},t)$ and $\boldsymbol{\xi}$ is not so direct anymore. First we introduce the concept of isovortical and isomagnetovortical disturbances. The isovortical disturbances are used in the study of hydrodynamics of inviscid fluid while isomagnetovortical disturbances are the extension of the first one in idea MHD.

1.2.3 Isovortical disturbance

In hydrodynamics of an inviscid fluid, the vorticity defined by

$$\frac{\partial \boldsymbol{\omega}}{\partial t} + (\boldsymbol{u}\cdot\nabla)\boldsymbol{\omega} - (\boldsymbol{\omega}\cdot\nabla)\boldsymbol{u} = 0. \tag{1.29}$$

is frozen into the flow. In other words, a vortex moves with the flow. For hydrodynamics of an inviscid incompressible fluid, the vortex equation is obtained by taking the curl of the Euler equation (1.19).

The evolution of $\boldsymbol{\omega}$ guarantees that the vortex line is moving with the fluid particle. Concomitantly (1.29) guarantees the well known Kelvin's circulation theorem which states, the circulation along any material loop or the vorticity flux across any material surface is invariant in the fluid motion [19].

$$\frac{\mathrm{d}}{\mathrm{d}t}\oint_C \boldsymbol{U}\cdot\mathrm{d}\boldsymbol{x} = \frac{\mathrm{d}}{\mathrm{d}t}\int_S \boldsymbol{\omega}\cdot\mathrm{d}\boldsymbol{S} = 0, \tag{1.30}$$

where C is an arbitrary closed material curve and S is the material surface surrounded by C.

The helicity is defined by quadratic integral

$$H_U = \int_D \boldsymbol{u} \cdot \boldsymbol{\omega} \mathrm{d}V, \tag{1.31}$$

where D is the whole fluid domain. It can be verified that for the circulation-preserving flow, the helicity is conservative, i.e.

$$\frac{\mathrm{d}H_U}{\mathrm{d}t} = 0. \tag{1.32}$$

If we constrain the disturbance to preserve the circulation for arbitrary closed loop and therefore the helicity disturbance, this class of disturbances are called the isovortical disturbances (kinematically accessible disturbance). It is important to notice that Kelvin's circulation theorem and the helicity conservation are satisfied only when the forces acting on the fluid are all potential forces. In the MHD, magnetic field is present and the Lorentz force is not a potential force. The circulation or the vorticity flux are not invariant any more. Instead there are new conservative quantities.

1.2.4 Isomagnetovortical Disturbance

For the ideal MHD, the fluid is inviscid and perfectly conducting, i.e. ν and η are both zero. Because of the influence of the Lorentz force $F_l = \boldsymbol{j} \times \boldsymbol{b}$, the vorticity flux is not a invariant in time anymore. However, if we exam (1.15), we can find by using of (1.16) and (1.17) the evolution of $\boldsymbol{b}$ becomes

$$\frac{\partial \boldsymbol{b}}{\partial t} + (\boldsymbol{u} \cdot \nabla)\boldsymbol{b} - (\boldsymbol{b} \cdot \nabla)\boldsymbol{u} = 0. \tag{1.33}$$

It can be noticed that the evolution of $\boldsymbol{b}$ is similar to the evolution of $\boldsymbol{\omega}$ in (1.29). It can be verified that for ideal MHD the magnetic flux, in an analogous way as the vortex flux

of a neutral fluid, is conserved [35, 20, 21]

$$\frac{\mathrm{d}}{\mathrm{d}t}\int_S \boldsymbol{b}\cdot\mathrm{d}\boldsymbol{s}=0. \tag{1.34}$$

On the other hand, there are two conservative quadratic integrals, with one corresponding to helicity in (1.31), the magnetic helicity[21]

$$H_M=\int_D \boldsymbol{b}\cdot(\nabla^{-1})\times\boldsymbol{b}\mathrm{d}V. \tag{1.35}$$

and the other one the cross-helicity [44, 20]

$$H_C=\int_D \boldsymbol{b}\cdot\boldsymbol{u}\mathrm{d}V. \tag{1.36}$$

If all of H_M, H_C and $\int_S \boldsymbol{b}\cdot\mathrm{d}\boldsymbol{S}$ do not change even after the disturbance, this kind of disturbances are called isomagnetovortical disturbances [21] (Kinematically accessible disturbance) and similarly we can obtain the relation between $\tilde{\boldsymbol{u}},\tilde{\boldsymbol{b}}$ and the Lagrangian displacement ξ [19, 37, 20, 21] as

$$\begin{aligned}\tilde{\boldsymbol{u}} &= \mathscr{P}\left[\boldsymbol{\xi}\times\Omega+\boldsymbol{\eta}\times\boldsymbol{B}\right],\\ \tilde{\boldsymbol{b}} &= \nabla\times(\boldsymbol{\xi}\times\boldsymbol{B}),\end{aligned} \tag{1.37}$$

where η is sort of 'magnetic displacement' indroduced similar to lagrangian displacement ξ and $\mathscr{P}[\cdot]$ is an operator projecting a vector field to a solenoidal one.8

Assume that the flow is incompressible and the density $\rho=1$, and that the permeability of the free space is $\mu_0=1$ for simplicity. The total energy in ideal MHD for incompressible flow is then

$$H=\frac{1}{2}\int_D \boldsymbol{u}^2+\boldsymbol{b}^2\mathrm{d}V, \tag{1.38}$$

which includes the kinetic energy $\int_D \boldsymbol{u}^2\mathrm{d}V/2$ and the magnetic energy $\int_D \boldsymbol{b}^2\mathrm{d}V/2$. If no

external disturbance or force introduced, total energy of the whole fluid is conserved in time. When a disturbance is added to the basic flow, the total energy will change (increase or decrease), and the sign of the wave energy holds a key to decide the stability of the flow according to Krein's theory of Hamiltonian spectra.

1.2.5 Frieman-Rotenberg equation and Hain-Lüst equation

In the book by J. P. Goedbloed *etal*., they use assumption of adiabatic development for obtaining the relation between $\tilde{p}_0$ and $\boldsymbol{\xi}$. In the incompressible case, $\tilde{p}_0$ can be obtained by the assistance of (1.19) and (1.21). Substituting $\tilde{\boldsymbol{u}}$, $\tilde{\boldsymbol{b}}$ and $\tilde{p}_0$ expressed in terms of $\boldsymbol{\xi}$ into (1.19), we can get by dropping the zeroth order, a linearized disturbance the equations for ξ only, which is called the Frieman-Rotenberg equation. [37]

$$\rho \frac{\partial^2 \boldsymbol{\xi}}{\partial t^2} + 2\rho(\boldsymbol{U}\cdot\boldsymbol{\nabla})\frac{\partial \boldsymbol{\xi}}{\partial t} - \boldsymbol{F}_0[\boldsymbol{\xi}] = 0. \tag{1.39}$$

where

$$\boldsymbol{F}_0[\boldsymbol{\xi}] = -\rho(\boldsymbol{U}\cdot\nabla)^2\boldsymbol{\xi} + \rho(\boldsymbol{\xi}\cdot\nabla)(\boldsymbol{U}\cdot\nabla)\boldsymbol{U} - \nabla\tilde{p} + \frac{1}{4\pi}(\nabla\times\tilde{\boldsymbol{b}})\times\boldsymbol{B} + \frac{1}{4\pi}(\nabla\times\boldsymbol{B})\times\tilde{\boldsymbol{b}}.$$

Here the basic velocity field $\boldsymbol{U}(\boldsymbol{r})$ and the magnetic field $\boldsymbol{B}(r)$ only depend on radius r. We will use then the Frieman-Rotenberg equation to calculate the wave energy to study the instability in Chapter 4. By the MHD version of Arnold theorem, for isomagnetovortical disturbances, if any disturbance has definite (positive energy or negative) wave energy, then the flow is stable. The wave energy is useful to judge the stability condition [37, 20]. Krein's theorem tells that collision of two imaginary eigenvalues with energy of opposite signature could bring in instability [47, 41].

Because the background fields (steady flow) have no dependence on t, θ, z, we can assume the disturbance to be in the normal-mode form i.e. $\propto \exp[\lambda t + i(m\theta + kz)]$. λ is the growth rate and θ, z are wavenumbers in azimuthal and axial direction. If we

eliminate ξ_θ and ξ_z in (1.39), then finally we are left with a second order differential equation of ξ_r. Furthermore, we can use a newly defined variable $\chi = r\xi_r$. The equation for χ is known as the Hain-Lüst equation [37]. The deduction of the Hain-Lüst equation in detail will be given in chapter 2 for ideal MHD and given in chapter 3 for inductionless MHD. We briefly show the Hain-Lüst equation for the ideal MHD as below.

$$\frac{\mathrm{d}}{\mathrm{d}r}\left(f\frac{\mathrm{d}\chi}{\mathrm{d}r}\right) = g\chi, \tag{1.40}$$

where,

$$\begin{aligned} f &= \frac{1}{h^2 r}\left(\tilde{\lambda}^2 + \frac{F^2}{\rho\mu_0}\right), \\ g &= \frac{\mathrm{d}}{\mathrm{d}r}\left(\frac{2im}{h^2 r^2}\left(\Omega\tilde{\lambda} - \frac{i\mu F}{\rho\mu_0}\right)\right) + \frac{1}{r}\left(\tilde{\lambda}^2 + \frac{F^2}{\rho\mu_0}\right) + \frac{\mathrm{d}\Omega^2}{\mathrm{d}r} - \frac{1}{\rho\mu_0}\frac{\mathrm{d}\mu^2}{\mathrm{d}r} + \frac{4k^2\left(\Omega\tilde{\lambda} - \frac{\mu i F}{\rho\mu_0}\right)^2}{h^2 r(\tilde{\lambda}^2 + \frac{F^2}{\rho\mu_0})}. \end{aligned}$$

for a given steady state rotating flow and magnetic field $\boldsymbol{U} = r\Omega(r)\boldsymbol{e}_\theta and \boldsymbol{B} = r\mu(r)\boldsymbol{e}_\theta + B_z\boldsymbol{e}_z$,, and with the definitions that $h^2 = m^2/r^2 + k^2$ and $F = m\mu + kB_z$.

We deduce (1.40) in a natural way in chapter 2 and extend it to resistive MHD to include the viscosity ν and electrical resistivity η in chapter 3. Based on Hain-Lüst equation for variable χ, we explore the WKB approximation to make local stability analysis.

1.2.6 WKB approximation

Let us think about the second order differential equation

$$(fx')' + h'x' - gx = 0, \tag{1.41}$$

where $f(r)$, $h(r)$, $g(r)$ are given functions of variable r and $x(r)$ is the unknown function of r to be decided; the prime denotes the differentiation $\mathrm{d}/\mathrm{d}r$. The solution is assumed to

be in the form

$$x(r) = p(r)exp\left[i\int q(r)\mathrm{d}r\right]. \tag{1.42}$$

Next step is to determine p and q in $x(r)$. Substitute (1.42) into (1.41), it yields

$$f'p' + fp'' + i(fpq)' - fpq^2 + h'p' + ih'pq - gp = 0. \tag{1.43}$$

Assume the wave length is very small compared to L such that $qL \gg 1$, the second order inhomogeneous terms $fp'' + h'p'$ can be neglected, and (1.41) can be written into two equations (zero order and first order of qL) [37]

$$fpq^2 + gp = 0, \;\; f(ln(fp^2q))' = -h'. \tag{1.44}$$

From the first one of (1.44), we instantaneously conclude

$$q = \sqrt{-\frac{g}{f}}, \tag{1.45}$$

and p also can be calculated from the second one in (1.44), but would need more efforts. After we obtain p and q, then we resubstitute them back into the solution form (1.42), the local solution of equation (1.41) is obtained. As a result, by using the WKB approximation, we can solve the equation in the short-wavelength limit. Equation (1.45) gives rise to the dispersion relation between the growth rate λ and axial, azimuthal and radial wavenumbers k, m and q. We use the WKB method to solve our Hain-Lüst equation in both the ideal MHD (zero ν and η) and the resistive MHD case (nonzero ν and η).

Chapter 2

Short-wavelength stability analysis of AMRI in ideal MHD

2.1 Short-wavelength stability analysis

We consider a circular symmetric flow of an incompressible inviscid fluid with infinite electric conductivity, subjected to a steady external magnetic field, and the linear stability of a localized disturbance along one of the streamlines. We assume that the radial wavelength is much small compared with the radius r of the streamline, being a sort of the WKB approximation. We introduce global cylindrical coordinates (r, θ, z) with the z-axis lying on the symmetric axis. The basic state is a rotating flow in equilibrium, with the angular velocity $\Omega(r)$, subject to a magnetic field having the azimuthal and the axial components $B_\theta(r) = r\mu(r)$ and B_z.

$$\boldsymbol{U} = r\Omega(r)\boldsymbol{e}_\theta, \ \boldsymbol{B} = r\mu(r)\boldsymbol{e}_\theta + B_z\boldsymbol{e}_z, \tag{2.1}$$

where $\boldsymbol{e}_\theta$ and $\boldsymbol{e}_z$ are the unit vectors in the azimuthal and the axial directions, respectively. After the second half of §3.2, we focus on the azimuthal field.

The linearized equations of the momentum and the induction equations for disturbance

$\tilde{\boldsymbol{u}}$, $\tilde{\boldsymbol{B}}$ and $\tilde{p}$ are

$$\frac{\partial \tilde{\boldsymbol{u}}}{\partial t} + (\tilde{\boldsymbol{u}} \cdot \nabla)\boldsymbol{U} + (\boldsymbol{U} \cdot \nabla)\tilde{\boldsymbol{u}} = -\frac{1}{\rho}(\nabla \tilde{p}) + \frac{1}{\rho \mu_0}(\tilde{\boldsymbol{B}} \cdot \nabla)\boldsymbol{B} + \frac{1}{\rho \mu_0}(\boldsymbol{B} \cdot \nabla)\tilde{\boldsymbol{B}}, \tag{2.2}$$

$$\frac{\partial \tilde{\boldsymbol{B}}}{\partial t} = \nabla \times (\boldsymbol{u} \times \tilde{\boldsymbol{B}}) + \nabla \times (\tilde{\boldsymbol{u}} \times \boldsymbol{B}), \tag{2.3}$$

$$\nabla \cdot \tilde{\boldsymbol{u}} = 0, \tag{2.4}$$

$$\nabla \cdot \tilde{\boldsymbol{B}} = 0, \tag{2.5}$$

where μ_0 is the magnetic permeability and the density ρ is assumed to be constant. The last equation is the solenoidal property of the magnetic field. The first step is to assume the disturbances in the normal-mode form

$$\begin{aligned} \tilde{\boldsymbol{u}} &= \tilde{\boldsymbol{u}_1} \exp[\lambda t + i(m\theta + kz)], \\ \tilde{\boldsymbol{B}} &= \tilde{\boldsymbol{B}_1} \exp[\lambda t + i(m\theta + kz)], \\ \tilde{\boldsymbol{p}} &= \tilde{\boldsymbol{p}_1} \exp[\lambda t + i(m\theta + kz)]. \end{aligned} \tag{2.6}$$

Later we will use $\tilde{\boldsymbol{u}}$, $\tilde{\boldsymbol{B}}$ and $\tilde{p}$ to denote $\tilde{\boldsymbol{u}_1}$, $\tilde{\boldsymbol{B}_1}$ and $\tilde{p_1}$for simplicity. Then the linearized equations (2.2)–(2.5) combine into matrix form for $\boldsymbol{\xi} = (\tilde{u_r},\ \tilde{u_\theta},\ \tilde{u_z},\ \tilde{B_r},\ \tilde{B_\theta},\ \tilde{B_z},\ \tilde{p})$ as

$$\mathsf{M}\boldsymbol{\xi} = 0, \tag{2.7}$$

where

$$\mathsf{M}=\begin{pmatrix}
\tilde{\lambda} & -2\Omega & 0 & -\frac{iF}{\rho\mu_0} & \frac{2\mu}{\rho\mu_0} & 0 & \frac{1}{\rho}\frac{d}{dr} \\
2\Omega+r\frac{d\Omega}{dr} & \tilde{\lambda} & 0 & -(2\mu+r\frac{d\mu}{dr}) & -\frac{iF}{\rho\mu_0} & 0 & \frac{1}{r\rho}im \\
0 & 0 & \tilde{\lambda} & 0 & 0 & -\frac{iF}{\rho\mu_0} & \frac{1}{\rho}ik \\
-iF & 0 & 0 & \tilde{\lambda} & 0 & 0 & 0 \\
r\frac{d\mu}{dr} & -iF & 0 & -r\frac{d\Omega}{dr} & \tilde{\lambda} & 0 & 0 \\
0 & 0 & -iF & 0 & 0 & \tilde{\lambda} & 0 \\
\frac{1}{r}+\frac{d}{dr} & \frac{im}{r} & ik & 0 & 0 & 0 & 0 \\
0 & 0 & 0 & \frac{1}{r}+\frac{d}{dr} & \frac{im}{r} & ik & 0
\end{pmatrix}, \tag{2.8}$$

with $\tilde{\lambda}=\lambda+im\Omega$ and $F=m\mu+B_z k$.

We can rule out, from (2.7), the disturbance magnetic field to obtain representations for $\tilde{\boldsymbol{u}}$ in terms of $\tilde{p}$ and its derivative as

$$\tilde{u_r}+\frac{1}{E\rho}\left(\tilde{\lambda}+\frac{F^2}{\tilde{\lambda}\rho\mu_0}\right)\frac{\mathrm{d}\tilde{p}}{\mathrm{d}r}+\frac{im}{E\rho r}\left(2\Omega-\frac{2i\mu F}{\tilde{\lambda}\rho\mu_0}\right)\tilde{p}=0, \tag{2.9}$$

$$\begin{aligned}\tilde{u_\theta}-\frac{1}{E\rho}&\left[2\Omega+\left(1+\frac{F^2}{\tilde{\lambda}^2\rho\mu_0}\right)r\frac{\mathrm{d}\Omega}{\mathrm{d}r}-\frac{2i\mu F}{\tilde{\lambda}\rho\mu_0}\right]\frac{\mathrm{d}\tilde{p}}{\mathrm{d}r}\\ &+\frac{im}{Er\rho}\left(\tilde{\lambda}+\frac{F^2}{\tilde{\lambda}\rho\mu_0}+\frac{2i\mu F}{\tilde{\lambda}^2\rho\mu_0}r\frac{\mathrm{d}\Omega}{\mathrm{d}r}-\frac{2\mu}{\tilde{\lambda}\rho\mu_0}r\frac{\mathrm{d}\mu}{\mathrm{d}r}\right)\tilde{p}=0,\end{aligned} \tag{2.10}$$

$$\tilde{u_z}+\frac{ik}{\rho\left(\tilde{\lambda}+F^2/(\tilde{\lambda}\rho\mu_0)\right)}\tilde{p}=0, \tag{2.11}$$

where

$$\begin{aligned}E \;=\;& \left(\tilde{\lambda}+\frac{F^2}{\tilde{\lambda}\rho\mu_0}\right)^2+\frac{2\mu r}{\tilde{\lambda}\rho\mu_0}\left(\tilde{\lambda}+\frac{F^2}{\tilde{\lambda}\rho\mu_0}\right)\left(\frac{iF}{\tilde{\lambda}}\frac{\mathrm{d}\Omega}{\mathrm{d}r}-\frac{\mathrm{d}\mu}{\mathrm{d}r}\right)\\ &+2\left[2\Omega+\left(1+\frac{F^2}{\tilde{\lambda}^2\rho\mu_0}\right)r\frac{\mathrm{d}\Omega}{\mathrm{d}r}-\frac{2i\mu F}{\tilde{\lambda}\rho\mu_0}\right]\left(\Omega-\frac{i\mu F}{\tilde{\lambda}\rho\mu_0}\right).\end{aligned} \tag{2.12}$$

Substitution of (2.9)-(2.11) into the continuity equation (2.4) then gives rise to a second-

order differential equation of $\tilde{p}$

$$\left(\frac{1}{r}+\frac{\mathrm{d}}{\mathrm{d}r}\right)\left[\left(\tilde{\lambda}+\frac{F^2}{\tilde{\lambda}\rho\mu_0}\right)\frac{1}{E}\frac{\mathrm{d}\tilde{p}}{\mathrm{d}r}+\frac{2im}{rE}\left(\Omega-\frac{i\mu F}{\tilde{\lambda}\rho\mu_0}\right)\tilde{p}\right]$$
$$-\frac{im}{rE}\left\{\left[2\Omega+\left(1+\frac{F^2}{\tilde{\lambda}^2\rho\mu_0}\right)r\frac{\mathrm{d}\Omega}{\mathrm{d}r}-\frac{2i\mu F}{\tilde{\lambda}\rho\mu_0}\right]\frac{\mathrm{d}\tilde{p}}{\mathrm{d}r}\right.$$
$$\left.-\frac{im}{r}\left(\tilde{\lambda}+\frac{F^2}{\tilde{\lambda}\rho\mu_0}+\frac{2ir\mu F}{\tilde{\lambda}^2\rho\mu_0}\frac{\mathrm{d}\Omega}{\mathrm{d}r}-\frac{2r\mu}{\tilde{\lambda}\rho\mu_0}\frac{\mathrm{d}\mu}{\mathrm{d}r}\right)\tilde{p}\right\}$$
$$-\frac{k^2}{\tilde{\lambda}+F^2/(\tilde{\lambda}\rho\mu_0)}\tilde{p}=0. \tag{2.13}$$

Introduce a new variable $\chi=-ru_r/\tilde{\lambda}$ associated with the radial Lagrangian displacement [35]. Equation (2.9) expresses χ in terms of $\tilde{p}$ and $\mathrm{d}\tilde{p}/\mathrm{d}r$. Next by taking differentiation, with respect to r, of (2.9) after multiplication by r, we relate $\mathrm{d}\chi/\mathrm{d}r$ with $\tilde{p}$, $\mathrm{d}\tilde{p}/\mathrm{d}r$ and $\mathrm{d}^2\tilde{p}/\mathrm{d}r^2$, the last of which is eliminated with the aid of (2.13). By using (2.9) again to further eliminate $\mathrm{d}\tilde{p}/\mathrm{d}r$, we are led to

$$\frac{\rho}{h^2r}\left(\tilde{\lambda}^2+\frac{F^2}{\rho\mu_0}\right)\frac{\mathrm{d}\chi}{\mathrm{d}r}-\frac{2im\rho}{h^2r^2}\left(\Omega\tilde{\lambda}-\frac{i\mu F}{\rho\mu_0}\right)\chi=\tilde{p}. \tag{2.14}$$

Substitution (2.14) for $\tilde{p}$ into (2.9) gives rise to

$$\frac{\mathrm{d}}{\mathrm{d}r}\left(f\frac{\mathrm{d}\chi}{\mathrm{d}r}\right)=g\chi, \tag{2.15}$$

where, by use of the definition $h^2=m^2/r^2+k^2$,

$$\begin{aligned} f &= \frac{1}{h^2r}\left(\tilde{\lambda}^2+\frac{F^2}{\rho\mu_0}\right),\\ g &= \frac{\mathrm{d}}{\mathrm{d}r}\left[\frac{2im}{h^2r^2}\left(\Omega\tilde{\lambda}-\frac{i\mu F}{\rho\mu_0}\right)\right]+\frac{1}{r}\left(\tilde{\lambda}^2+\frac{F^2}{\rho\mu_0}\right)+\frac{\mathrm{d}\Omega^2}{\mathrm{d}r}-\frac{1}{\rho\mu_0}\frac{\mathrm{d}\mu^2}{\mathrm{d}r}\\ &\quad+\frac{4k^2\left(\Omega\tilde{\lambda}-\mu iF/(\rho\mu_0)\right)^2}{h^2r(\tilde{\lambda}^2+F^2/(\rho\mu_0))}. \end{aligned}$$

This is no other than the Hain-Lüst equation [37], as extended to accommodate the effect

of a rotating flow. We seek the solution of (2.15) in the WKB approximation. For this purpose, we substitute into (2.15) the form $\chi(r) = p(r)\exp[i\int q(r)\mathrm{d}r]$ with the constraint that the radial wavelength $2\pi/q$ is assumed to be much shorter than the characteristic length L, a measure for radial inhomogeneity, namely, $qL \gg 1$. Neglecting the second-order terms in $qL \gg 1$, the dispersion relation is gained from (2.15) as $q^2 = -g/f$, producing

$$
\begin{aligned}
&(h^2+q^2)\left(\tilde{\lambda}^2+\frac{F^2}{\rho\mu_0}\right)^2+4k^2\left(\Omega\tilde{\lambda}-\frac{i\mu F}{\rho\mu_0}\right)^2\\
&+4h^2\left[\frac{imr}{2}\frac{\mathrm{d}}{\mathrm{d}r}\left(\frac{\Omega\tilde{\lambda}-\frac{i\mu F}{\rho\mu_0}}{h^2r^2}\right)+\Omega^2 Ro-\frac{\mu^2}{\rho\mu_0}Rb\right]\left(\tilde{\lambda}^2+\frac{F^2}{\rho\mu_0}\right)=0, \quad (2.16)
\end{aligned}
$$

where we have introduced the Rossby number Ro [8, 9] and the magnetic Rossby number Rb [32] by

$$
Ro=\frac{1}{2}\frac{r}{\Omega}\frac{\mathrm{d}\Omega}{\mathrm{d}r}, \quad Rb=\frac{1}{2}\frac{r}{\mu}\frac{\mathrm{d}\mu}{\mathrm{d}r}. \quad (2.17)
$$

2.2 Axisymmetric perturbations

For the standard MRI (SMRI), that is for $\boldsymbol{B} = B_z\boldsymbol{e}_z$ with B_θ left out, the maximum growth rate is the Oort A-value $\nu_A/\Omega = \frac{1}{2}|\mathrm{d}\log\Omega/\mathrm{d}\log r| = |Ro|$ [22] which is attained at $m = 0$, the radial wavenumber $q = 0$ and the axial wavenumber k satisfying $\omega_A/\Omega = \pm\sqrt{1-\kappa^4/(16\Omega^4)}$, with $\omega_A = kB_z/\sqrt{\rho\mu_0}$ and κ being the epicyclic frequency [15, 27]. At the outset, we shall confirm that our approach of using (2.15) restores this well known result.

For the SMRI, the dispersion relation (2.16) simplifies, when $m = 0$, to

$$
\frac{\lambda^2}{\Omega^2}+Ro\left(\frac{\lambda^2}{\Omega^2}+\frac{\omega_A^2}{\Omega^2}\right)+\frac{1}{4\alpha^2}\left(\frac{\lambda^2}{\Omega^2}+\frac{\omega_A^2}{\Omega^2}\right)^2=0, \quad (2.18)
$$

where $\alpha = k/\sqrt{q^2+k^2}$. We read off from (2.18) limited to $\lambda = 0$ the stability boundary as

$$
Ro_c=-\frac{\omega_A^2}{4\alpha^2\Omega^2}(<0), \quad \text{or} \quad \frac{\omega_A}{\Omega}=0. \quad (2.19)
$$

As the magnetic field $\sqrt{k^2+q^2}B_z \to 0$, the above representation $Ro_c \to 0$, and the Velikhov-Chandrasekhar paradox [4, 5], a glamour of the MRI, is retrieved. We note in passing that this paradox was resolved by taking account of the electric resistivity and the viscosity [**?**, 9]. The eigenvalue λ, the root of (2.18), is

$$\frac{\lambda}{\Omega} = \pm\sqrt{\alpha^2 Ro^2 - \left(|\alpha| \mp \sqrt{\alpha^2(1+Ro)^2 + \left(\frac{\omega_A}{\Omega}\right)^2}\right)^2}. \tag{2.20}$$

The growth rate $\mathrm{Re}[\lambda]$, the real part of λ, reaches the maximum value $|\alpha Ro|$ at $(\omega_A/\Omega)^2 = \alpha^2[1-(1+Ro)^2]$, among which the maximum growth rate $\nu_\mathrm{A}/\Omega = |Ro|$, being the Oort A-value, is attained at $|\alpha| = 1$. It should be born in mind that the Oort A-value is realizable only when $-2 < Ro < 0$ as required by $(\omega_\mathrm{A}/\Omega)^2 > 0$ with k a disposable parameter. For a Keplerian rotation ($Ro = -3/4$), $\nu_\mathrm{A} = 3|\Omega|/4$ when $\omega_A = \pm\sqrt{15}\Omega/4$ in accord with ref [15].

The critical wavenumber for the instability is read off from (2.19) to be $\omega_A/\Omega = \pm\sqrt{-4Ro}$, meaning that the instability is invited when $\omega_A/\Omega \in (-\sqrt{-4Ro}, 0) \cup (0, \sqrt{-4Ro})$. For the SMRI, the most unstable mode is likely to be axisymmetric. The axisymmetric mode is tractable since the eigenvalues λ are either real or pure imaginary, whereas for a non-axisymmetric perturbation, the eigenvalues are complex, being less analytically tractable.

Next, we turn to the azimuthal MRI (AMRI), for which the magnetic field has an azimuthal component $\boldsymbol{B} = r\mu(r)e_\theta$ only. For the axisymmetric case ($m = 0$), the growth rate calculated from (2.16) is

$$\lambda = \pm 2\Omega\alpha\sqrt{-1 - Ro + Rb\,\omega_{A\theta}^2/\Omega^2}, \quad \lambda = 0, \tag{2.21}$$

where $\omega_{A\theta} = \mu/\sqrt{\rho\mu_0}$, and $\lambda = 0$ is a double root. The instability region is $Ro < Rb\,\omega_{A\theta}^2/\Omega^2 - 1$, i.e., the critical Rossby number $Ro_c = Rb\,\omega_{A\theta}^2/\Omega^2 - 1$, which recovers Michael's criterion [38] (See also refs [5, 39]). Recently, this criterion is extended

to include the viscosity and the electric resistivity [26]. In case of $Rb\,\omega_{A\theta} = 0$, the criterion reduces to that of Rayleigh's centrifugal instability; when either magnetic field or the magnetic shear vanishes, the Keplerian flow is stable. The magnetic shear acts to either lower ($Rb < 0$) or to raise ($Rb > 0$) the critical Rossby number for the axisymmetric mode. In view of (2.21), for a Keplerian flow ($Ro = -3/4$), the instability occurs for $Rb\,\omega_{A\theta}^2/\Omega^2 > 1/4$. Either increase of Rb on the side of $Rb > 0$ or $\omega_{A\theta}^2$ increases the growth rate.

2.3 Non-axisymmetric perturbations: overview

Inclusion of non-axisymmetric perturbations ($m \neq 0$) supplies rich characteristics of the AMRI. In order to gain an insight into the three-dimensional AMRI, we start with the stability analysis for motionless state and then proceed to the case of a very weak magnetic field. The former corresponds to the strong-field limit.

By trial and error of numerical calculation, it is probable that the maximum growth rate is attained in the limit of $k \to \infty$. The dispersion relation (2.16) reduces, in the limit of $k^2 + q^2 \to \infty$, to

$$4(\tilde{\lambda}\Omega - im\omega_{A\theta}^2)^2 + \frac{1}{\alpha^2}(\tilde{\lambda}^2 + m^2\omega_{A\theta}^2)^2 + (\tilde{\lambda}^2 + m^2\omega_{A\theta}^2)(4\Omega^2 Ro - 4Rb\,\omega_{A\theta}^2) = 0. \quad (2.22)$$

Equation (2.22), which is valid for a strong magnetic field as well, was derived by Ogilvie and Pringle [31], and coincides with equation in the inductionless limit [26] if the viscous and resistive terms are dropped off.

For motionless state ($\Omega \equiv 0$), the roots λ of (2.22) are written out explicitly in compact form as

$$\lambda = \pm\sqrt{-m^2 + 2\alpha^2 Rb \pm 2\alpha\sqrt{m^2 + \alpha^2 Rb^2}}\,\omega_{A\theta}. \quad (2.23)$$

One of the roots (2.23) becomes positive, signifying instability, when $2|\alpha|\sqrt{m^2 + \alpha^2 Rb^2} > m^2 - 2\alpha^2 Rb$. For an axisymmetric perturbation ($m = 0$), the instability criterion is $Rb > 0$.

For non-axisymmetric perturbations, this condition is superseded by $Rb > m^2/(4\alpha^2) - 1$. A glance at (2.23) shows that the growth rate is zero for $\alpha = 0$. When m exhausts all the integers and α exhausts all the real numbers contained in the range of $0 < |\alpha| \leq 1$, the magnetic Rossby number $Rb > -3/4$ is the widest possible Rb-range for instability [31]. This condition coincides with the necessary condition for the instability derived in a wider context by Newcomb's energy principle [13, 3], which takes the form

$$-rp' > \frac{1}{2\mu_0} m^2 \boldsymbol{B}^2, \tag{2.24}$$

where $p' = \mathrm{d}p/\mathrm{d}r$ [35]. Substituting $\boldsymbol{B}(r) = B_\theta(r)\boldsymbol{e}_\theta$ into the equilibrium condition $\boldsymbol{0} = -\nabla p + (\nabla \times \boldsymbol{B}) \times \boldsymbol{B}/\mu_0$, we have, $p' = -B_\theta/(\mu_0 r)(rB_\theta)'$. As noted in ref [35], (2.24) is not valid for the axisymmetric case $m = 0$, for which (2.24) is taken place of by Suydam's criterion for the local interchange condition. As a consequence, $m = \pm 1$ in (2.24) provides the maximum possible range for instability, and this condition is exactly $Rb > -3/4$.

The maximum growth rate is found by rewriting (2.23) as

$$\lambda = \pm \sqrt{\alpha^2 (Rb+1)^2 - \left(\sqrt{m^2 + \alpha^2 Rb^2} \mp \alpha \right)^2}\, \omega_{A\theta}. \tag{2.25}$$

Since m takes integral values but α is confined to the range $0 < |\alpha| \leq 1$, the maximum of λ is attained either at $m = 0$ or $m = \pm 1$. When Rb is larger than 3/4, the maximum is $\lambda_{\max} = 2\sqrt{Rb}|\omega_{A\theta}|$ attained at $m = 0$ and $|\alpha| = 1$. For $-3/4 < Rb \leq 3/4$, the maximum is attained at $m = \pm 1$ with its value $\lambda_{\max} = \sqrt{-1 + 2Rb + 2\sqrt{1+Rb^2}}|\omega_{A\theta}|$.

For comparison, we look into the case of $k = 0$. The dispersion relation (2.16) reduces to

$$\left(\tilde{\lambda}^2 + m^2 \omega_{A\theta}^2\right) \left[\left(q^2 + \frac{m^2}{r^2} \right) (\tilde{\lambda}^2 + m^2 \omega_{A\theta}^2) + \frac{4m^2}{r^2} (\Omega^2 Ro + Rb\, \omega_{A\theta}^2) \right.$$
$$\left. + \frac{4im\Omega Ro}{r^2} (\lambda + 2im\Omega) \right] = 0. \tag{2.26}$$

For motionless state ($\Omega \equiv 0$), the eigenvalues are

$$\lambda = \begin{cases} \pm \dfrac{m\omega_{A\theta}}{\sqrt{m^2+q^2r^2}} \sqrt{-4Rb - m^2 - q^2r^2}, \\ \pm im\omega_{A\theta}. \end{cases} \tag{2.27}$$

The criterion for instability is read off, from (2.27) as,

$$Rb < -\frac{m^2+q^2r^2}{4} \leq -\frac{1}{4}. \tag{2.28}$$

with the maximum value of growth rate

$$\lambda \quad = \quad |\omega_{A\theta}| \sqrt{-4Rb-1} \tag{2.29}$$

being attained at $m = \pm 1$ and $q = 0$. The instability relevant to the current-free magnetic field $\boldsymbol{B}_\theta(r) \propto 1/r$ (Rb=-1) is this mode rather than that of $k \to \infty$. The growth rate is proportional to $|\omega_{A\theta}|$.

It is instructive to look into the eigenvalues and eigenfunctions of waves, of $k \to \infty$, on a rotating flow with no external magnetic field. For a non-axisymmetric perturbation $m \neq 0$ and simultaneously in the presence of a rotational flow with angular velocity $\Omega \neq 0$, the energy principle is difficult to apply, and we appeal to the WKB method by restricting to short-wavelength perturbations. In the absence of magnetic field ($\omega_{A\theta} \equiv 0$), (2.22) has roots $\lambda_{1,2}/\Omega = -im \pm 2\alpha\sqrt{-(1+Ro)}$ and $\lambda_{3,4}/\Omega = -im$. The latter pertain to the mode characterized by the advection of the disturbance magnetic field frozen into the local rotating flow. The root $\lambda_{1,2}$ pertain to the inertial wave or the Kelvin wave [42]. Its frequency $\omega_{1,2}$ as defined by $\lambda_{1,2} = -i\omega_{1,2}$ is given by $\omega_{1,2} = m \mp 2\alpha\sqrt{1+Ro}$. This distinction between $\lambda_{1,2}$ and $\lambda_{3,4}$ manifests itself by constructing the eigenfunction $\boldsymbol{\xi}$ of (2.7). For simplicity, we take $Ro = 0$, $\alpha = 1$ and $|m| \ll |k|$. The eigenfunctions corresponding to $\lambda_{1,2} = -i(m \mp 2)$ are $\boldsymbol{\xi}_{1,2} = (\mp i, 1, 0, 0, 0, 0, 0)$, and those corresponding to $\lambda_{3,4} = -i\omega_{3,4}$ are $\boldsymbol{\xi}_3 = (0,0,0,1,0,0,0)$ and $\boldsymbol{\xi}_4 = (0,0,0,0,1,0,0)$. It is simply the disturbance magnetic

field $\xi_{3,4}$ that is advected by the fluid ($\omega_{3,4} = m$). For a uniform rotation ($Ro = 0$), the frequency $\omega_{1,2} = m \mp 2\alpha$ is confined to $-2 \leq \omega_1 \leq 0$ (upper sign) and $0 \leq \omega_2 \leq 2$ (lower sign) [41]. The parameter α plays the role of a counter for the radial nodal structure, with $|\alpha| = 1$, or $|q/k| \ll 1$, corresponding to a simple structure and with $|\alpha| \ll 1$, or $|q/k| \gg 1$, corresponding to a highly fine radial structure. The mode with eigenfrequecy ω_1, being smaller than $m\Omega$, is called the retrograde mode, while the one with eigenfrequency ω_2, being larger than $m\Omega$, is called the cograde mode [42]. Alternatively, from the viewpoint of the way approaching the limiting frequency m for $\alpha = 0$, ω_1 and ω_2 are referred to as the Sturmian and the anti-Sturmian, respectively [37]. There is no growing perturbation unless $Ro < -1$. This implies that the same criterion as Rayleigh's one for the centrifugal instability applies to the non-axisymmetric perturbations too. Fig. 2.1 depicts $\mathrm{Re}[\lambda]$ (left) and $\mathrm{Im}[\lambda] = -\omega$ (right) of the eigenvalue for the helical perturbation $m = 1$ with the simplest nodal structure $\alpha = 1$ when no external magnetic field is applied ($\omega_{A\theta} \equiv 0$).

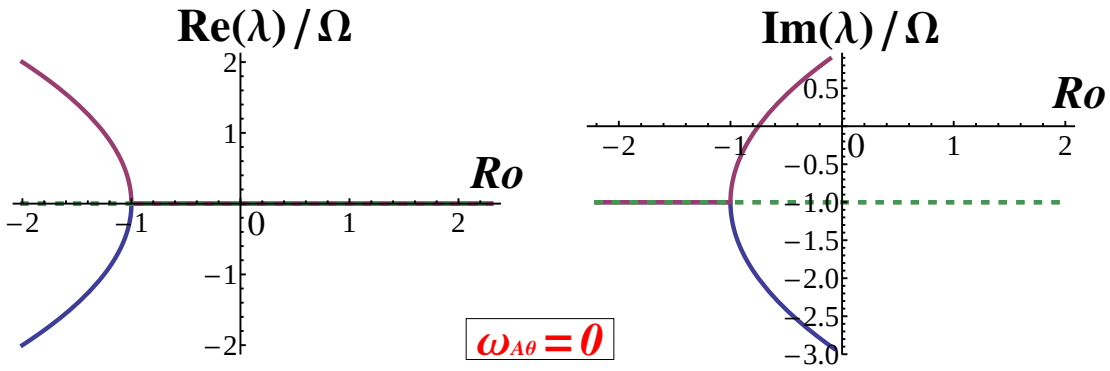

Figure 2.1: The growth rate $\mathrm{Re}[\lambda]$ (left) and the frequency $\mathrm{Im}[\lambda] = -\omega$ (right) of the perturbation of $m = 1$ and $\alpha = 1$ in the absence of the external magnetic field ($\omega_{A\theta} \equiv 0$ and consequently $Rb = 0$).

We are now ready to inquire into how a weak azimuthal magnetic field deforms the above dispersion relation. When $\omega_{A\theta} \neq 0$, but with $|\omega_{A\theta}/\Omega| \ll 1$, the expression for the eigenvalue can be expanded to second order in a small parameter $\omega_{A\theta}/\Omega$ as, unless

$|\alpha| \ll 1$,

$$\frac{\lambda_{1,2}}{\Omega} \approx \begin{cases} -im \pm 2|\alpha|\sqrt{-(1+Ro)} - \dfrac{1}{1+Ro}\left(im \pm Rb|\alpha|\sqrt{-(1+Ro)} \right. \\ \qquad \left. \pm \dfrac{m^2}{4|\alpha|}\dfrac{2+Ro}{\sqrt{-(1+Ro)}} \right)\left(\dfrac{\omega_{A\theta}}{\Omega}\right)^2 & (Ro \neq -1), \\ -im \pm \sqrt{\dfrac{2\alpha m\omega_{A\theta}}{\Omega}} + i\dfrac{\alpha\omega_{A\theta}}{\Omega} \pm \dfrac{\alpha^2 - m^2 + \alpha^2 Rb}{2\sqrt{2\alpha m}}\left(\dfrac{\omega_{A\theta}}{\Omega}\right)^{3/2} & (Ro = -1), \end{cases} \tag{2.30}$$

$$\frac{\lambda_{3,4}}{\Omega} \approx \begin{cases} -im \pm m\sqrt{\dfrac{Ro}{-(1+Ro)}}\dfrac{\omega_{A\theta}}{\Omega} + \dfrac{im}{1+Ro}\left(\dfrac{\omega_{A\theta}}{\Omega}\right)^2 & (Ro \neq -1, 0), \\ -im \pm i\sqrt{\dfrac{2\alpha m\omega_{A\theta}}{\Omega}} - i\dfrac{\alpha\omega_{A\theta}}{\Omega} \mp i\dfrac{\alpha^2 - m^2 + \alpha^2 Rb}{2\sqrt{2\alpha m}}\left(\dfrac{\omega_{A\theta}}{\Omega}\right)^{3/2} & (Ro = -1), \\ -im + m\left(i \mp \sqrt{Rb - m^2/(4\alpha^2)} \right)\left(\dfrac{\omega_{A\theta}}{\Omega}\right)^2 & (Ro = 0), \end{cases} \tag{2.31}$$

where the double-sign corresponds, and the upper sign corresponds to λ_1 and λ_3, and the lower sign corresponds to λ_2 and λ_4. For both $\lambda_{1,2}$ and $\lambda_{3,4}$, the first expansions are singular at $Ro = -1$, where a separate treatment is necessary. For the expansion at $Ro = -1$, we have ignored terms of $O\left((\omega_{A\theta}/\Omega)^2\right)$. For $\lambda_{3,4}$, the first expansion for $Ro \neq -1, 0$ of (2.31) is invalidated in the limit of $Ro \to 0$ as well, because the coefficient of the third term $(\omega_{A\theta}/\Omega)^3$ is proportional to $Ro^{-1/2}$, which diverges in the limit $Ro \to 0$. This singularity requires a separate treatment for the case of $Ro = 0$ and the resulting expression is the third expression of (2.31). The branches $\lambda_{1,2}$ of the inertial waves, subjected to the azimuthal magnetic field, are called the fast magneto-Coriolis (MC) waves. The branches $\lambda_{3,4}$ are called the slow magneto-Coriolis (MC) waves [9]. In case of $|\alpha| \ll 1$, (2.30) and (2.31) give way to

$$\frac{\lambda_{1,2}}{\Omega} \approx -im\left(1 + \frac{\omega_{A\theta}}{\Omega}\right) \pm i\left(1 + \frac{\omega_{A\theta}}{\Omega}\right)|\alpha| + O(\alpha^2), \tag{2.32}$$

$$\frac{\lambda_{3,4}}{\Omega} \approx -im\left(1 - \frac{\omega_{A\theta}}{\Omega}\right) \pm i\left(1 - \frac{\omega_{A\theta}}{\Omega}\right)|\alpha| + O(\alpha^2). \tag{2.33}$$

By applying the magnetic field, the frequency m degenerate at $\alpha = 0$ is split into $m(1 \pm \omega_{A\theta}/\Omega)$. In the limit of $|\alpha| \to 0$, the frequency defined via $\lambda_{1,2} = -i\omega_{1,2}$ of the fast MC

waves degenerate to $m(\Omega+\omega_{A\theta})$ with ω_1 (upper sign) approaching from below and ω_2 (lower sign) from above, and that of the slow MC waves, stemming from the frozen-in advection, degenerate to $m(\Omega-\omega_{A\theta})$with ω_3 (upper sign) approaching from below and ω_4 (lower sign) from above. For this reason, the fast and slow MC waves may refer to the forward and the backward modes, with the upper sign Sturmian and the lower sign anti-Sturmian [37].

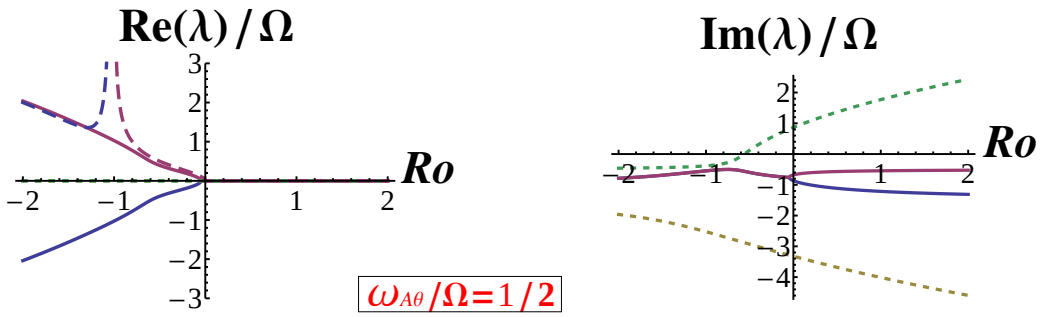

Figure 2.2: The growth rate $\mathrm{Re}[\lambda]$ (left) and the frequency $\mathrm{Im}[\lambda]=-\omega$ (right) of the perturbation of $m=1$ and $\alpha=1$ for $\omega_{A\theta}/\Omega=0.5$. The magnetic shear is $Rb=0$. The long dashed lines (left) draw the positive real part of the first of (2.30) for $Ro<-1$ and that of (2.31) for $-1<Ro<0$.

The first expansion of (2.31) suggests that the instability occurs when $Ro \lesssim 0$. This property is reminiscent of the SMRI for which the critical Rossby number (2.19) is close to but less than zero if the resistivity is zero [9]. The situation is slightly different for the AMRI. The first of (2.31) becomes invalid at $Ro=0$, to which the third expansion of (2.31) applies. The third one implies that, when $Rb>m^2/(4\alpha^2)\geq m^2/4$ by varying $|\alpha|\in(0,1]$, $Ro_c>0$, but otherwise, $Ro_c\leq 0$. In the following, we determine Ro_c

It turns out that Ro_c is very small. Near $Ro_c\approx 0$, we seek the eigenvalues of the slow MC wave in a power series in small parameter $\omega_{A\theta}/\Omega$, and, in the keeping, we represent Ro in a power series in $\omega_{A\theta}/\Omega$. The result for the slow MC wave is

$$\frac{\lambda_{3,4}}{\Omega}\approx -im+m\left(i\pm\sqrt{Rb-Ro_2-m^2/(4\alpha^2)}\right)\left(\frac{\omega_{A\theta}}{\Omega}\right)^2, \tag{2.34}$$

for $0 < |\alpha| \leq 1$ and $Ro = Ro_2 \left(\omega_{A\theta}/\Omega\right)^2 + \cdots$. It follows from (2.34) that the slow MC wave is amplified when $Ro_2 < Rb - m^2/(4\alpha^2)$. For small values of $(\omega_{A\theta}/\Omega)^2$, the AMRI is caused when approximately

$$Ro < \left(Rb - \frac{m^2}{4\alpha^2}\right)\left(\frac{\omega_{A\theta}}{\Omega}\right)^2 \leq Ro_c \approx \left(Rb - \frac{1}{4}\right)\left(\frac{\omega_{A\theta}}{\Omega}\right)^2. \tag{2.35}$$

Fig. 2.2 draws the growth rate (left) and the frequency (right) for $\omega_{A\theta}/\Omega = 0.5$. The other parameters $m = 1$, $\alpha = 1$ and $Rb = 0$ are common with Fig. 2.1. For this choice of the parameters, $Ro_c = -1/16$. It is observed that the instability is driven when the frequencies ω_3 and ω_4 of the slow MC wave (= backward wave) collide at around $\omega = m = 1$ at the critical value Ro_c. To clarify the source for the instability, the positive values of the asymptotic formulas $\mathrm{Re}[\lambda_{1,2}/\Omega]$ and $\mathrm{Re}[\lambda_{3,4}/\Omega]$ provided by the first equations of (2.30) and (2.31) respectively are superposed, with long dashed lines, on the left panel of Fig. 2.2. For $Ro > -1$, the instability originates from the slow MC waves, but, for $Ro < -1$, the dominant role in the instability is played by the fast MC waves. At the dividing point $Ro = -1$, the flow is necessarily unstable; for $\alpha m \omega_{A\theta}/\Omega > 0$, $\mathrm{Re}[\lambda_{1,2}] \neq 0$ as is seen from the second of (2.30) and the fast MC wave is amplified, but, for $\alpha m \omega_{A\theta}/\Omega < 0$, the slow MC wave is amplified, with growth rate given by $|\mathrm{Re}[\lambda_{3,4}]|$, the real part of the second of (2.31).

Here we point out that, unlike the axisymmetric SMRI, the axisymmetric AMRI is of the fast MC-wave origin. The growth rate of the axisymmetric AMRI, the left values of (2.21) in the limit of $k \to \infty$, has a link with the first of (2.30) specialized to $m = 0$. For the fast MC wave, the critical Rossby number Ro_c is close to -1 when $|\omega_{A\theta}/\Omega| \ll 1$, being in consistent with the argument of §3.2. On the contrary, the eigenvalues (2.31) of the slow MC wave become zero for $m = 0$, in agreement with the second values of (2.21), which does not contribute to the axisymmetric AMRI. For the AMRI, the slow MC wave, raising the critical value to $Ro_c \approx 0$, close to Velikhov-Chandrasekhar's value for the SMRI, is intrinsic to non-axisymmetric perturbations.

Given a small value of $|\omega_{A\theta}/\Omega|$, the maximum growth rate increases with $|m|$. Interestingly, the maximum growth rate approaches, as $|m|$ is increased, the same value as that of the SMRI. Fig. 2.3 displays the growth rate $\nu = \mathrm{Re}[\lambda_{3,4}]$ as functions of the Alfvén frequency $\omega_{A\theta}$ with azimuthal wavenumbers $m = 1$, 5 and 10 for $Ro = -3/4$ and $Rb = -1$. Since the system is Hamiltonian, to each damping perturbation ($\nu < 0$) corresponds the growing perturbation ($\nu > 0$) and therefore we display only the solution with positive real part ν. The change of the sign of Rb, namely, the choice of $Rb = 1$, does not change much the growth rate. We observe from Fig. 2.3 that, as m increases, the maximum growth rate approaches $3|\Omega|/4$, though the width of the instability band in $\omega_{A\theta}/\Omega$ is narrowed with m. This was examined by Ogilvie et al. and the maximum growth rate $3|\Omega|/4$ was also obtained [31]. Indeed, by taking $m\omega_{A\theta}^2 = 0$ and $Rb\omega_{A\theta}^2 = 0$ in (2.22) as a limit of small values of $|\omega_{A\theta}/\Omega|$ with maintaining $|m\omega_{A\theta}/\Omega|$ finite, we can show that the maximum growth rate happens to coincides with the Oort A-value $\nu_{\mathrm{A}}/|\Omega| = |Ro|$. In this limit, (2.22) is solved for $\tilde{\lambda}$, yielding

$$\frac{\lambda}{\Omega} = -im \pm \sqrt{\alpha^2 Ro^2 - \left(\sqrt{\left(m\frac{\omega_{A\theta}}{\Omega}\right)^2 + \alpha^2(1+Ro)^2} \mp \alpha\right)^2}. \tag{2.36}$$

The growth rate $\nu = |\mathrm{Re}[\lambda]|$ takes the maximum value close to $|\alpha Ro|$ when $\sqrt{(m\omega_{A\theta}/\Omega)^2 + \alpha^2(1+Ro)^2} = |\alpha|$, or at $m \approx \pm(\Omega/\omega_{A\theta})\alpha\sqrt{1-(1+Ro)^2}$. Actually m should be an integer closest to the right hand side. By varying α, the maximum value among the above is close to the Oort A-value $\nu_{\mathrm{A}}/|\Omega| = |Ro|$ at $\alpha = \pm 1$ [22]. The instability window is found from (2.36) as $\alpha^2 Ro^2 > (\sqrt{(m\omega_{A\theta}/\Omega)^2 + \alpha^2(1+Ro)^2} - |\alpha|)^2$. The instability takes place for $0 < |\omega_{A\theta}/\Omega| < 2\sqrt{|\alpha Ro|}/|m|$, whose upper bound $2\sqrt{|Ro|}/|m|$ is reached at $|\alpha| = 1$, The width of the instability band is narrowed with $|m|$ in inversely proportional to $|m|$ as is confirmed from Fig. 2.3.

The AMRI shares common features with the SMRI that the instability occurs for $Ro < Ro_c \approx 0$ no matter how weak the external magnetic field may be, when it is applied,

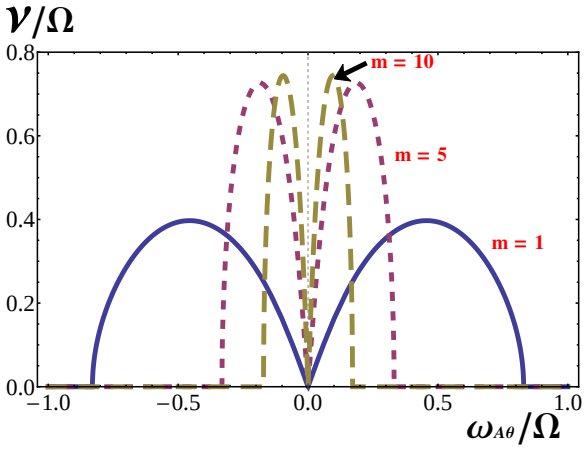

Figure 2.3: The growth rate, in the limit $k \to \infty$ with fixing $\alpha = 1$, of the non-axisymmetric AMRI versus $\omega_{A\theta}/\Omega$, in the range of small values, for different azimuthal wavenumbers $m = 1$ (solid line), 5 (dashed line) and 10 (long dashed line) for $Ro = -3/4$, a Keplerian rotation. The magnetic Rossby number is $Rb = -1$.

and the maximum growth rate is $|Ro|$, regardless of strength of the external field. This resemblance holds true as far as $|\omega_{A\theta}/\Omega| \ll 1$. However, a distinctive behavior manifests itself when the azimuthal magnetic field B_θ is intensified to the level $|\omega_{A\theta}/\Omega| = O(1)$ as will be described in the subsequent section.

2.4 Non-axisymmetric perturbations: strong external field

This section is concerned with the case of $|\omega_{A\theta}/\Omega| \sim 1$. A purely magnetic instability of $|k| \to \infty$ is excited when $Rb > -3/4$. The both cases $Ro < 0$ and $Ro \geq 0$ entail this instability, or, put another way, there is no critical Rossby number. But this mode subsides down as Rb is decreased and dies down at $Rb = -3/4$. Another unstable mode of $k = 0$ is born at $Rb = -1/4$, develops as Rb is decreased, and surpasses the mode of $|k| \to \infty$ for $Rb \leq -1/\sqrt{8}$. The instability mode of $k = 0$ is confined to a finite range in Ro centered on $Ro = 0$, $Ro^2 < (|Rb| - 1/4)(\omega_{A\theta}/\Omega)^2$ for $-1/2 \leq Rb < -1/4$, and $Ro^2 < Rb^2(\omega_{A\theta}/\Omega)^2$ for $Rb < -1/2$. We should keep in mind the results of the previous section that, for small value of $|\omega_{A\theta}/\Omega|$, the unstable mode of $|k| \to \infty$ prevails for the entire range of Rb, though

restricted to $Ro < Ro_c$, with Ro_c depending on Rb as given by (2.35).

The numerical calculation for $m = 1$, for instance, shows that, for $Rb > 0$, the maximum growth rate is taken in the limit of $k \to \infty$ and that the maximum value overshoots the Oort A-value $\nu_{\rm A}$ when $|\omega_{a\theta}|$ and Rb are increased. In the limit of $k \to \infty$ with fixing α, the asymptotics of the growth rate for $|\omega_{A\theta}/\Omega| \gg 1$ is deduced with ease by manipulating the expansion of (2.22) in $\Omega/\omega_{A\theta}$, up to $O(1)$, as

$$\frac{\lambda_{1,2}}{\Omega} \approx \pm\sqrt{2\alpha^2 Rb - m^2 + 2|\alpha|\sqrt{m^2+\alpha^2 Rb^2}}\,\frac{\omega_{A\theta}}{\Omega} - im\left(1 - \frac{|\alpha|}{\sqrt{m^2+\alpha^2 Rb^2}}\right) \quad (2.37)$$

$$\frac{\lambda_{3,4}}{\Omega} \approx \pm\sqrt{2\alpha^2 Rb - m^2 - 2|\alpha|\sqrt{m^2+\alpha^2 Rb^2}}\,\frac{\omega_{A\theta}}{\Omega} - im\left(1 + \frac{|\alpha|}{\sqrt{m^2+\alpha^2 Rb^2}}\right) \quad (2.38)$$

The parameter Ro resides only in higher-order terms in $\Omega/\omega_{A\theta}$. The both sides of $Ro < 0$ and $Ro \geq 0$ entail the instability, as opposed the case of small values of $|\omega_{A\theta}/\Omega|$. When $Rb > 0$, (2.37) and (2.38) are reduced, if specialized to $m = 0$, to the large $\omega_{A\theta}/|\Omega|$ asymptotics of the left and the right of (2.21). Unlike the case of $|\omega_{A\theta}/\Omega| \ll 1$, the unstable mode is necessarily the fast MC wave ($\lambda_{1,2}$) regardless of the value of Ro. When $Rb < 0$, the roles of $\lambda_{1,2}$ and $\lambda_{3,4}$ are exchanged. The growth rate is proportional to $\omega_{A\theta}/\Omega$. The maximum value of the growth rate $\nu_{1,2} = \mathrm{Re}[\lambda_{1,2}]$ with respect to m and α is evaluated by rewriting (2.37) into

$$\frac{\nu_{1,2}}{\Omega} \approx \pm\sqrt{\alpha^2(Rb+1)^2 - \left(\sqrt{m^2+\alpha^2 Rb^2} - |\alpha|\right)^2}\,\frac{\omega_{A\theta}}{\Omega}. \quad (2.39)$$

For an integer m and $0 < |\alpha| \leq 1$, this is real when $Rb \geq m^2/(4\alpha^2) - 1 \geq -3/4$ ($m \neq 0$) and $Rb \geq 0$ ($m = 0$). The maximum value is taken at $|\alpha| = 1$, and at $m = 0$ for $Rb \geq 3/4$, but at $|m| = 1$ for $-3/4 < Rb < 3/4$, with the maximum values

$$\frac{\nu_{\max}}{\Omega} \approx \begin{cases} 2\sqrt{Rb}\,|\omega_{A\theta}/\Omega| & (Rb \geq 3/4), \\ \sqrt{2Rb - 1 + 2\sqrt{1+Rb^2}}\,|\omega_{A\theta}/\Omega| & (-3/4 < Rb < 3/4). \end{cases} \quad (2.40)$$

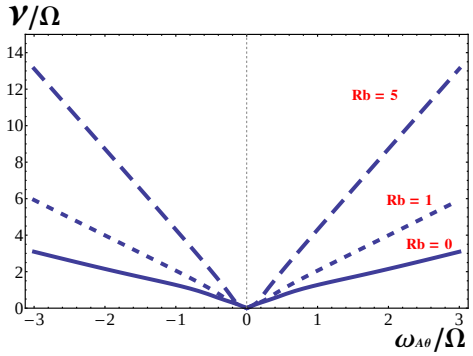

Figure 2.4: The growth rate, for $m = 1$ and $k \to \infty$ with fixing $\alpha = 1$, of the non-axisymmetric AMRI over a wide range of $\omega_{A\theta}/\Omega$ for negative $Ro = -3/4$ and different non-negative magnetic Rossby numbers Rb: $Rb = 0$ (solid line), 1 (dashed line) and 5 (long dashed line).

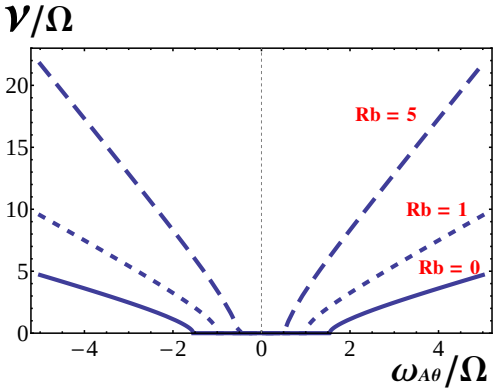

Figure 2.5: The growth rate, for $m = 1$ and $k \to \infty$, of the non-axisymmetric AMRI over a wide range of $\omega_{A\theta}/\Omega$ for positive $Ro = 1$ and different non-negative Rb: $Rb = 0$ (solid line), 1 (dashed line), 5 (long dashed line).

This value decreases to zero as Rb decreases to $-3/4$.

Fig. 2.4 shows the growth rate, for $m = 1$ in the limit of $k \to \infty$, over a wide range of the Alfvén frequency $\omega_{A\theta}/\Omega$ and for typical values of Rb ($= 0,\ 1,\ 5$) in the range of $Rb > -3/4$. The flow is Keplerian ($Ro < 0$). Fig. 2.5 is the counterpart for positive $Ro(= 1)$. The difference lies in the neighborhood of the origin $(\omega_{A\theta}/\Omega, \nu/\Omega) = (0,0)$. The critical condition (2.35), if rearranged, implies that, for $Rb > 1/4$, the unstable mode of $|k| \to \infty$ is excited for $(\omega_{A\theta}/\Omega)^2 > Ro/(Rb - 1/4)$, though the validity is limited to $|\omega_{A\theta}/\Omega| \ll 1$. Fig. 2.5 for $Ro > 0$ exhibits the disappearance of instability in a finite range in $|\omega_{A\theta}/\Omega|$, being wider for a smaller value of Rb ($> 1/4$). For instance, the $k \to \infty$ mode arises at $\omega_{A\theta}/\Omega \approx 0.48$ for $Ro = 1$ and $Rb = 5$, for which $\sqrt{Ro/(Rb - 1/4)} \approx 0.4588$.

An unstable mode of the other extreme $k \to 0$ is seeded at $Rb = -1/4$, is strengthened and becomes dominant as Rb is decreased on the side of $Rb < 0$ and $|\omega_{A\theta}/\Omega| \sim 1$. In this limit, the dispersion relation (2.16) admits its roots in a tidy form as

$$\begin{aligned} \frac{\lambda}{\Omega} &= \frac{-im(m^2 + q^2r^2 + 2Ro) \pm m\sqrt{(-4Rb - m^2 - q^2r^2)(m^2 + q^2r^2)(\omega_{A\theta}/\Omega)^2 - 4Ro^2}}{m^2 + q^2r^2}, \\ \frac{\lambda}{\Omega} &= -im\left(1 \pm \frac{\omega_{A\theta}}{\Omega}\right). \end{aligned} \tag{2.41}$$

The instability is driven on the side of $-4Rb - m^2 - q^2r^2 > 0$ with $m \neq 0$, namely, $Rb < -(m^2+q^2r^2)/4 \leq -1/4$. The possible real part ν of the first of (2.41) reads

$$\frac{\nu}{\Omega} = \pm\frac{m}{m^2+q^2r^2}\sqrt{[4Rb^2-(m^2+q^2r^2+2Rb)^2]\left(\frac{\omega_{A\theta}}{\Omega}\right)^2-4Ro^2}. \quad (2.42)$$

It follows from (2.42) that the sign of Ro is irrelevant to the growth rate, The instability occurs in a finite range in Ro centered on $Ro = 0$. Noting that the realizability of $m^2+q^2r^2+2Rb = 0$ for $m \neq 0$ is confined to $Rb \leq -1/2$, the maximum width of the instability band is obtained, for $-1/2 \leq Rb < -1/4$, by taking $|m| = 1$ and $q = 0$, with the instability range $Ro^2 < (|Rb|-1/4)(\omega_{A\theta}/\Omega)^2$. For $Rb < -1/2$, the instability range is $Ro^2 < Rb^2(\omega_{A\theta}/\Omega)^2$, and the large-magnetic-field asymptotics of the growth rate ν is obtained from (2.42) as

$$\frac{\nu}{\Omega} \approx \sqrt{\frac{4|Rb|}{m^2+q^2r^2}-1}\left|\frac{m\omega_{A\theta}}{\Omega}\right| \leq \sqrt{4|Rb|-1}\left|\frac{\omega_{A\theta}}{\Omega}\right|, \quad (2.43)$$

with the upper bound taken at $q = 0$ and $|m| = 1$. Comparison with (2.40) shows that the instability mode of $k = 0$ prevails over that of $|k| \to \infty$ for approximately $Rb \leq -1/\sqrt{8}$.

The condition $1 \leq m^2+q^2r^2 < -4Rb$, under restriction of $m \neq 0$, for existence of the unstable mode of $k = 0$ signifies that the value of $|Rb|$ limits the range of $|m|$ for instability. For instance, $Rb = -1$ admits only $m = \pm 1$ for instability. To have an idea of the instability parameters for the case of $Rb < -1/4$ and $|\omega_{A\theta}/\Omega| \sim 1$, we draw in Fig. 2.6 the instability region, in the space of (m, Ro), of the $k = 0$ wave, for a Keplerian flow ($Ro = -3/4$). The left panel of Fig. 2.6 fixes $Rb = -1$ and varies the values of $|\omega_{A\theta}/\Omega|$. The right panel fixes $|\omega_{A\theta}/\Omega| = 1$ and varies the values of Rb. The gray region indicates the set of parameters for which the AMRI occurs, painted with darker gray as the parameter value is increased. Fig. 2.6 shows that the increase of $|\omega_{A\theta}(r)/\Omega|$ and/or $|Rb|$ enlarges the instability range in Ro, though limited the case of $Rb < -1/4$ with $|\omega_{A\theta}/\Omega| \sim 1$. The left figure confirms that Rb determines the range of azimuthal

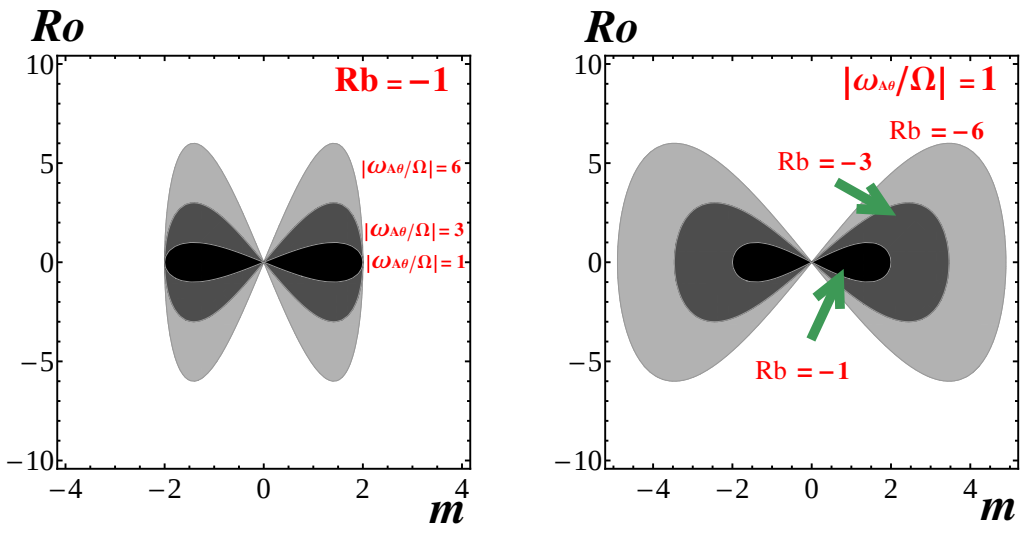

Figure 2.6: The instability region of the non-axisymmetric wave of $k = 0$ for $Rb < -1/4$. The flow is Keplerian ($Ro = -3/4$). The left figure fixes $Rb = -1$ and depicts the instability region with increasing $|\omega_{A\theta}(r)/\Omega|$ from dark gray to light gray. The right figure fixes $|\omega_{A\theta}(r)/\Omega| = 1$ and depicts the instability region with increasing $|Rb|$ from dark gray to light gray.

wavenumber m for the instability. The right figure shows that increases in $|Rb|$ results in widening of the instability range both in Ro and m.

For $Rb \geq -1/\sqrt{8}$, the shortest waves ($k \to \infty$) dominate over the long waves ($k = 0$) for $|\omega_{A\theta}/\Omega| \sim 1$, and the transition of behavior from the regime of $|\omega_{A\theta}/\Omega| \ll 1$ to the regime $|\omega_{A\theta}/\Omega| \sim 1$ is displayed in a single figure Fig. 2.4 for the case of $Ro \leq 0$ and in Fig. 2.5 for the case of $Ro > 0$. A distinctive feature of Fig. 2.5 arises around the origin $(\omega_{A\theta}/\Omega, \nu/\Omega) = (0,0)$, where the instability disappears in a finite range of $\omega_{A\theta}/\Omega$ with its width depending on Rb. Notably, the maximum growth rate increases, beyond the Oort A-value, indefinitely with $|\omega_{A\theta}/\Omega|$ linearly in it.

On the other hand, a smooth transition may not be expected from the regime of $|\omega_{A\theta}/\Omega| \ll 1$ to that of $|\omega_{A\theta}/\Omega| \sim 1$, when $Rb < -1/\sqrt{8}$, because the maximum growth rate occurs in the short-wave limit ($k \to \infty$) for $|\omega_{A\theta}/\Omega| \ll 1$, but in the long-wave limit for $|\omega_{A\theta}/\Omega| \sim 1$. With a choice of $Ro = -3/4$ and $Rb = -1/2$, Fig. 2.7 draws the

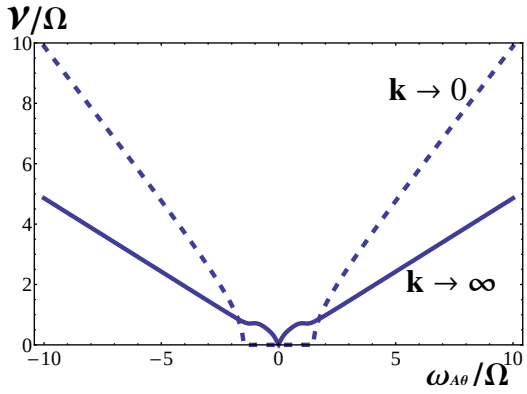

Figure 2.7: The crossover of the most unstable mode of $m = 1$ from the regime of $|\omega_{A\theta}/\Omega| \ll 1$ to that of $|\omega_{A\theta}/\Omega| \sim 1$ in the case of $Rb = -1/2$. The maximum growth rates occurs at $k \to \infty$ (solid line) in the former regime but at $k = 0$ in the latter (dashed line), and they are simultaneously drawn as a function of $\omega_{A\theta}/\Omega$. The flow is Keplerian ($Ro = -3/4$). In the both limits, the maxima are taken at $|\alpha| = 1$.

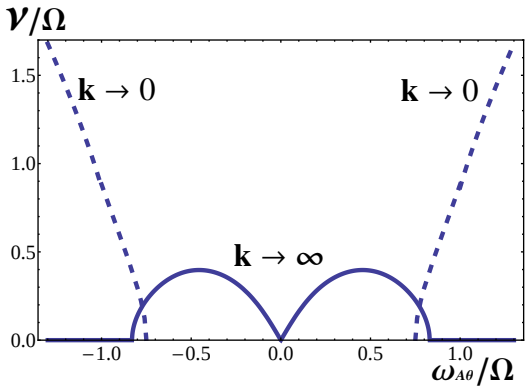

Figure 2.8: The crossover of the most unstable mode of $m = 1$ from the regime of $|\omega_{A\theta}/\Omega| \ll 1$ to that of $|\omega_{A\theta}/\Omega| \sim 1$ in the case of $Rb = -1$ for a Keplerian flow ($Ro = -3/4$). For the limit of $k = 0$, $|qr| = 1$ at the critical point $\omega_{A\theta}/\Omega = 3/4$ and $|qr|$ decreases, with $\omega_{A\theta}/\Omega$, to zero along the graph.

maximum growth rate of $m = 1$ mode, in the limit of $k \to \infty$ and in the opposite limit $k \to 0$ simultaneously. For the former, the maximum occurs at $|\alpha| = 1$ and for the latter, the maximum occurs at $q = 0$, being mathematically equivalent to each other. As argued above, because $Rb < -1/\sqrt{8}$, the mode of $k \to 0$ overweighs that of $k \to \infty$ in the regime of $|\omega_{A\theta}/\Omega| \sim 1$. The maximum growth rate of the former increases without bound in proportion to $|\omega_{A\theta}/\Omega|$. The instability mode of $k = 0$, being admitted only for $|\omega_{A\theta}/\Omega| > |Ro/Rb| = |Ro|/\sqrt{|Rb| - 1/4} = 3/2$ when $Rb = -1/2$, is excluded in the regimes of $|\omega_{A\theta}/\Omega| \ll 1$

Fig. 2.8 chooses $Rb = -1$, with the other parameters being unchanged. The regime $|\omega_{A\theta}/\Omega| \ll 1$ accommodates the instability modes of $|k| \to \infty$ with $|m| \geq 2$ as well with the overall maximum growth rate being close to the Oort A-value, as illustrated by Fig. 2.3. In the regime $|\omega_{A\theta}/\Omega| \sim 1$, the instability mode of $k \to \infty$ disappears because $Rb \leq -3/4$. The maximum growth rate for $k \to \infty$ corresponds to $|\alpha| = 1$. But this is not the case

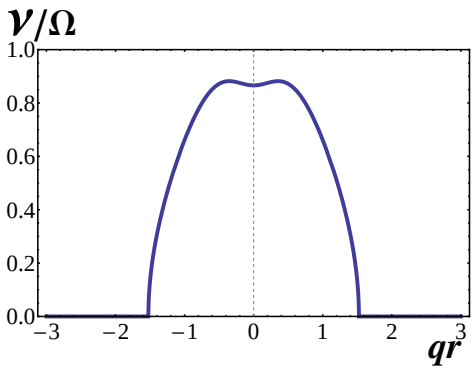

Figure 2.9: The growth rate of the non-axisymmetric wave of $m = 1$ and $k \to 0$, versus qr with q being the radial wavenumber, for $Rb = -1$ and $\omega_{A\theta}/\Omega = 1$. The flow is Keplerian ($Ro = -3/4$). The maximum growth rate is $\nu_{max} = \sqrt{7}\Omega/3$ taken at $qr = \pm 1/\sqrt{8}$.

with the wave of $k = 0$. Near the critical point $|\omega_{A\theta}/\Omega| = |Ro/Rb| = 3/4$, the most unstable mode has $|qr| = 1$ in favor of $m^2 + q^2r^2 + 2Rb = 0$. As $|\omega_{A\theta}/\Omega|$ is increased, $|qr|$ decreases monotonically to zero as is seen from (2.43). In between, the maximum is taken at an intermediate value of qr. On the whole, for $|\omega_{A\theta}/\Omega| \gtrsim 0.8$ approximately, the mode of $k = 0$ prevails over that of $k \to \infty$.

For $Ro = -3/4$ and $Rb = -1$, we draw in Fig. 2.9 the growth rate ν as a function of the radial wavenumber qr. The maximum growth rate is found with ease to be $\nu_{\max}/|\Omega| = \sqrt{7}/3$ which is attained at $q = 1/\sqrt{8}$. This value is larger than the Oort A-value $\nu_{\rm A}/|\Omega| = 3/4$.

2.5 Discussions

We have explored the AMRI of a perfectly conducting fluid to non-axisymmetric as well as axisymmetric perturbations of short wavelengths, based on the Hain-Lüst equation (2.15) augmented with the terms originating from a background flow of differential rotation. The present investigation is capable of dealing with a rotating flow of arbitrary angular velocity profile $\Omega(r)$. The advantage of using the Hain-Lüst equation is that a risk of dropping-off the terms with radial derivatives can be avoided. If we substitute

the WKB ansatz $\xi \propto \exp[i\int q(r)\mathrm{d}r]$, at an earlier stage, into (2.7) say, the derivative in r is replaced by multiplication iq, and after this stage, the operation of radial derivative $iq = \mathrm{d}/\mathrm{d}r$ is liable to be inactive, though it should be. It is safer to keep all the derivative terms to the very last stage where we apply the short wavelength approximation. Retaining all the relevant terms has disclosed rich aspects of the AMRI to non-axisymmetric perturbations than known ones (*cf.* ref [15]).

Given Rb, for small values of $|\omega_{A\theta}/\Omega|$, a rotating flow is unstable to non-axisymmetric perturbations of $|k| \to \infty$ if $Ro < (Rb - 1/4)(\omega_{A\theta}/\Omega)^2$ as dictated by (2.35). It is recovered that the maximum growth rate is the Oort A-value $|Ro|$ [31]. For $|\omega_{A\theta}/\Omega| \sim 1$, the situation is changed. When $Rb > -3/4$, the rotating flow is unstable to perturbations of $|k| \to \infty$ in the whole range of Ro. But the mode of $|k| \to \infty$ subsides down as Rb is decreased and disappears at $Rb = -3/4$. Another unstable mode of $k = 0$ emerges at $Rb = -1/4$, develops as Rb is decreased, and surpasses the mode of $|k| \to \infty$ for $Rb \leq -1/\sqrt{8}$. The instability mode of $k = 0$ is confined to a finite range in Ro centered on $Ro = 0$, $Ro^2 < (|Rb| - 1/4)(\omega_{A\theta}/\Omega)^2$ for $-1/2 \leq Rb < -1/4$, and $Ro^2 < Rb^2(\omega_{A\theta}/\Omega)^2$ for $Rb < -1/2$, as is derived from (2.42). The behavior, over the whole range of $\omega_{A\theta}/\Omega$, of the modes of $m = 1$ and $|k| \to \infty$ and of $m = 1$ and $k = 0$ is summarized as follows. For $Ro < 0$ and $Rb < -3/4$, the mode of $|k| \to \infty$ is confined approximately to $0 < |\omega_{A\theta}/\Omega| < \sqrt{|Ro|/(|Rb| + 1/4)}$ as is read off from (2.35). The unstable mode of $k = 0$ exists for $|\omega_{A\theta}/\Omega| > |Ro/Rb|$ when $Ro < -1/2$, and for $|\omega_{A\theta}/\Omega| > |Ro|/\sqrt{|Rb| - 1/4}$ when $-1/2 \leq Ro < -1/4$. The overall behavior for $Ro < 0$ and $Rb < -3/4$ looks like Fig. 2.8. For $Rb > -3/4$, the mode of $|k| \to \infty$ extends to the entire range of $\omega_{A\theta}/\Omega$, and for $-3/4 < Rb < -1/\sqrt{8}$, the graph looks like Fig. 2.7. For $Ro < 0$ and $Rb > -1/\sqrt{8}$, the mode of $|k| \to \infty$ predominates over the mode of $k = 0$ over the entire range of $\omega_{A\theta}/\Omega$. For $Rb \geq -1/4$, the mode of $k = 0$ disappears. The asymptotic behavior at large values of $|\omega_{A\theta}/\Omega|$ is common for all values of Ro and is given by (2.40). At small values of $|\omega_{A\theta}/\Omega|$, the mode of $|k| \to \infty$ is confined to $0 < |\omega_{A\theta}/\Omega| < \sqrt{|Ro/(Rb - 1/4)|}$ for

$-1/4 < Rb < 1/4$ and $Ro < 0$. This branch is absent for $Ro \geq 0$. For $Rb > 1/4$, this branch exists for $|\omega_{A\theta}/\Omega| > \sqrt{Ro/(Rb-1/4)}$. As a whole, for $Rb > -1/4$, the graph looks like Fig. 2.4 for $Ro < 0$ and like Fig. 2.5 for $Ro > 0$. It is remarkable that the growth rate exceed the Oort A-value by increasing $|\omega_{A\theta}/\Omega|$.

This is not the end of story. We have exclusively explored the unstable modes in the two extremes, $|k| \to \infty$ and $k = 0$, as either of the two is likely to be dominant. However, a detailed examination shows that there are cases that, given Ro and Rb, the mode of the largest growth rate occurs at an intermediate value of k. For instance, given a Keplerian rotation ($Ro = -3/4$), for $|\omega_{A\theta}/\Omega| \ll 1$ and fixing $m = 1$ and $q = 0$, the most unstable mode occurs at an intermediate value of k when $Rb \lesssim -17.5$. Furthermore, the transition of the behavior from $|\omega_{A\theta}/\Omega| \ll 1$ to that of $|\omega_{A\theta}/\Omega| \sim 1$ calls for elaboration.

It is probable that these properties, in particular, non-existence of critical Rossby number for large values of Rb ($Rb > -3/4$ for the AMRI) may carry over to the helical MRI (HMRI) for which the both axial and azimuthal magnetic fields are externally imposed. From the practical view point, the inductionless limit is worth pursuing, since the laboratory experiments of using a liquid metal, such as PROMISE (Potsdam ROssendorf Magnetic InStability Experiment) [34], belongs to this regime. From previous papers on AMRI [26] and HMRI [32] in the inductionless limit, the condition for non-existence of critical Rossby number is obtained to be $Rb > -1/2$.

Care should be excised for the most unstable mode of $k = 0$ and $q = 0$ which is dominant $|\omega_{A\theta}/\Omega| \sim 1$ for $Rb < -1/\sqrt{8}$. This mode may lie outside the range of validity of the WKB approximation to short-wavelength waves. Moreover, the perturbation of large m invites the action of the viscous and/or resistive cut off. To draw a definite conclusion on the AMRI or HMRI to non-axisymmetric perturbations, the global modal analyses are indispensable. For the purpose of the global stability analyses as well, the Hain-Lüst equation provides us with a sound basis [40]. The determination of the maximum growth rate for the AMRI and the HMRI is left for a future investigation.

Chapter 3

Short-wavelength stability analysis of AMRI in resistive MHD

3.1 Equations and short wavelength approximation

We consider a circular symmetric rotating flow of an incompressible viscous fluid with finite electric conductivity, and its linear stability to localized disturbance of three dimensions, along one of the streamlines, when a steady azimuthal magnetic field $B_\theta(r) = r\mu(r)$ is applied. In chapter 2 and a companion paper[23], we dealt with a steady rotating flow of an incompressible inviscid fluid with infinite electric conductivity, subjected to the same magnetic field. We assume that the radial wavelength is much shorter than the radius of the circular streamline, a setting to which the WKB approximation is applicable. We employ the global cylindrical coordinates (r, θ, z) with the z-axis lying on the symmetric axis. The basic state is a rotating flow in equilibrium, with the angular velocity $\Omega(r)$ of the basic flow $\boldsymbol{U}$, applied by a steady magnetic field $\boldsymbol{B}$ with the azimuthal and the axial components $r\mu(r)$ and $B_z(r)$, respectively. Later in §3.3, we focus on the former field.

$$\boldsymbol{U} = r\Omega(r)\boldsymbol{e}_\theta, \ \boldsymbol{B} = r\mu(r)\boldsymbol{e}_\theta + B_z\boldsymbol{e}_z, \tag{3.1}$$

where e_θ is the unit vector in the azimuthal direction, and the axial magnetic field B_z is assumed to be constant.

The Navier-Stokes equation and induction equation, the equations for incompressibility assumption and the solenoidal property of the magnetic field are

$$\frac{\partial \boldsymbol{u}}{\partial t} + (\boldsymbol{u}\cdot\nabla)\boldsymbol{u} = -\frac{1}{\rho}\nabla P + \frac{1}{\rho\mu_0}(\boldsymbol{b}\cdot\nabla\boldsymbol{b}) + \nu\nabla^2\boldsymbol{u}, \tag{3.2}$$

$$\frac{\partial}{\partial t} = \nabla\times(\boldsymbol{u}\times\boldsymbol{b}) + \eta\nabla^2\boldsymbol{b}, \tag{3.3}$$

$$\nabla\cdot\boldsymbol{u} = 0, \tag{3.4}$$

$$\nabla\cdot\boldsymbol{b} = 0, \tag{3.5}$$

where $\boldsymbol{u}$ is the velocity field, $\boldsymbol{b}$ is the magnetic field, ρ is density, $p = p_0 + \boldsymbol{b}^2/(2\mu_0)$ is the total pressure consisting the hydrodynamic pressure p_0 and the magnetic pressure $\boldsymbol{b}^2/(2\mu_0)$, and $\mu_0,\ \nu$ and η represent the magnetic permeability, the kinematic viscosity and the electrical resistivity, respectively. We assume that $\rho,\ \mu_0,\ \nu,\ \eta$ are all constant[26]. The velocity, the magnetic and the total pressure fields are partioned into the steady flow, being assumed to be steady, and the disturbance as

$$\boldsymbol{u} = \boldsymbol{U} + \tilde{\boldsymbol{u}},\ \boldsymbol{b} = \boldsymbol{B} + \tilde{\boldsymbol{b}},\ \boldsymbol{p} = P + \tilde{p}. \tag{3.6}$$

The Navier-Stokes and the induction equations linearized in the disturbance are

$$\frac{\partial \tilde{\boldsymbol{u}}}{\partial t} + (\tilde{\boldsymbol{u}}\cdot\nabla)\boldsymbol{U} + (\boldsymbol{U}\cdot\nabla)\tilde{\boldsymbol{u}} = -\frac{1}{\rho}\nabla\tilde{p} + \frac{1}{\rho\mu_0}(\boldsymbol{B}\cdot\nabla)\tilde{\boldsymbol{b}} + \frac{1}{\rho\mu_0}(\tilde{\boldsymbol{b}}\cdot\nabla)\boldsymbol{B} + \nu\nabla^2\tilde{\boldsymbol{u}}, \tag{3.7}$$

$$\frac{\partial \tilde{\boldsymbol{b}}}{\partial t} = \nabla\times(\boldsymbol{u}\times\tilde{\boldsymbol{b}}) + \nabla\times(\tilde{\boldsymbol{u}}\times\boldsymbol{B}) + \eta\nabla^2\tilde{\boldsymbol{b}}, \tag{3.8}$$

$$\nabla\cdot\tilde{\boldsymbol{u}} = 0, \tag{3.9}$$

$$\nabla\cdot\tilde{\boldsymbol{b}} = 0.. \tag{3.10}$$

Owing to the steadiness and to the symmetries with respect to translation along and ro-

tation about the z-axis, we may pose the disturbances in the normal-mode form $\exp[\lambda t + i(m\theta + kz)]$. The azimuthal wavenumber m takes an integer and the axial wavenumber k is taken to be a real number. The remaining task is to determine the radial dependence. Substitution of this normal-mode form into (3.7)–(3.10) yields a coupled system of 8 ordinary differential equations, with r independent variable. The viscous and the resistive terms stand as obstacles to carry through the stability analysis. With a view to incorporate only the leading-order effect of short-wave disturbances under the assumption of ν and η being small, we may simply replace $-\nabla^2$ by $|\boldsymbol{k}|^2 = k^2 + q^2 + m^2/r^2$ with an introduction of the radial wavenumber $q(r)$. This procedure amounts to discarding the terms including the derivative of $q(r)$ and m/r, and should be justified *a posteriori*. The resulting equations are combined into matrix form for $\boldsymbol{\xi} = (\tilde{u_r},\ \tilde{u_\theta},\ \tilde{u_z},\ \tilde{b_r},\ \tilde{b_\theta},\ \tilde{B_z},\ \tilde{p})$ as

$$\mathsf{M}\boldsymbol{\xi} = 0, \tag{3.11}$$

where

$$\mathsf{M} = \begin{pmatrix}
\tilde{\lambda}_\nu & -2\Omega & 0 & -\dfrac{iF}{\rho\mu_0} & \dfrac{2\mu}{\rho\mu_0} & 0 & \dfrac{1}{\rho}\dfrac{d}{dr} \\
2\Omega + r\dfrac{d\Omega}{dr} & \tilde{\lambda}_\nu & 0 & -(2\mu + r\dfrac{d\mu}{dr}) & -\dfrac{iF}{\rho\mu_0} & 0 & \dfrac{1}{r\rho}im \\
0 & 0 & \tilde{\lambda}_\nu & 0 & 0 & -\dfrac{iF}{\rho\mu_0} & \dfrac{1}{\rho}ik \\
-iF & 0 & 0 & \tilde{\lambda}_\eta & 0 & 0 & 0 \\
r\dfrac{d\mu}{dr} & -iF & 0 & -r\dfrac{d\Omega}{dr} & \tilde{\lambda}_\eta & 0 & 0 \\
0 & 0 & -iF & 0 & 0 & \tilde{\lambda}_\eta & 0 \\
\dfrac{1}{r} + \dfrac{d}{dr} & \dfrac{im}{r} & ik & 0 & 0 & 0 & 0 \\
0 & 0 & 0 & \dfrac{1}{r} + \dfrac{d}{dr} & \dfrac{im}{r} & ik & 0
\end{pmatrix}, \tag{3.12}$$

where $\omega_\nu = |\boldsymbol{k}|^2\nu$ and $\omega_\eta = |\boldsymbol{k}|^2\eta$, $\tilde{\lambda}_\nu = \lambda + im\Omega + \omega_\nu$, $\tilde{\lambda}_\eta = \lambda + im\Omega + \omega_\eta$ and $F =$

$m\mu + B_z k$. By the 4th to 6th equations in (3.11), the magnetic field disturbance $\tilde{b_r}$, $\tilde{b_\theta}$ and $\tilde{b_z}$ can be expressed in terms of the other variables. As a consequence, by eliminating the magnetic-field disturbance, we can reduce (3.11) to equations for $\boldsymbol{\xi_1} = (\tilde{u_r}, \tilde{u_\theta}, \tilde{u_z}, \tilde{p})$ asas

$$\mathsf{M}_1 \boldsymbol{\xi}_1 = 0, \tag{3.13}$$

where

$$\mathsf{M}_1 = \tag{3.14}$$
$$\begin{pmatrix} \Lambda + \dfrac{2\mu r}{\rho\mu_0\tilde{\lambda}_\eta}\left(\dfrac{iF}{\tilde{\lambda}_\eta}\dfrac{\mathrm{d}\Omega}{\mathrm{d}r}\right) - \dfrac{\mathrm{d}\mu}{\mathrm{d}r} & -2\Omega + \dfrac{2iF\mu}{\rho\mu_0\tilde{\lambda}_\eta} & 0 & \dfrac{1}{\rho}\dfrac{\mathrm{d}}{\mathrm{d}r} \\ 2\Omega + r\dfrac{\mathrm{d}\Omega}{\mathrm{d}r}\left(1 + \dfrac{F^2}{\rho\mu_0\tilde{\lambda}_\eta^2}\right) - \dfrac{2iF\mu}{\rho\mu_0\tilde{\lambda}_\eta} & \Lambda & 0 & \dfrac{1}{r\rho}im \\ 0 & 0 & \Lambda & \dfrac{1}{\rho}ik \\ \dfrac{1}{r} + \dfrac{\mathrm{d}}{\mathrm{d}r} & \dfrac{im}{r} & ik & 0 \end{pmatrix},$$

where we have introduced the notation $\Lambda = \tilde{\lambda}_\nu + F^2/\tilde{\lambda}_\eta$ to simplify the expressions.

We then embark on combining all the equations into a single second-order differential equation for the radial component of the Lagrangian displacement field. As an intermediate step, we solve algebraic equations (3.13) and express $(\tilde{u_r}, \tilde{u_\theta}, \tilde{u_z})$ in terms of $\tilde{p}$ as

$$\begin{aligned} \tilde{u_r} &= -\frac{\Lambda}{E\rho}\frac{\mathrm{d}\tilde{p}}{\mathrm{d}r} + \frac{im}{E\rho r}\left(\frac{2iF\mu}{\tilde{\lambda}_\eta\rho\mu_0} - 2\Omega\right)\tilde{p}, \\ \tilde{u_\theta} &= \frac{1}{E\rho}\left[2\Omega + r\frac{\mathrm{d}\Omega}{\mathrm{d}r}\left(1 + \frac{F^2}{\rho\mu_0\tilde{\lambda}_\eta^2}\right) - \frac{2iF\mu}{\rho\mu_0\tilde{\lambda}_\eta}\right]\frac{\mathrm{d}\tilde{p}}{\mathrm{d}r} \\ &\quad -\frac{im}{Er\rho}\left[\Lambda + \frac{2\mu r}{\rho\mu_0\tilde{\lambda}_\eta}\left(\frac{iF}{\tilde{\lambda}_\eta}\frac{\mathrm{d}\Omega}{\mathrm{d}r} - \frac{\mathrm{d}\mu}{\mathrm{d}r}\right)\right]\tilde{p}, \\ \tilde{u_z} &= -\frac{ik}{\rho\Lambda}\tilde{p}, \end{aligned} \tag{3.15}$$

where

$$
\begin{aligned}
E &= \Lambda^2 + \frac{2\Lambda\mu r}{\tilde{\lambda}_\eta \rho \mu_0}\left(\frac{iF}{\tilde{\lambda}_\eta}\frac{\mathrm{d}\Omega}{\mathrm{d}r} - \frac{\mathrm{d}\mu}{\mathrm{d}r}\right) + 2\left(\Omega - \frac{i\mu F}{\tilde{\lambda}_\eta \rho \mu_0}\right) \\
&\quad \times \left[2\Omega + \left(1 + \frac{F^2}{\tilde{\lambda}_\eta^2 \rho \mu_0}\right) r\frac{\mathrm{d}\Omega}{\mathrm{d}r} - \frac{2i\mu F}{\tilde{\lambda}_\eta \rho \mu_0}\right].
\end{aligned} \tag{3.16}
$$

Upon substitution from (3.15) for $\tilde{u_r}$, $\tilde{u_\theta}$ and $\tilde{u_z}$, the continuity equation (3.9) produces a second-order differential equation of $\tilde{p}$

$$
\begin{aligned}
&\frac{\mathrm{d}}{\mathrm{d}r}\left(\frac{\Lambda}{\rho E}\frac{\mathrm{d}\tilde{p}}{\mathrm{d}r}\right) + \left[\frac{\Lambda}{rE\rho} - \frac{im}{E\rho}\left(1 + \frac{F^2}{\rho\mu_0\tilde{\lambda}_\eta^2}\right)\frac{\mathrm{d}\Omega}{\mathrm{d}r}\right]\frac{\mathrm{d}\tilde{p}}{\mathrm{d}r} \\
&+ \frac{2im}{Er^2\rho}\left(\Omega - \frac{iF\mu}{\rho\mu_0\tilde{\lambda}_\eta}\right)\tilde{p} + \frac{\mathrm{d}}{\mathrm{d}r}\left[\frac{2im}{Er\rho}\left(\Omega - \frac{iF\mu}{\rho\mu_0\tilde{\lambda}_\eta}\right)\right]\tilde{p} \\
&- \frac{2m^2}{Er^2\rho}\left(\frac{\Lambda}{2} + \frac{\mu r}{\rho\mu_0\tilde{\lambda}_\eta}\left(\frac{iF}{\tilde{\lambda}_\eta}\frac{\mathrm{d}\Omega}{\mathrm{d}r} - \frac{\mathrm{d}\mu}{\mathrm{d}r}\right)\right)\tilde{p} - \frac{k^2}{\Lambda\rho}\tilde{p} = 0.
\end{aligned} \tag{3.17}
$$

We are now ready to deduce an equation of the Lagrangian displacement $\xi_r = u_r/\tilde{\lambda}$ in the radial direction. With η effect, we introduce a new variable $\chi = -ru_r/\tilde{\lambda}_\eta$, with the minus sign for convenience of the later calculation. The first equation of (3.15) reads the expression of χ in terms of $\tilde{p}$ and $\mathrm{d}\tilde{p}/\mathrm{d}r$

$$
\chi = \frac{\Lambda r}{\tilde{\lambda}_\eta E\rho}\frac{\mathrm{d}\tilde{p}}{\mathrm{d}r} + \frac{2im}{E\rho\tilde{\lambda}_\eta}\left(\Omega - \frac{iF\mu}{\rho\mu_0\tilde{\lambda}_\eta}\right)\tilde{p}. \tag{3.18}
$$

In order to derive the equation for χ, our target, first we take the radial derivative of (3.18),

and simplify it, with the help of (3.17), leaving

$$\begin{aligned}\frac{\mathrm{d}\chi}{\mathrm{d}r} &= \frac{im}{E\rho\tilde{\lambda}_\eta}\left[\left(1-\frac{\tilde{\lambda}_\nu}{\tilde{\lambda}_\eta}\right)r\frac{\mathrm{d}\Omega}{\mathrm{d}r}+2\left(\Omega-\frac{iF\mu}{\rho\mu_0\tilde{\lambda}_\eta}\right)\right]\frac{\mathrm{d}\tilde{p}}{\mathrm{d}r}\\ &+\frac{2m^2}{E\rho\tilde{\lambda}_\eta^2}\left(\Omega-\frac{iF\mu}{\rho\mu_0\tilde{\lambda}_\eta}\right)\frac{\mathrm{d}\Omega}{\mathrm{d}r}\tilde{p}\\ &+\frac{h^2r}{\Lambda E\rho\tilde{\lambda}_\eta}\left[\Lambda^2+\frac{2\mu r}{\tilde{\lambda}_\eta\rho\mu_0}\Lambda\left(\frac{iF}{\tilde{\lambda}_\eta}\frac{\mathrm{d}\Omega}{\mathrm{d}r}-\frac{\mathrm{d}\mu}{\mathrm{d}r}\right)\right]\tilde{p}\\ &+\frac{2k^2r}{\Lambda E\rho\tilde{\lambda}_\eta}\left[2\Omega+\left(1+\frac{F^2}{\tilde{\lambda}_\eta^2\rho\mu_0}\right)r\frac{\mathrm{d}\Omega}{\mathrm{d}r}-\frac{2i\mu F}{\tilde{\lambda}_\eta\rho\mu_0}\right]\left(\Omega-\frac{i\mu F}{\tilde{\lambda}_\eta\rho\mu_0}\right)\tilde{p},\end{aligned} \tag{3.19}$$

where $h^2=k^2+m^2/r^2$. A combination of (3.18) and (3.19) brings the expression of $\mathrm{d}\tilde{p}/\mathrm{d}r$ in terms of χ and $\mathrm{d}\chi/\mathrm{d}r$

$$\begin{aligned}\frac{\mathrm{d}\tilde{p}}{\mathrm{d}r} &= -\frac{2i\rho m\tilde{\lambda}_\eta}{h^2r^2}\left(\Omega-\frac{iF\mu}{\rho\mu_0\tilde{\lambda}_\eta}\right)\frac{\mathrm{d}\chi}{\mathrm{d}r}+\frac{\rho\tilde{\lambda}_\eta E}{\Lambda r}\chi\\ &-\frac{2\rho m^2\tilde{\lambda}_\eta}{h^2r^3\Lambda}\left(\Omega-\frac{iF\mu}{\rho\mu_0\tilde{\lambda}_\eta}\right)\left[\left(1-\frac{\tilde{\lambda}_\nu}{\tilde{\lambda}_\eta}\right)r\frac{\mathrm{d}\Omega}{\mathrm{d}r}+2\left(\Omega-\frac{iF\mu}{\rho\mu_0\tilde{\lambda}_\eta}\right)\right]\chi\end{aligned} \tag{3.20}$$

With this help in (3.19), we reach a tidy equation,

$$\Lambda r\frac{\mathrm{d}\chi}{\mathrm{d}r}-im\left[\left(1-\frac{\tilde{\lambda}_\nu}{\tilde{\lambda}_\eta}\right)r\frac{\mathrm{d}\Omega}{\mathrm{d}r}+2\left(\Omega-\frac{iF\mu}{\rho\mu_0\tilde{\lambda}_\eta}\right)\right]\chi=\frac{h^2r^2}{\rho\tilde{\lambda}_\eta}\tilde{p}. \tag{3.21}$$

Multiplying both side of (3.21) by $\rho\tilde{\lambda}_\eta/(h^2r^2)$ and taking r derivative, then substituting $\mathrm{d}\tilde{p}/\mathrm{d}r$ expressed in terms of χ and $\mathrm{d}\chi/\mathrm{d}r$ using (3.18) and (3.19), we eventually arrive at a desired equation for χ

$$\frac{\mathrm{d}}{\mathrm{d}r}\left(f\frac{\mathrm{d}\chi}{\mathrm{d}r}\right)+s\frac{\mathrm{d}\chi}{\mathrm{d}r}-g\chi=0, \tag{3.22}$$

where

$$
\begin{aligned}
f &= \frac{\tilde{\lambda}_\eta \Lambda}{h^2 r}, \\
s &= \frac{im\rho E(\tilde{\lambda}_\nu - \tilde{\lambda}_\eta)}{h^2 r}\frac{\mathrm{d}\Omega}{\mathrm{d}r}, \\
g &= \frac{\mathrm{d}}{\mathrm{d}r}\left[\frac{im\tilde{\lambda}_\eta}{h^2 r^2}\left(\left(1-\frac{\tilde{\lambda}_\nu}{\tilde{\lambda}_\eta}\right)\frac{\mathrm{d}\Omega}{\mathrm{d}r}+2\left(\Omega-\frac{iF\mu}{\rho\mu_0\tilde{\lambda}_\eta}\right)\right)\right] \\
&\quad +\frac{E\tilde{\lambda}_\eta}{\Lambda r}-\left(\Omega-\frac{iF\mu}{\rho\mu_0\tilde{\lambda}_\eta}\right) \\
&\quad \times\frac{2m^2\tilde{\lambda}_\eta}{\Lambda h^2 r^3}\left[\left(1-\frac{\tilde{\lambda}_\nu}{\tilde{\lambda}_\eta}\right)\frac{\mathrm{d}\Omega}{\mathrm{d}r}+2\left(\Omega-\frac{iF\mu}{\rho\mu_0\tilde{\lambda}_\eta}\right)\right].
\end{aligned}
$$

This is thought of as a version of the Hain-Lüst equation [37] extended with allowance for the effect of the viscous dissipation and the magnetic diffusion.

We seek the solution of (3.22) in the WKB approximation. To this end, we substitute into (3.22) the form $\chi(r) = p(r)\exp[i\int q(r)\mathrm{d}r]$ and get

$$
f'p' + fp'' - fpq^2 + sp' - g = 0 \tag{3.23}
$$

where the prime $'$ denotes the radial derivative. We make the assumption that the radial wavelength $2\pi/q$ is assumed to be much shorter than the characteristic length L, a measure for radial inhomogeneity, $qL \gg 1$. Under this assumption, for instance, $qp \gg p'$, and for this reason, the second order inhomogenous terms $f'p' + fp''$ are ignored in (3.23), and so is sp', because s includes the derivative term $\mathrm{d}\Omega/\mathrm{d}r$. Finally the dispersion relation (3.23) is approximated, in the short-wavelength limit, by $q^2 = -g/f$, which is written out as

$$
\begin{aligned}
&(h^2+q^2)\tilde{\lambda}_\eta^2\Lambda^2 + 4k^2\left(\Omega\tilde{\lambda}_\eta - \frac{iF\mu}{\rho\mu_0}\right)\left[\Omega Ro(\omega_\eta - \omega_\nu) + \left(\Omega\tilde{\lambda}_\eta - \frac{iF\mu}{\rho\mu_0}\right)\right] \\
&+4\Lambda h^2\tilde{\lambda}_\eta\left[(\Omega^2 Ro - \frac{\mu^2}{\rho\mu_0}Rb) + \frac{imr}{2}\frac{\mathrm{d}}{\mathrm{d}r}\left(\frac{\Omega\tilde{\lambda}_\eta - \frac{i\mu F}{\rho\mu_0}}{h^2 r^2}\right)\right] = 0,
\end{aligned} \tag{3.24}
$$

where we have introduced the Rossby number Ro and the magnetic Rossby number Rb by [8, 9]

$$Ro = \frac{1}{2}\frac{r}{\Omega}\frac{\mathrm{d}\Omega}{\mathrm{d}r}, \quad Rb = \frac{1}{2}\frac{r}{\mu}\frac{\mathrm{d}\mu}{\mathrm{d}r}. \tag{3.25}$$

Two kinds of Alfvén frequency ω_A and $\omega_{A\theta}$ as well as their comparative parameter β are defined as follows

$$\omega_A = \frac{kB_z}{\sqrt{\rho\mu_0}}, \quad \omega_{A\theta} = \frac{\mu^2}{\sqrt{\rho\mu_0}}, \quad \beta = \frac{\omega_{A\theta}}{\omega_A}. \tag{3.26}$$

In addition, we introduce three dimensionless parameters, namely, the magnetic Prandtl number Pm, the Reynolds number Re and the Hartmann number Ha by

$$Pm = \frac{\omega_\nu}{\omega_\eta}, \quad Re = \frac{\Omega}{\omega_\nu}, \quad Ha = \frac{\omega_A}{\sqrt{\omega_\nu\omega_\eta}}. \tag{3.27}$$

The dispersion relation for non-dimensional variables, with the derivative term in (3.24) being expanded out, leads to

$$\begin{aligned}
&(\Lambda_1\Lambda_2 + \widetilde{Ha}^2)^2 + 4\frac{h^2(\Lambda_1\Lambda_2 + \widetilde{Ha}^2)}{h^2+q^2}(Re^2 PmRo - \beta^2 Ha^2 Rb) \\
&+\frac{4im(\Lambda_1\Lambda_2 + \widetilde{Ha}^2)}{r^2(h^2+q^2)}\Big[ReRo\sqrt{Pm}(\Lambda_2 + imRe\sqrt{Pm}) \\
&-i(2m\beta+1)\beta Ha^2 Rb + (i\widetilde{Ha}\beta Ha - Re\sqrt{Pm}\Lambda_2)\frac{k^2}{h^2}\Big] \\
&+4\alpha^2\Big[(Re\Lambda_2\sqrt{Pm} - i\widetilde{Ha}\beta Ha)\Big(Re\Lambda_2\sqrt{Pm} - i\widetilde{Ha}\beta Ha + RoRe(1-Pm)\Big)\Big] = 0.
\end{aligned} \tag{3.28}$$

where

$$\begin{aligned}
\Lambda_1 &= \lambda + imRe\sqrt{Pm} + \sqrt{Pm}, \\
\Lambda_2 &= \lambda + imRe\sqrt{Pm} + \frac{1}{\sqrt{Pm}}, \\
\widetilde{Ha} &= Ha(1+m\beta) \\
\alpha &= \frac{k^2}{h^2+k^2}
\end{aligned}$$

This form of the dispersion relation plays the key role, in the following sections, for determining the instability criterion and for calculating the growth rate for both the axisymmetric ($m = 0$) and the non-axisymmetric ($m \neq 0$) MRI.

3.2 Axisymmetric perturbations

For the axisymmetric SMRI ($m = 0$, $\boldsymbol{B} = B_z \boldsymbol{e}_z$), the dispersion relation (3.28) simplifies, in the inductionless limit ($Pm \to 0$), to

$$4\alpha^2 Re^2(1+Ro) + (1+Ha^2 + \frac{\lambda}{\Omega}Re)^2 = 0. \tag{3.29}$$

The growth rate can be solved from (3.29) as

$$\frac{\lambda}{\Omega} = -\frac{1+Ha^2}{Re} \pm 2\sqrt{-\alpha^2(1+Ro)} \tag{3.30}$$

where $\alpha^2 = k^2/(q^2+k^2)$ when $m = 0$. From (3.30), the instability region is

$$Ro < Ro_c = -1 - \left(\frac{1+Ha^2}{\alpha Re}\right)^2. \tag{3.31}$$

As Re goes to infinity the critical Rossby number approaches $Ro_c = -1$. Here magnetic field or Ha lowered the critical Rossby number, which is different from ideal SMRI where magnetic field, no matter how weak, can raise the critical Rossby number from $Ro_c = -1$

for hydrodynamic flows to $Ro_c = 0$ for MHD flows, i.e. Velikhov-Chandrasekhar paradox [8]. The viscosity acts to stabilize the MHD flow when the magnetic field is weak.

Next, we consider the inductionless azimuthal MRI (AMRI), where the magnetic field has only the azimuthal component $\boldsymbol{B} = r\mu(r)\boldsymbol{e}_\theta$. Putting $m = 0$, and taking account of only the azimuthal magnetic field by replacing $\beta Ha = Ha_\theta$ and then taking $Ha \to 0$, where $\omega_{A\theta} = \mu/\sqrt{\rho\mu_0}$ and $Ha_\theta = \omega_{A\theta}/\sqrt{\omega_\nu\omega_\eta}$, the growth rate is found from (3.28) to be

$$\lambda = \frac{-1 + 2\alpha^2 Ha_\theta^2 Rb \pm 2\alpha\sqrt{\alpha^2 Ha_\theta^4 Rb^2 - (1+Ro)Re^2}}{Re}. \tag{3.32}$$

We expand (3.32) in small $1/Re$ to the first order for large Reynolds number as

$$\lambda = 2\sqrt{-\alpha^2(1+Ro)} + (-1 + 2\alpha^2 Ha_\theta^2 Rb)\frac{1}{Re} \tag{3.33}$$

When $Re \to \infty$, the instability region from the zero order and first order coefficients of $1/Re$ in (3.33) becomes

$$Ro < -1 \text{ or } Ro \geq 0,\ Rb > \frac{1}{2\alpha^2 Ha_\theta^2} \tag{3.34}$$

In the rest of this section, we revisit the axisymmetric HMRI occurring in the presence of both azimuthal and axial components of magnetic field $\boldsymbol{B} = r\mu(r)\boldsymbol{e}_\theta + B_z\boldsymbol{e}_z$. The dispersion relation (3.28) is solved for the eigenvalue as

$$\begin{aligned}\lambda &= -\frac{1}{Re} + \frac{Ha^2}{Re}(-1 + 2\alpha^2\beta^2 Rb) \\ &\quad \pm \frac{2\alpha}{Re}\left[\beta^2 Ha^4 + \alpha^2\beta^4 Ha^4 Rb^2 - Re^2(1+Ro) + i\beta Ha^2 Re(2+Ro)\right]^{1/2}\end{aligned} \tag{3.35}$$

When Reynolds number tends to infinity, we expand (3.35) as

$$\begin{aligned}
\lambda &= \pm 2i\alpha\sqrt{1+Ro} + \left[-1 + Ha^2 \left(2\alpha^2\beta^2 Rb - 1 \right.\right. \\
&\quad \left.\left. \pm \frac{(2+Ro)\alpha\beta}{\sqrt{1+Ro}} \right) \right] \frac{1}{Re}, \quad (Ro \neq -1), \\
\lambda &= \pm 2\alpha Ha\sqrt{i\beta}\frac{1}{\sqrt{Re}} + (-1 - Ha^2 + 2\alpha^2\beta^2 Ha^2 Rb)\frac{1}{Re}, \\
&\quad (Ro = -1).
\end{aligned} \tag{3.36}$$

Obviously from the zero order term in (3.36), $Ro < -1$ always guarantees the instability and $Ro = -1$ is also unstable if $Ha,\ \beta$ are nonzero. So it is left to consider the case when $Ro > -1$, from (3.36), if growth rate is positive, then it must grow with $|Ha|$.

For $1 \ll Ha \ll Re$ and $Ro \neq -1$, from (3.36), the growth rate (λ_R=Re[λ]) becomes

$$\begin{aligned}
\lambda_R &= \left(2\alpha^2\beta^2 Rb - 1 \pm \frac{(2+Ro)\alpha\beta}{\sqrt{1+Ro}} \right) \frac{Ha^2}{Re} - \frac{1}{Re} \\
&= \left[2Rb \left(\alpha\beta \pm \frac{2+Ro}{4Rb\sqrt{1+Ro}} \right)^2 - \frac{(2+Ro)^2}{8Rb(1+Ro)} - 1 \right] \frac{Ha^2}{Re} - \frac{1}{Re}.
\end{aligned} \tag{3.37}$$

From second line in (3.37), the criterion for instability for $1 \ll Ha \ll Re$ case is

$$2Rb \left(\alpha\beta \pm \frac{2+Ro}{4Rb\sqrt{1+Ro}} \right)^2 - \frac{(2+Ro)^2}{8Rb(1+Ro)} > 1. \tag{3.38}$$

We can also write it from the first line in (3.37) to be

$$\sqrt{1+Ro} + \frac{1}{\sqrt{1+Ro}} > \frac{1 - 2\alpha^2\beta^2 Rb}{|\alpha\beta|}. \tag{3.39}$$

So the critical Rossby number depends on $Rb,\ \alpha,\ \beta$ and the criterion for instability is

separated into two cases as

$$\begin{cases} Ro & \in & \forall \text{ Reals, } (c<2), \\ Ro & \in & \left(\left(\frac{c}{2}+\frac{1}{2}\sqrt{c^2-4}\right)^2-1,+\infty\right) \\ & & \bigcup\left(-\infty,\left(\frac{c}{2}-\frac{1}{2}\sqrt{c^2-4}\right)^2-1\right) \ (c\geq 2) \\ c & = & \dfrac{1-2\alpha^2\beta^2 Rb}{|\alpha\beta|} \end{cases} \tag{3.40}$$

When $Rb<0$ the maximum growth rate turns out to be $-\left(\dfrac{(2+Ro)^2}{8Rb(1+Ro)}+1\right)\dfrac{Ha^2}{Re}$, so the instability region is

$$\begin{aligned} Ro \ \in \ & \left[-\infty, 2\left(-\sqrt{2}\sqrt{2Rb^2+Rb}-1-2Rb\right)\right] \\ & \cup\left[2\left(\sqrt{2}\sqrt{2Rb^2+Rb}-1-2Rb\right),+\infty\right]. \end{aligned} \tag{3.41}$$

Especially when $Rb=-1$, $Ro_c=2(1\pm\sqrt{2})$ corresponding to $\alpha\beta=\pm\sqrt{2}/2$, and thus Liu's limit was recovered. [36, 8, 9]

3.3 Non-axisymmetric perturbations

3.3.1 Weak external field

After a discussion of axisymmetric perturbations, we want to focus on the non-axisymmetric perturbations in the inductionless limit. Inclusion of non-axisymmetric perturbations ($m\neq 0$) entirely alters the characteristics of the inductionless AMRI. At the beginning, we deduce the inductionless ($Pm\to 0$) dispersion relation. Making ($Pm\to 0$) in (3.28),

we get

$$\hat{\lambda}^2 - \frac{4h^2 Ha_\theta^2 Rb\hat{\lambda}}{h^2+q^2} - 4i\alpha^2 Ha_\theta^2 mReRo$$
$$+\frac{4\hat{\lambda}(2h^2 Ha_\theta^2 m^2 Rb - Ha_\theta^2 k^2 m^2 - ik^2 mRe + ih^2 mReRo)}{(h^2+q^2)h^2 r^2}$$
$$+\alpha^2(-2iHa_\theta^2 m + 2Re)^2 + 4\alpha^2 Re^2 Ro = 0, \tag{3.42}$$

where $\alpha = k^2/(k^2+q^2+m^2/r^2)$, $\hat{\lambda} = 1 + Ha_\theta^2 m^2 + \lambda Re + imRe$ and $Ha_\theta = \omega_{A\theta}/\sqrt{\omega_\nu \omega_\eta}$.

To see the instability when magnetic field is weak, we do the small Ha_θ expansion of the solution of (3.42)

$$\begin{aligned}\frac{\lambda}{\Omega} &= \pm 2\sqrt{-\alpha^2(1+Ro) - \frac{m^2(k^2r^2(Ro-1)+m^2Ro)^2}{h^4 r^8 (h^2+q^2)^2}} \\ &\quad -\frac{1}{Re} - \frac{im(h^2(h^2r^2+q^2r^2+2Ro)-2k^2)}{h^2r^2(h^2+q^2)} + o(Ha_\theta).\end{aligned} \tag{3.43}$$

In (3.43), Thesquare root term is the hope for positive growth rate. There are two terms in the square root, one is $-\alpha^2(1+Ro)$ which can become positive by $Ro < -1$ and the second term is definitely non-positive $-(m^2(k^2r^2(Ro-1)+m^2Ro)^2)/(h^4r^8(h^2+q^2)^2) \leq 0$. This non-positive term has the effect of decreasing the growth rate. So $m = 0$ is an appropriate choice connecting with the largest growth rate. We should reconsider the simpler case of $m = 0$ when $Ha = 0$.

In §3.2, we considered the growth rate of axisymmetric AMRI in large Re expansion as (3.33). If we set $Ha_\theta = 0$ in (3.33) we get the same result as when we set $m = 0$ in (3.43) except $o(Ha_\theta)$ terms. In this case the growth rate becomes

$$\frac{\lambda}{\Omega} = \pm 2\alpha\sqrt{-1-Ro} - 1/Re, \tag{3.44}$$

by setting $Ha_\theta = 0$ in (3.33). As a result, the instability requires $Ro < Ro_c$, where $Ro_c = -1 - 1/(4Re^2)$. Comparing to ideal hydrodynamics, whose critical Rossby num-

ber is $Ro_c = -1$, the famous Rayleigh criterion and the maximum growth rate becomes $2\alpha\sqrt{-1-Ro}$ by $Re \to \infty$, the critical Rossby number is lowered by $1/4Re^2$ and the maximum growth rate is also lowered by $1/Re$ when viscosity exists.

When $Ro > -1$, for instance, the Keplerian flow $Ro = -3/4$, for the non-axisymmetric waves as well as the axisymmetic ones, the $1/Re$ in zero order term of Ha_θ (3.43), stops the instability from the higher order terms $o(Ha_\theta)$. It breaks down the similar singularity of the ideal AMRI. In ideal AMRI, weak magnetic fields arouse magneto-Coriolis waves, raise the critical Rossby number from $Ro_c = -1$ for hydrodynamic flows to $Ro_c \approx 0$ for MHD flows- the resolution of Velikhov-Chandrasekhar paradox to the ideal AMRI case. The $1/Re$ term in the zeroth order term in (3.43) for $Ro > -1$ prevents the occurrence of instability for very weak magnetic field. The disappearance of the singularity is the same as in the inductionless AMRI as discussed in (3.2).

3.3.2 Strong external field

Now we turn to strong magnetic fields. We consider that viscosity is small, i.e. Reynolds number is large. When $Re \to \infty$ the leading order (zero order to $1/Re$) of growth rate solved from (3.42) becomes

$$\frac{\lambda}{\Omega} = \pm 2\sqrt{-\alpha^2(1+Ro) - \frac{m^2(k^2r^2(Ro-1)+m^2Ro)^2}{h^4r^8(h^2+q^2)^2}}. \tag{3.45}$$

We may check that for instability in (3.45), $Ro < -1$ is necessary. We are more interested in the cases when $Ro > -1$, for example $Ro = -3/4$ for an Keplerian flow, so the zeroth order is far from enough. We have to look for the first order of $1/Re$ term of the eigenvalues in (3.42) to seek instability for $Ro \geq -1$.

The axial wavenumber k is important when we decide the maximum growth rate and the instability region. Fig. 3.1 shows the growth rate to k for different Rb. For the case, $m = 1$, $Ro = -3/4$ and $q = 0$ (because numerically $q = 0$ mode likely corresponds to the

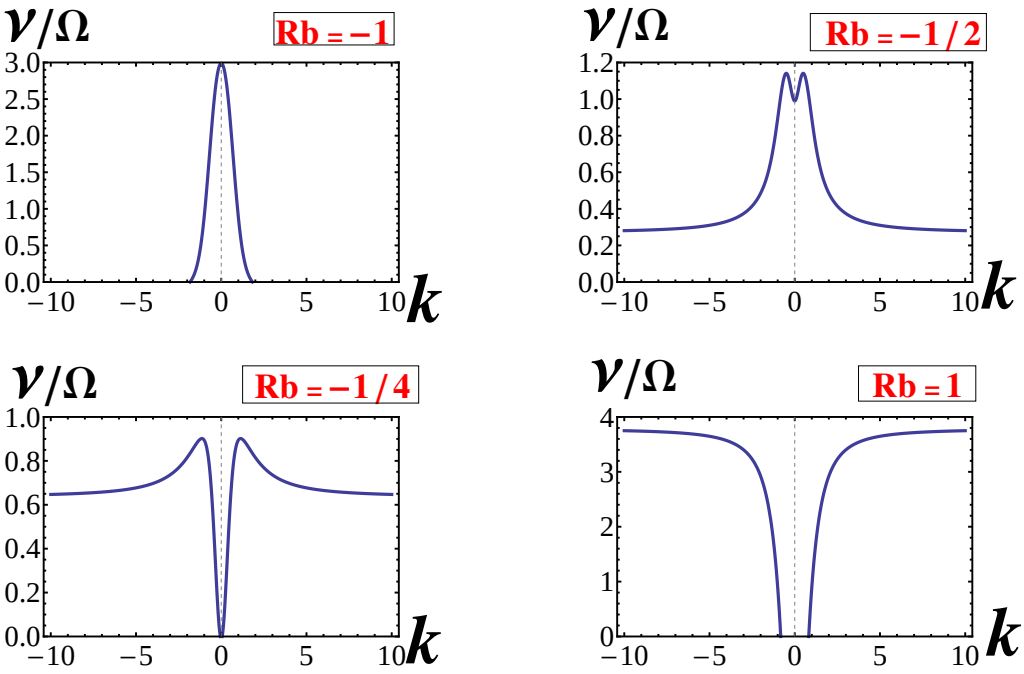

Figure 3.1: The normalized growth rate ν/Ω to the axial wavenumber k for a Keplerian flow with the Reynolds $Re = 10^4$, the Hartmann number $Ha_\theta = 100$ in the inductionless limit $Pm = 0$. When the magnetic Rossby number Rb increases from -1 to 1, the axial wavenumber k corresponding to the maximum growth rate quickly changes from 0 to ∞.

fastest growth rate), when Rb has the value around $-1/4$ there is some finite k, which corresponds to the maximum growth rate. But when Rb goes smaller than $-1/4$, the fast growth rate quickly moves to $k=0$ mode. And at the same time, if Rb increases to the more right side, the infinite k mode grows fastest. It is important and easier to analytically consider $k=0$ and $k=\infty$ for understanding.

When $Rb < -m^2/4$, we consider the limit of $k \to 0$ and $q \to 0$. So, we fix $k=0$. By small $1/Re$ expansion to the first order, the growth rate can be expanded to the first order in $1/Re$ as

$$\begin{aligned} \frac{\lambda_1}{\Omega} &= -im - (1+Ha_\theta^2 m^2)\frac{1}{Re}, \\ \frac{\lambda_2}{\Omega} &= -i(m+4\frac{mRo}{m^2+q^2r^2}) - \left(1+Ha_\theta^2 m^2\left(1+4\frac{Rb}{m^2+q^2r^2}\right)\right)\frac{1}{Re}. \end{aligned} \tag{3.46}$$

From λ_2 in (3.46) the instability region, we can immediately get the instability region

$$Rb < -\frac{m^2}{4} \text{ and } Ha_\theta^2 > \frac{1}{m^2+4Rb}. \tag{3.47}$$

From (3.47), Rb is essential rather than Ro to decide the instability. When $Rb=-1$, the $m=\pm 1$ modes are the only possible modes for instability and it is notable that the Liu's limit disappear, i.e. instability exists for arbitrary Rossby number. When $m=1$ is fixed, $Rb<-1/4$ is the promising of the $k=0$ mode instability.

Fig. 3.2 displays the growth rate to Ha_θ when $Re=10^4$, $m=1$, $k=q=0$, $Ro=-3/4$ and $Rb=-1$. The left one shows that the growth rate increases with the increase of Ha_θ and the right one confirms that there is an onset of $|Ha_\theta| = \sqrt{3}/3 \approx 0.5774$ for instability which is quite small but nonzero.

When $Rb > -m^2/4$, the maximum growth rate for $Ro > -1$ occurs when $k \to \infty$. We

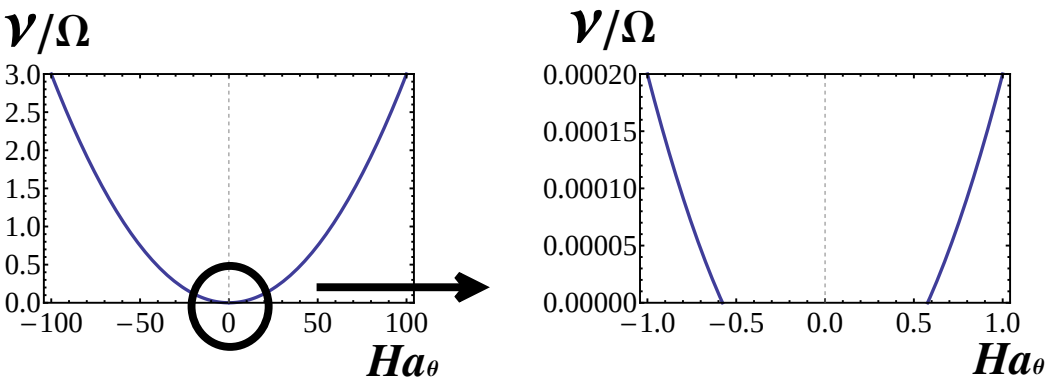

Figure 3.2: The growth rate Re$[\lambda]$ to Ha_θ when $Re = 10^4$, $m = 1$, $k = q = 0$, $Ro = -3/4$ and $Rb = -1$. The left figure shows that large Ha_θ increase the growth rate and the right one is the amplification of the left one when Ha_θ is small, which demonstrates that a certain strength of magnetic field is necessary for instability.

expand the eigenvalues to the first order in small $1/Re$ for the case $k \to \infty$.

$$\begin{aligned}\frac{\lambda_{1,2}}{\Omega} &= -im \pm 2\alpha\sqrt{-1-Ro} \\ &\quad + \left[Ha_\theta^2\left(2\alpha^2 Rb - m^2 \pm \frac{\alpha m(2+Ro)}{\sqrt{1+Ro}}\right) - 1\right]\frac{1}{Re}.\end{aligned} \tag{3.48}$$

From (3.48), when $Ro < -1$, it is unstable from the zeroth order term, and if $Ro > -1$, the instability criterion becomes

$$\begin{aligned}&2\alpha^2 Rb - m^2 + \frac{|\alpha m|(2+Ro)}{\sqrt{1+Ro}} > 0, \\ &\text{and } Ha^2 > \frac{\sqrt{1+Ro}}{(2\alpha^2 Rb - m^2)\sqrt{1+Ro} + |\alpha m|(2+Ro)}.\end{aligned} \tag{3.49}$$

To decide the critical Rossby number, the first inequality in (3.49) is equal to

$$\sqrt{1+Ro} + \frac{1}{\sqrt{1+Ro}} > \frac{m^2 - 2\alpha^2 Rb}{|\alpha m|}. \tag{3.50}$$

The criterion for instability by use of Ro is separated into two cases expressed similarly as in (3.40)

$$\begin{cases} Ro & \in & \forall \text{ Reals, } (c<2)\,, \\ Ro & \in & \left(\left(\frac{c}{2}+\frac{1}{2}\sqrt{c^2-4}\right)^2-1,+\infty\right) \\ & & \bigcup\left(-\infty,\left(\frac{c}{2}-\frac{1}{2}\sqrt{c^2-4}\right)^2-1\right) \ (c\geq 2) \\ c & = & \dfrac{m^2-2\alpha^2 Rb}{|\alpha m|} \end{cases} \tag{3.51}$$

When $Rb=-1$, the first inequality in (3.49) can be written as

$$\begin{aligned} &-1<Ro<\frac{4+n^4}{2n^2}-\frac{1}{2}\sqrt{\frac{(n^4+4)(n^2+2)^2}{n^4}}\leq 2-2\sqrt{2}, \\ &\text{or, Ro}>\frac{4+\mathrm{n}^4}{2\mathrm{n}^2}-\frac{1}{2}\sqrt{\frac{(\mathrm{n}^4+4)(\mathrm{n}^2+2)^2}{\mathrm{n}^4}}\geq 2+2\sqrt{2}, \end{aligned} \tag{3.52}$$

where $n=\alpha m$ and the two equalities are obtained when $n=\alpha m=\pm\sqrt{2}$. (3.52) also reveals the *Liu's limit* for the instability in the axisymmetric HMRI.

From Keplerian flow $Ro=-3/4$, $Rb>-25/32$ is necessary for instability. Actually, choosing $m/\alpha=\pm\frac{5}{4}$ in (3.49), the critical Rossby number $Rb_c=-25/32$ can be obtained. If we furthermore choose that $Rb=0$, it can be calculated that the $|Ha_\theta|=\sqrt{6}/3\approx 0.8165$ is the onset of AMRI as show in Fig. 3.3.

Recall from (3.47), $Rb<-1/4$ is necessary for $k=0$, $m=1$ mode instability. And from (3.49), $Rb>-25/32$ is necessary for the $k=\infty$, $m=1$ mode instability. Because the later one overlaps with the former one, it concludes that the instability exists for arbitrary magnetic Rossby number. Maybe you will be curious about other mode of finite and nonzero k mode. Those modes has the maximum growth rate when Rb in an narrow region as show in 3.4 and for a large range of Rb the $k=0$ or the $k=\infty$ modes take the maximum growth rate. Fig. 3.4 shows the growth rate to magnetic Rossby number Rb

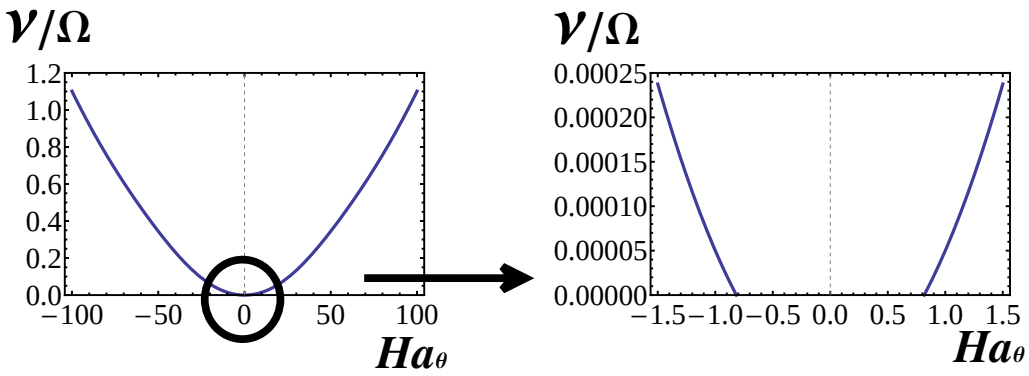

Figure 3.3: The growth rate $\mathrm{Re}[\lambda]$ to Ha_θ when $Re = 10^4$, $m = 1$, $k = q = 0$, $Ro = -3/4$ and $Rb = -1$. Left figure shows that large Ha_θ increase the growth rate and the right one is the amplification of the left one when Ha_θ is small, which demonstrates that a certain strength of magnetic field is needed for instability.

for $Re = 10^4$, $Ha_\theta = 100$, $m = 1$, and $Re = -3/4$. We can see the the crossover of the $k = 0,\ q = 0$ mode and the $k = \infty$ mode and the maximum growth rate, whose left part coincides with the $k = 0$ mode, the right part coincides with the $k = \infty,\ \alpha = 1$ mode, and in between there is a narrow range the maximum is taken for finite and nonzero k mode.

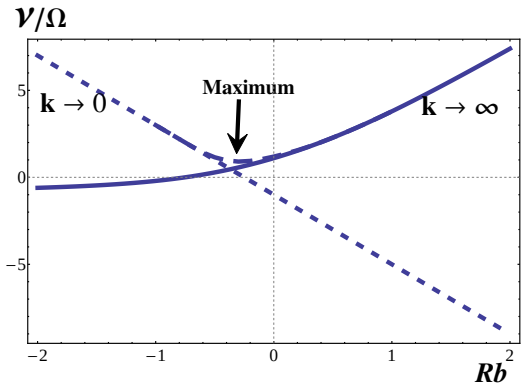

Figure 3.4: the growth rate to magnetic Rossby number Rb for $Re = 10^4$, $Ha_\theta = 100$, $m = 1$, and $Re = -3/4$. Dotted one is $k = 0,\ q = 0$ mode, solid line is the $k = \infty$ mode and dashed line stands for the maximum growth rate, whose left part coincide with the $k = 0$ mode and the right part coincides with the $k = \infty,\ \alpha = 1$ mode.

Chapter 4

Energy of ideal MHD

This chapter is different from the previous two chapters in that we make a global modal analysis rather than the local analysis with respect to the short-wavelength waves. We still use the cylindrical coordinates (r, θ, z) and the flow is confined between two coaxial cylinders. The ideal MHD is an Hamiltonian system of infinite degree of freedom. By the Arnold theorem, the signature of the energies of eigenmodes plays a vital role for stability of a steady state; if the wave energies for all the admissible disturbances are all positive or all negative, then the steady state is linearly stable [43, 47, 44, 45, 46]. Krein's theorem tells for a Hamiltonian system of finite degree of freedom that the collision of two imaginary eigenvalues with energy of opposite signature, instability could occur. In this chapter, we will deduce two energy formulas for the MHD waves, and by using one of them, calculate the wave energy and put the bifurcation on the ground of Krein's theorem [47, 41].

We confine our analysis to ideal MHD of an incompressible flow with constant density $\rho = 1$ and the magnetic permeability $\mu_0 = 1$ for simplicity. The flow has the velocity field

$$\boldsymbol{u} = \boldsymbol{U} + \tilde{\boldsymbol{u}}, \tag{4.1}$$

and the magnetic field

$$\boldsymbol{b} = \boldsymbol{B} + \tilde{\boldsymbol{b}}, \tag{4.2}$$

being constituted from a steady flow $\boldsymbol{U}$ and $\boldsymbol{B}$ and a small disturbance $\tilde{\boldsymbol{u}}$ and $\tilde{\boldsymbol{b}}$ to them. The flow is bounded by two concentric cylinders and the boundary conditions should be

$$\boldsymbol{n} \cdot \boldsymbol{u} = 0,\ \boldsymbol{n} \cdot \boldsymbol{b} = 0. \tag{4.3}$$

The boundary conditions mean that the flow and magnetic field do not go out or come in through the boundary.

4.1 Second formula of energy

As introduced in §1.2.5 the Lagrangian displacement satisfies the Frieman-Rotenberg equation.

$$\rho \frac{\partial^2 \boldsymbol{\xi}}{\partial t^2} + 2\rho(\boldsymbol{U} \cdot \boldsymbol{\nabla}) \frac{\partial \boldsymbol{\xi}}{\partial t} - \boldsymbol{F}_0[\boldsymbol{\xi}] = 0. \tag{4.4}$$

where

$$\boldsymbol{F}_0[\boldsymbol{\xi}] = -\rho(\boldsymbol{U} \cdot \nabla)^2 \boldsymbol{\xi} + \rho(\boldsymbol{\xi} \cdot \nabla)(\boldsymbol{U} \cdot \nabla)\boldsymbol{U} - \nabla \tilde{p} + \frac{1}{4\pi}(\nabla \times \tilde{\boldsymbol{b}}) \times \boldsymbol{B} + \frac{1}{4\pi}(\nabla \times \boldsymbol{B}) \times \tilde{\boldsymbol{b}}.$$

In (4.4) we can regard $\boldsymbol{F}_0$ as the force operator, which can be used to define the potential energy. The energy of the disturbance $\boldsymbol{\xi}$ directly obtained from (4.4) is an integral over the whole domain D [37]

$$H = \frac{1}{2} \int_D \rho \left| \frac{\partial \boldsymbol{\xi}}{\partial t} \right|^2 - \boldsymbol{\xi}^* \cdot F_0[\boldsymbol{\xi}] dV. \tag{4.5}$$

Here the * is used to express the complex conjugate. Equation (4.5) is regarded as the first energy formula.

H includes two parts, the kinetic energy K and the potential energy W

$$K = \frac{1}{2}\int_D |\frac{\partial \boldsymbol{\xi}}{\partial t}|^2 dV, \;\; W = -\frac{1}{2}\int_D \boldsymbol{\xi}^* \cdot F_0[\boldsymbol{\xi}] dV \tag{4.6}$$

One may directly calculate energy from (4.5), but $\boldsymbol{F}_0$ is a complicated operator and makes the calculation awkward. We make an attempt to simplify it. Multiplying the Frieman-Rotenberg equation by $\boldsymbol{\xi}^*$, it yields

$$\frac{\partial^2 \boldsymbol{\xi}}{\partial t^2} \cdot \boldsymbol{\xi}^* + 2(\boldsymbol{U} \cdot \boldsymbol{\nabla}) \frac{\partial \boldsymbol{\xi}}{\partial t} \cdot \boldsymbol{\xi}^* - \boldsymbol{F}_0[\boldsymbol{\xi}] \cdot \boldsymbol{\xi}^* = 0. \tag{4.7}$$

Substitute $\boldsymbol{F}_0[\boldsymbol{\xi}] \cdot \boldsymbol{\xi}^*$in (4.5 by using (4.7)

$$\begin{aligned} H &= \frac{1}{2}\int_D |\frac{\partial \boldsymbol{\xi}}{\partial t}|^2 - \boldsymbol{\xi}^* \cdot F_0[\boldsymbol{\xi}] dV. \\ &= \frac{1}{2}\int_D |\frac{\partial \boldsymbol{\xi}}{\partial t}|^2 - \frac{\partial^2 \boldsymbol{\xi}}{\partial t} \cdot \boldsymbol{\xi}^* - 2(\boldsymbol{U} \cdot \boldsymbol{\nabla}) \frac{\partial \boldsymbol{\xi}}{\partial t} \cdot \boldsymbol{\xi}^* dV. \\ &= \int_D |\frac{\partial \boldsymbol{\xi}}{\partial t}|^2 - (\boldsymbol{U} \cdot \boldsymbol{\nabla}) \frac{\partial \boldsymbol{\xi}}{\partial t} \cdot \boldsymbol{\xi}^* - \frac{\partial}{\partial t}(\frac{\partial \boldsymbol{\xi}}{\partial t} \cdot \boldsymbol{\xi}^*) dV \end{aligned} \tag{4.8}$$

Usually $\boldsymbol{\xi}$ is assumed to be in eigenmode $\boldsymbol{\xi} = \hat{\boldsymbol{\xi}}(r)\exp[-i\omega t + i(kz + m\theta)]$. So it can be verified the last term in (4.8)

$$\frac{\partial}{\partial t}(\frac{\partial \boldsymbol{\xi}}{\partial t} \cdot \boldsymbol{\xi}^*) = 0. \tag{4.9}$$

Consequently we obtained our second formula for energy

$$H = \int_D |\frac{\partial \boldsymbol{\xi}}{\partial t}|^2 - (\boldsymbol{U} \cdot \boldsymbol{\nabla}) \frac{\partial \boldsymbol{\xi}}{\partial t} \cdot \boldsymbol{\xi}^* dV \tag{4.10}$$

4.2 Third formula of energy

We consider *isomagnetovortical* perturbations as introduced in §1.2.4. By using the conservation of magnetic helicity H_M [21]

$$H_M = \int_D \boldsymbol{b} \cdot (\nabla\times)^{-1}\boldsymbol{b}\mathrm{d}V \tag{4.11}$$

and the cross-helicity

$$H_C = \int_D \boldsymbol{b} \cdot \boldsymbol{u}\mathrm{d}V, \tag{4.12}$$

the disturbances $\tilde{\boldsymbol{u}}$ and $\tilde{\boldsymbol{b}}$ can be expressed by $\boldsymbol{\xi}$[21, 44, 45, 46].

We rely on the formula for the *isomagnetovortical* perturbations derived by Vladimirov, Moffatt and Ilin (1999).

$$\begin{aligned} \tilde{\boldsymbol{u}} &= \mathscr{P}\left[\boldsymbol{\xi}\times\Omega+\boldsymbol{\eta}\times\boldsymbol{B}\right], \\ \tilde{\boldsymbol{b}} &= \nabla\times(\boldsymbol{\xi}\times\boldsymbol{B}), \end{aligned} \tag{4.13}$$

where η describes magnetic displacement, similar to how ξ describes the Lagrangian displacement and $\mathscr{P}[\cdot]$ is an operator projecting a vector field to a solenoidal field. And we restate the other relation between $\boldsymbol{\xi}$ and $\tilde{\boldsymbol{u}}$ as shown in (1.28) of §1.2.2

$$\tilde{\boldsymbol{u}}(\boldsymbol{x_0},t) = \frac{\partial\boldsymbol{\xi}}{\partial t} + \boldsymbol{U}\cdot\nabla\boldsymbol{\xi} - \boldsymbol{\xi}\cdot\nabla\boldsymbol{U}. \tag{4.14}$$

By a combination of (4.13) and (4.14), $\partial\boldsymbol{\xi}/\partial t$ can be written as

$$\frac{\partial\boldsymbol{\xi}}{\partial t} = \tilde{\boldsymbol{u}} - \boldsymbol{U}\cdot\nabla\boldsymbol{\xi} + \boldsymbol{\xi}\cdot\nabla\boldsymbol{U} = \boldsymbol{\xi}\times\boldsymbol{\Omega} + \boldsymbol{\eta}\times\boldsymbol{B} - \boldsymbol{U}\cdot\nabla\boldsymbol{\xi} + \boldsymbol{\xi}\cdot\nabla\boldsymbol{U} \tag{4.15}$$

In order to make no confusion, we regards $\boldsymbol{\xi}$ to be real. From (4.8) in §4.1,

$$\begin{aligned} H &= \frac{1}{2}\int_D \frac{\partial \boldsymbol{\xi}}{\partial t} - \boldsymbol{\xi}\cdot \boldsymbol{F_0}(\boldsymbol{\xi})dV \\ &= \frac{1}{2}\int_D \frac{\partial \boldsymbol{\xi}}{\partial t} - \boldsymbol{\xi}\cdot (2(\boldsymbol{u}\cdot\boldsymbol{\nabla})\frac{\partial \boldsymbol{\xi}}{\partial t} + \frac{\partial^2 \boldsymbol{\xi}}{\partial t^2})dV \\ &= \int_D (\frac{\partial \boldsymbol{\xi}}{\partial t})^2 - (\boldsymbol{u}\cdot\boldsymbol{\nabla})\frac{\partial \boldsymbol{\xi}}{\partial t}\cdot\boldsymbol{\xi} - \frac{1}{2}\frac{\partial}{\partial t}(\frac{\partial \boldsymbol{\xi}}{\partial t}\cdot\boldsymbol{\xi})dV, \end{aligned} \tag{4.16}$$

Substitute (4.15) into (4.16) we can obtain the following result

$$\begin{aligned} H &= \int_D \frac{\partial \boldsymbol{\xi}}{\partial t}\cdot\big(\boldsymbol{\xi}\times\boldsymbol{\Omega} + \boldsymbol{\eta}\times\boldsymbol{B} - \boldsymbol{U}\cdot\nabla\boldsymbol{\xi} + \boldsymbol{\xi}\cdot\nabla\boldsymbol{U}\big) - (\boldsymbol{U}\cdot\boldsymbol{\nabla})\frac{\partial \boldsymbol{\xi}}{\partial t}\cdot\boldsymbol{\xi} - \frac{1}{2}\frac{\partial}{\partial t}(\frac{\partial \boldsymbol{\xi}}{\partial t}\cdot\boldsymbol{\xi})dV \\ &= \int_D \frac{\partial \boldsymbol{\xi}}{\partial t}\cdot(\boldsymbol{\xi}\times\boldsymbol{\Omega}) + \frac{\partial \boldsymbol{\xi}}{\partial t}\cdot(\boldsymbol{\eta}\times\boldsymbol{B}) + \frac{\partial \boldsymbol{\xi}}{\partial t}\cdot(\boldsymbol{\xi}\cdot\nabla\boldsymbol{U}) - \frac{1}{2}\frac{\partial}{\partial t}((\boldsymbol{\eta}\times\boldsymbol{B} + \boldsymbol{\xi}\cdot\boldsymbol{\nabla}\boldsymbol{U})\cdot\boldsymbol{\xi})dV \\ &= \int_D \frac{\partial \boldsymbol{\xi}}{\partial t}\cdot(\boldsymbol{\xi}\times\boldsymbol{\Omega}) + \frac{\partial \boldsymbol{\xi}}{\partial t}\cdot(\boldsymbol{\eta}\times\boldsymbol{B}) + \frac{1}{2}\frac{\partial \boldsymbol{\xi}}{\partial t}\cdot(\boldsymbol{\xi}\cdot\nabla\boldsymbol{U}) - \frac{1}{2}\frac{\partial \boldsymbol{\xi}}{\partial t}\cdot\nabla\boldsymbol{U}\cdot\boldsymbol{\xi} - \frac{1}{2}\frac{\partial}{\partial t}(\boldsymbol{\eta}\times\boldsymbol{B}\cdot\boldsymbol{\xi})dV \\ &= \int \frac{1}{2}\frac{\partial \boldsymbol{\xi}}{\partial t}\cdot(\boldsymbol{\xi}\times\boldsymbol{\Omega}) + \frac{1}{2}\left(\frac{\partial \boldsymbol{\xi}}{\partial t}\cdot(\boldsymbol{\eta}\times\boldsymbol{B}) - \boldsymbol{\xi}\cdot(\frac{\partial \boldsymbol{\eta}}{\partial t}\times\boldsymbol{B})\right)dV \end{aligned} \tag{4.17}$$

where we have used the divergence theorem and the boundary condition at the surface for several times. The evolution of $\boldsymbol{\eta}$ can be found in Appendix A

4.3 Energy of rigid rotaion

We consider an example flow between two coaxial cylinders. The steady velocity and magnetic field are

$$\begin{aligned} &\boldsymbol{U} = r\Omega\boldsymbol{e}_\theta,\ \boldsymbol{B} = r\mu\boldsymbol{e}_\theta + B_z\boldsymbol{e}_z, \\ &B.C.\ \ \boldsymbol{n}\cdot\boldsymbol{U} = 0,\ \boldsymbol{n}\cdot\boldsymbol{B} = 0. \\ &\text{where, } \Omega,\ B_z \text{ and } \mu \text{ are all constant .} \end{aligned} \tag{4.18}$$

The disturbance is assumed to be in the eigenmode $\hat{f}(r)\exp[\lambda t + i(m\theta + kz)] = \hat{f}(r)\exp[-i\omega t + i(m\theta + kz)]$. The equation for $\chi = r\hat{\xi}_r(r)$ from Hain-Lüst equation (1.40) in §1.2.5 can be

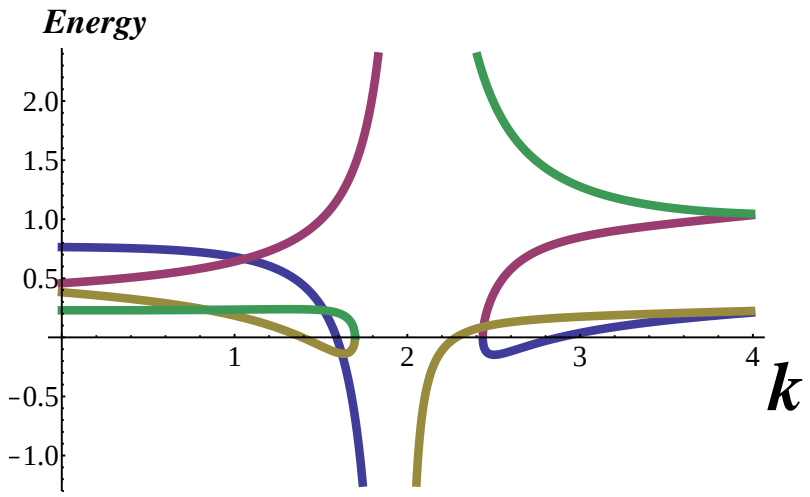

Figure 4.1: The wave energy to axial wavenumber k. The parameters are $m = -5$, $\Omega = 0.25$, $\mu = 1$, $B_z = 0$.

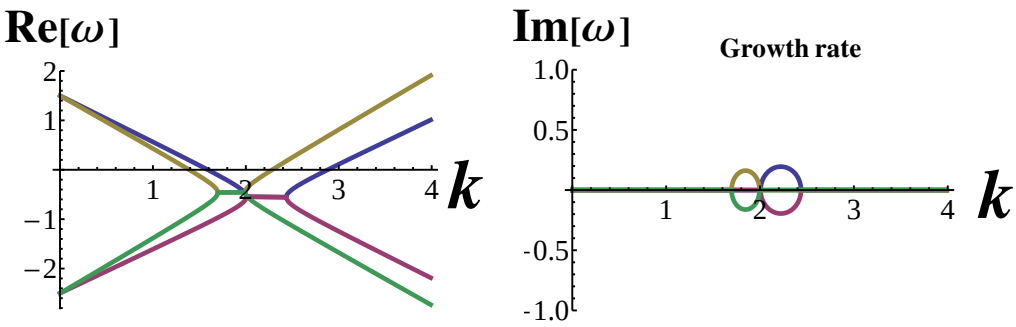

Figure 4.2: The eigenvalue to axial wavenumber k. The parameters are $m = -5$, $\Omega = 0.25$, $\mu = 1$, $B_z = 0$. The left one shows the real part of ω, and the right one shows the imaginary part of ω, which is the growth rate

simplified to [37]

$$
\begin{aligned}
& r\frac{\mathrm{d}}{\mathrm{d}r}\left[\frac{1}{h^2 r}\frac{\mathrm{d}\chi}{\mathrm{d}r}\right]-\left[1-\left(\alpha^2-\frac{2m\alpha}{h^2r^2}\right)\frac{k^2}{h^2}\right]\chi=0, \\
& \text{with } \alpha=\frac{2(\mu F+\Omega\tilde{\omega})}{\tilde{\omega}^2-F^2},\ F=m\mu+B_z,\ \tilde{\omega}=\omega-m\Omega, \\
& \text{B. C. } \chi=0.
\end{aligned} \tag{4.19}
$$

Take into consideration the boundary condition, (4.19) can be solved and the solution χ can be analytically expressed in terms of the Bessel functions as

$$
\chi=\frac{1}{(\alpha^2-1)(\rho\tilde{\lambda}^2-F^2)}\left[rJ'_m(lr)-m\alpha J_m(lr)\right], \tag{4.20}
$$

with $l=k\sqrt{\alpha^2-1}$, J_m is the Bessel function and the prime designates the derivative in r. After a long calculation which can be found in Appendix B, the energy is calculated as

$$
H_R=\frac{1}{2}\int_D\left[\omega(\omega-m\Omega-kB_z)-\frac{\Omega\omega}{\alpha}\right]|\xi|^2dV. \tag{4.21}
$$

In (4.21), the coefficient $\left[\omega(\omega-m\Omega-kB_z)-\frac{\Omega\omega}{\alpha}\right]$ decides the signature of energy, so we can view $\left[\omega(\omega-m\Omega-kB_z)-\frac{\Omega\omega}{\alpha}\right]$ as the normalized energy.

In Fig. 4.1, we draw the energy with dependence to the axial wavenumber. The parameters are

$$
m=-5,\ \Omega=0.25,\ \mu=1,\ B_z=0. \tag{4.22}
$$

In Fig. 4.2, we draw the eigenvalue with dependence to the axial wavenumber k as the varying parameter. The left graph shows the real part of ω and the right graph corresponds to the imaginary part of ω which is thus the growth rate.

From Fig. 4.1 and Fig. 4.2 we can clearly see the collision of two pure imaginary (corresponding to that ω is a real number) eigenvalues of zero energy collide and they

bifurcate to eigenvalues which have real part (corresponding to that ω is complex) and instability occurs there. This is the fact of the Krein's theorem.

Chapter 5

Conclusion

We studied three-dimensional linear stabilities of rotating flows of an electrically conducting fluid, subject to azimuthal magnetic field. The basic field is assumed to be axisymmetric. We addressed this problem from both the local stability analysis of using the WKB method and the global modal analysis.

In chapter 2 we explored the AMRI of a perfectly conducting fluid to non-axisymmetric as well as axisymmetric perturbations of short wavelengths, based on the Hain-Lüst equation (1.40) augmented with the terms originating from a background flow of differential rotation. The present investigation is capable of dealing with a rotating flow of arbitrary angular velocity profile $\Omega(r)$. The advantage of using the Hain-Lüst equation is that a risk of dropping-off the terms including radial derivatives can be avoided. If we substitute the WKB ansatz $\boldsymbol{\xi} \propto \exp[i\int q(r)\mathrm{d}r]$, at an earlier stage, into (3.11) say, the derivative in r is replaced by multiplication iq, and after this stage, the operation of radial derivative $iq = \mathrm{d}/\mathrm{d}r$ is liable to be inactive, though it should be. For example, the continuity equation (2.4)

$$\frac{\partial \tilde{u_r}}{\partial r} + \frac{im}{r}\tilde{u_\theta} + ik\tilde{u_z} = 0. \tag{5.1}$$

is approximated by

$$iq\tilde{u_r} + \frac{im}{r}\tilde{u_\theta} + ik\tilde{u_z} = 0. \tag{5.2}$$

Substitution of (2.9) into (5.1) or (5.2) gives different results. It is safer to keep all the derivative terms to the very last stage when the equations are combined to one second order differential equation for $\chi = r\xi_r(r)$. Then we apply the short wavelength approximation where the appropriate assumption becomes $\boldsymbol{\xi} \propto p(r)\exp[i\int q(r)\mathrm{d}r]$. This approach retains all the relevant terms which has disclosed a novel instability mode, of long wavelengths, of the AMRI to non-axisymmetric perturbations than known ones (*cf.* ref [15]).

Given Rb, for small values of $|\omega_{A\theta}/\Omega|$, a rotating flow is unstable to non-axisymmetric perturbations of $|k| \to \infty$ if $Ro < (Rb - 1/4)(\omega_{A\theta}/\Omega)^2$ as dictated by (2.35), with the maximum growth rate close to the Oort A-value $|Ro|$. For $|\omega_{A\theta}/\Omega| \sim 1$, the situation is changed. When $Rb > -3/4$, the rotating flow is unstable to perturbations of $|k| \to \infty$ in the whole range of Ro. But the mode of $|k| \to \infty$ subsides down as Rb is decreased and disappears at $Rb = -3/4$. Instead, another unstable mode of $k = 0$ emerges at $Rb = -1/4$, develops as Rb is decreased, and surpasses the mode of $|k| \to \infty$ for $Rb \leq -1/\sqrt{8}$. The instability mode of $k = 0$ is confined to a finite range in Ro centered on $Ro = 0$.

In chapter 3 we extended the Hain-Lüst equation to include the viscosity and the electric resistivity. This extended Hain-Lüst equation serves as a basis for the linear stability analysis of the AMRI and the HMRI in the inductionless limit. By making the WKB analysis of the extended Hain-Lüst equation, we obtained the dispersion relation in the short wavelength limit. We showed that this approach restores the known results of the axisymmetric SMRI and the axisymmetric AMRI. Liu's limit for the critical Rossby number is restored; in the presence of the axial as well as the azimuthal magnetic field, the critical Rossby number is raised from -1 of Rayleigh's criterion to at most Liu's limit $Ro_c = 2(1-\sqrt{2})$ for $B_\theta/B_z = \pm\sqrt{2}/2$. In §3.3 we also showed that for non-axisymmetric AMRI in weak magnetic field, the critical Rossby number is lower than Rayleigh's value $Ro_c = -1$. When the azimuthal magnetic field is sufficiently strong, we dealt exclusively with two extreme modes of $k \to 0$ and $k \to \infty$. For a Keplerian flow, the $k \to 0$ mode is excited for $Rb < -1/4$, with the growth rate proportional to square of the magnetic-

field strength. On the other hand, the $k \to \infty$ mode is excited for $Rb > -25/32$, with the growth rate proportional to square of the field strength the field strength. Either of these two modes is excitable at any value of Rb, and we are led to a conclusion that the Keplerian flow is unstable in the presence of a strong azimuthal magnetic field.

Chapter 4 sheds light on the aspect that the ideal MHD is a Hamiltonian system. Krein's collision theorem makes the wave-energy an essential factor to distinguish instability from stability. We simplified the lengthy energy formula and then obtained two new energy formula. Based on the simplified energy formula, we revisited an rigidly rotating flow whose eigenfunction of disturbance can be written out explicitly in terms of the Bessel functions. We obtained the energy of this rigidly rotating flow and confirmed that the bifurcation complies with Krein's theorem.

Appendix A

Evolution of η

In the appendix, the δ stands for the disturbance and is the same as previous˜, e.g. $\delta \boldsymbol{u} = \tilde{\boldsymbol{u}}$, and δ^2 will be used to denote the second order disturbance.

Vorticity equation for steady state:

$$0 = \frac{\partial \Omega}{\partial t} = \boldsymbol{\nabla} \times (\boldsymbol{U} \times \boldsymbol{\Omega}) + \boldsymbol{\nabla} \times (\boldsymbol{J} \times \boldsymbol{B}).$$

For *Dynamicallyaccessibleperturbations* [44, 45]

$$\delta \boldsymbol{u} = \boldsymbol{\xi} \times \boldsymbol{\Omega} + (\boldsymbol{\nabla} \times \boldsymbol{\eta}) \times \boldsymbol{B}. \tag{A.1}$$

Taking the curl of it, we obtain

$$\delta \boldsymbol{\omega} = \boldsymbol{\nabla} \times (\boldsymbol{\xi} \times \boldsymbol{\Omega}) + \boldsymbol{\nabla} \times ((\boldsymbol{\nabla} \times \boldsymbol{\eta}) \times \boldsymbol{B}). \tag{A.2}$$

Moreover by taking time derivative of both sides, and substituting the relation $\partial \boldsymbol{\xi} / \partial t +$

$\boldsymbol{U}\cdot\nabla\xi-\xi\cdot\nabla U=\delta u$, it yields,

$$\begin{aligned}
\frac{\partial\delta\omega}{\partial t} &= \boldsymbol{\nabla}\times(\frac{\partial\boldsymbol{\xi}}{\partial t}\times\boldsymbol{\Omega})+\boldsymbol{\nabla}\times(\frac{\partial(\boldsymbol{\nabla}\times\boldsymbol{\eta})}{\partial t}\times\boldsymbol{B})\\
&= \boldsymbol{\nabla}\times((\boldsymbol{\delta u}-\boldsymbol{U}\cdot\boldsymbol{\nabla\xi}+\boldsymbol{\xi}\cdot\boldsymbol{\nabla U})\times\boldsymbol{\Omega})+\boldsymbol{\nabla}\times(\frac{\partial(\boldsymbol{\nabla}\times\boldsymbol{\eta})}{\partial t}\times\boldsymbol{B})\\
&= \boldsymbol{\nabla}\times(\boldsymbol{\delta u}\times\boldsymbol{\Omega})-\boldsymbol{\Omega}\cdot\boldsymbol{\nabla}(\boldsymbol{U}\cdot\boldsymbol{\nabla\xi}-\boldsymbol{\xi}\cdot\boldsymbol{\nabla U})+(\boldsymbol{U}\cdot\boldsymbol{\nabla\xi}-\boldsymbol{\xi}\cdot\boldsymbol{\nabla U})\cdot\boldsymbol{\nabla\Omega}\\
&\quad+\boldsymbol{\nabla}\times(\frac{\partial(\boldsymbol{\nabla}\times\boldsymbol{\eta})}{\partial t}\times\boldsymbol{B})\\
&= \boldsymbol{\nabla}\times(\boldsymbol{\delta u}\times\boldsymbol{\Omega})+[-\boldsymbol{\Omega}\cdot\boldsymbol{\nabla U}\cdot\boldsymbol{\nabla\xi}-\boldsymbol{U}\cdot\boldsymbol{\nabla}(\boldsymbol{\Omega}\cdot\boldsymbol{\nabla\xi})+\boldsymbol{U}\cdot\boldsymbol{\nabla\Omega}\cdot\boldsymbol{\nabla\xi}]\\
&\quad+[\boldsymbol{\Omega}\cdot\boldsymbol{\nabla\xi}\cdot\boldsymbol{\nabla U}+\boldsymbol{\xi}\cdot\boldsymbol{\nabla}(\boldsymbol{\Omega}\cdot\boldsymbol{\nabla U})-\boldsymbol{\xi}\cdot\boldsymbol{\nabla\Omega}\cdot\boldsymbol{\nabla U}]\\
&\quad+(\boldsymbol{U}\cdot\boldsymbol{\nabla\xi})\cdot\boldsymbol{\nabla\Omega}+[-\boldsymbol{\xi}\cdot\boldsymbol{\nabla}(\boldsymbol{U}\cdot\boldsymbol{\nabla\Omega})+\boldsymbol{U}\cdot\boldsymbol{\nabla}(\boldsymbol{\xi}\cdot\boldsymbol{\nabla\Omega})-\boldsymbol{U}\cdot\boldsymbol{\nabla\xi}\cdot\boldsymbol{\nabla\Omega}]\\
&\quad+\boldsymbol{\nabla}\times(\frac{\partial(\boldsymbol{\nabla}\times\boldsymbol{\eta})}{\partial t}\times\boldsymbol{B})\\
&= \boldsymbol{\nabla}\times(\boldsymbol{\delta u}\times\boldsymbol{\Omega})+\boldsymbol{\nabla}\times(\boldsymbol{U}\times\boldsymbol{\delta\Omega})+(\boldsymbol{U}\cdot\boldsymbol{\nabla\Omega}-\boldsymbol{\Omega}\cdot\boldsymbol{\nabla U})\cdot\boldsymbol{\nabla\xi}\\
&\quad+\boldsymbol{\xi}\cdot\boldsymbol{\nabla}(\boldsymbol{\Omega}\cdot\boldsymbol{\nabla U}-\boldsymbol{U}\cdot\boldsymbol{\nabla\Omega})+\boldsymbol{\nabla}\times(\frac{\partial(\boldsymbol{\nabla}\times\boldsymbol{\eta})}{\partial t}\times\boldsymbol{B})\\
&= \boldsymbol{\nabla}\times(\boldsymbol{\delta u}\times\boldsymbol{\Omega})+\boldsymbol{\nabla}\times(\boldsymbol{U}\times\boldsymbol{\delta\Omega})+(\boldsymbol{\nabla}\times(\boldsymbol{J}\times\boldsymbol{B}))\cdot\boldsymbol{\nabla\xi}+\boldsymbol{\xi}\cdot\boldsymbol{\nabla}(-\boldsymbol{\nabla}\times(\boldsymbol{J}\times\boldsymbol{B}))\\
&\quad+\boldsymbol{\nabla}\times(\frac{\partial(\boldsymbol{\nabla}\times\boldsymbol{\eta})}{\partial t}\times\boldsymbol{B}). \qquad \text{(A.3)}
\end{aligned}$$

where we used that $\boldsymbol{\nabla}\times(\boldsymbol{U}\times\boldsymbol{\Omega})+\boldsymbol{\nabla}\times(\boldsymbol{J}\times\boldsymbol{B})=0$, and the relationships

$$\boldsymbol{\Omega}\cdot\boldsymbol{\nabla\xi}\cdot\boldsymbol{\nabla U}-\boldsymbol{\xi}\cdot\boldsymbol{\nabla\Omega}\cdot\boldsymbol{\nabla U}=\boldsymbol{\nabla}\times(\boldsymbol{\xi}\times\boldsymbol{\Omega})\cdot\boldsymbol{\nabla U}$$

$\boldsymbol{and}\boldsymbol{U}\cdot\boldsymbol{\nabla}(\boldsymbol{\xi}\cdot\boldsymbol{\nabla\Omega})-\boldsymbol{U}\cdot\boldsymbol{\nabla}(\boldsymbol{\Omega}\cdot\boldsymbol{\nabla\xi})=-\boldsymbol{U}\cdot\boldsymbol{\nabla}(\boldsymbol{\nabla}\times(\boldsymbol{\xi}\times\boldsymbol{\Omega}))$.

On the other hand, we linearize the vorticity equation as

$$\frac{\partial\delta\boldsymbol{\omega}}{\partial t}=\boldsymbol{\nabla}\times(\boldsymbol{\delta u}\times\boldsymbol{\Omega})+\nabla\times(\boldsymbol{U}\times\boldsymbol{\delta\omega})+\boldsymbol{\nabla}\times(\boldsymbol{\delta J}\times\boldsymbol{B})+\boldsymbol{\nabla}\times(\boldsymbol{J}\times\boldsymbol{\delta B}). \quad \text{(A.4)}$$

First we calculate the last two terms of this equation but in opposite sign as

$$
\begin{aligned}
& \boldsymbol{\nabla} \times (\boldsymbol{J} \times \boldsymbol{\delta B}) + \boldsymbol{\nabla} \times (\boldsymbol{\delta J} \times \boldsymbol{B}) \\
= \; & \boldsymbol{\nabla} \times (\boldsymbol{J} \times (\boldsymbol{\nabla} \times (\boldsymbol{\xi} \times \boldsymbol{B})) + \boldsymbol{\nabla} \times (\boldsymbol{\delta J} \times \boldsymbol{B}) \\
= \; & (\boldsymbol{B} \cdot \boldsymbol{\nabla} \boldsymbol{\xi} - \boldsymbol{\xi} \cdot \boldsymbol{\nabla} \boldsymbol{B}) \cdot \boldsymbol{\nabla} \boldsymbol{J} - \boldsymbol{J} \cdot \boldsymbol{\nabla} (\boldsymbol{B} \cdot \boldsymbol{\nabla} \boldsymbol{\xi} - \boldsymbol{\xi} \cdot \boldsymbol{\nabla} \boldsymbol{B}) + \boldsymbol{\nabla} \times (\boldsymbol{\delta J} \times \boldsymbol{B}) \\
= \; & [\boldsymbol{B} \cdot \boldsymbol{\nabla} (\boldsymbol{\xi} \cdot \boldsymbol{\nabla} \boldsymbol{J}) - \boldsymbol{\xi} \cdot \boldsymbol{\nabla} (\boldsymbol{B} \cdot \boldsymbol{\nabla} \boldsymbol{J}) + \boldsymbol{\xi} \cdot \boldsymbol{\nabla} \boldsymbol{B} \cdot \boldsymbol{\nabla} \boldsymbol{J}] - \boldsymbol{\xi} \cdot \boldsymbol{\nabla} \boldsymbol{B} \cdot \boldsymbol{\nabla} \boldsymbol{J} \\
& + [-\boldsymbol{J} \cdot \boldsymbol{\nabla} \boldsymbol{B} \cdot \boldsymbol{\nabla} \boldsymbol{\xi} - \boldsymbol{B} \cdot \boldsymbol{\nabla} (\boldsymbol{J} \cdot \boldsymbol{\nabla} \boldsymbol{\xi}) + \boldsymbol{B} \cdot \boldsymbol{\nabla} \boldsymbol{J} \cdot \boldsymbol{\nabla} \boldsymbol{\xi}] \\
& + [\boldsymbol{J} \cdot \boldsymbol{\nabla} \boldsymbol{\xi} \cdot \boldsymbol{\nabla} \boldsymbol{B} + \boldsymbol{\xi} \cdot \boldsymbol{\nabla} (\boldsymbol{J} \cdot \boldsymbol{\nabla} \boldsymbol{B}) - \boldsymbol{\xi} \cdot \boldsymbol{\nabla} \boldsymbol{J} \cdot \boldsymbol{\nabla} \boldsymbol{B}] + \boldsymbol{\nabla} \times (\boldsymbol{\delta J} \times \boldsymbol{B}) \\
= \; & (\boldsymbol{\nabla} \times (\boldsymbol{J} \times \boldsymbol{B}) \cdot \boldsymbol{\nabla} \boldsymbol{\xi} + \boldsymbol{\xi} \cdot \boldsymbol{\nabla} (-\boldsymbol{\nabla} \times (\boldsymbol{J} \times \boldsymbol{B})) + \boldsymbol{\nabla} \times ((\boldsymbol{\delta J} - \boldsymbol{\nabla} \times (\boldsymbol{\xi} \times \boldsymbol{J})) \times \boldsymbol{B}).
\end{aligned}
\tag{A.5}
$$

(A.4) can be written as

$$
\begin{aligned}
\frac{\partial \boldsymbol{\delta \omega}}{\partial t} = \; & \boldsymbol{\nabla} \times (\boldsymbol{\delta u} \times \boldsymbol{\Omega}) + \boldsymbol{\nabla} \times (\boldsymbol{U} \times \boldsymbol{\delta \omega}) + (\boldsymbol{\nabla} \times (\boldsymbol{J} \times \boldsymbol{B}) \cdot \boldsymbol{\nabla} \boldsymbol{\xi} + \boldsymbol{\xi} \cdot \boldsymbol{\nabla} (-\boldsymbol{\nabla} \times (\boldsymbol{J} \times \boldsymbol{B})) \\
& + \boldsymbol{\nabla} \times ((\boldsymbol{\delta J} - \boldsymbol{\nabla} \times (\boldsymbol{\xi} \times \boldsymbol{J})) \times \boldsymbol{B}).
\end{aligned}
\tag{A.6}
$$

Comparing (A.6) and (A.3), we get

$$
\frac{\partial (\nabla \times \eta)}{\partial t} = \delta J - \nabla \times (\xi \times J) + c_0 \boldsymbol{B}. \tag{A.7}
$$

Appendix B

Energy of rigid flow

Define a, b, c as

$$\begin{aligned}
&\xi_r = ae^{\Theta} = \frac{1}{r}\chi e^{\Theta}, \\
&\xi_\theta = be^{\Theta} = \frac{i}{h^2 r}\left(\frac{m}{r}\chi' - k^2\alpha\chi\right)e^{\Theta}, \\
&\xi_z = ce^{\Theta} = \frac{i}{h^2 r}\left(k\chi' + \frac{m}{r}k\alpha\chi\right)e^{\Theta}, \\
&\text{where } \Theta = -i\omega t + i(m\theta + kz).
\end{aligned} \tag{B.1}$$

$$\mathrm{Re}[\boldsymbol{\xi}] = \begin{pmatrix} a\cos\Theta \\ b\sin\Theta \\ c\sin\Theta \end{pmatrix}, \quad \mathrm{Re}[\frac{\partial\boldsymbol{\xi}}{\partial t}] = \begin{pmatrix} \omega a\sin\Theta \\ -\omega b\cos\Theta \\ -\omega c\cos\Theta \end{pmatrix}, \tag{B.2}$$

From (4.10), energy is written as

$$\begin{aligned}
H &= \int_D |\frac{\partial\boldsymbol{\xi}}{\partial t}|^2 - (\boldsymbol{U}\cdot\boldsymbol{\nabla})\frac{\partial\boldsymbol{\xi}}{\partial t}\boldsymbol{\xi}^* dV \\
&= \frac{1}{2}\int_D \omega^2(a^2+b^2+c^2-(\Omega m + B_z k)\omega(a^2+b^2+c^2-2\Omega ab\omega))dV
\end{aligned} \tag{B.3}$$

Now we calculate $a^2+b^2+c^2$ and ab as

$$\begin{aligned}\int_D a^2+b^2+c^2 dV &= \left(\frac{\chi}{r}\right)^2+\frac{1}{h^4r^2}\left[h^2\chi'^2+k^2\alpha^2h^2\chi^2\right]\\ &= \left(\frac{\chi}{r}\right)^2+\frac{1}{h^2r^2}(\chi'^2+k^2\alpha^2\chi^2)\\ &= |\boldsymbol{\xi}|^2\\ &\quad \text{(Substitute the Bessel solution:)}\\ &= \frac{2\pi J_m^2}{(\alpha^2-1)(\rho\tilde{\lambda}^2-F^2)^2}(\alpha m+\alpha^2k^2+\alpha^2k^2), \qquad \text{(B.4)}\end{aligned}$$

and

$$\begin{aligned}\int_D abdV &= -\frac{1}{h^2r^2}\chi\left(\frac{m}{r}\chi'-k^2\alpha\chi\right)=\frac{i}{2}(\xi_\theta\xi_r^*-\xi_r\xi_\theta^*)\\ &\quad \text{(Substitute the Bessel solution:)}\\ &= \frac{\pi J_m^2}{(\alpha^2-1)(\rho\tilde{\lambda}^2-F^2)^2}\left(\alpha m+\alpha^2k^2+\alpha^2k^2\right). \qquad \text{(B.5)}\end{aligned}$$

From (B.4) and (B.5) we conclude that

$$\begin{aligned}H_R &= \frac{1}{2}\int_D\left((\omega^2-(\Omega m+B_zk)^2+F^2)-\frac{2}{\alpha}(\Omega(\Omega m+B_zk)-\mu F)\right)|\boldsymbol{\xi}|^2dV\\ &= \frac{1}{2}\int_D\left[\omega(\omega-m\Omega-kB_z)-\frac{\Omega\omega}{\alpha}\right]|\boldsymbol{\xi}|^2dV. \qquad \text{(B.6)}\end{aligned}$$

Bibliography

[1] R. J. Tayler, Proc. Phys. Soc. **B70**, 31(1957).

[2] P. Markey, and R. J. Tayler, Mon. Not. R. Astron. Soc. **161**, 365 (1973).

[3] R. J. Tayler, Mon. Not. R. Astron. Soc. **163**, 77 (1973).

[4] E. Velikhov, JETP (USSR) **36**, 1398 (1959).

[5] S. Chandrasekhar, Proc. Natl. Acad. Sci. **46**, 253 (1960).

[6] A. Balbus, and J. F. Hawley, Astrophys. J. **376**, 214 (1991).

[7] S. Chandrasekhar, *Hydrodynamic and Hydromagnetic Stability* (Clarendon Press, Oxford, 1961).

[8] O. N. Kirillov, and F. Stefani, Astrophys. J. **712**, 52 (2010).

[9] O. N. Kirillov, and F. Stefani, Acta Appl. Math. **120**, 177 (2012).

[10] R. Salmeron, and M. Wardle, Mon. Not. R. Astron. Soc. **345**, 992 (2003).

[11] F. Ebrahimi, B. Lefebvre, C. B. Forest and A. Bhattacharjee, Phys. Plasmas **18**, 062904 (2011).

[12] G. Rüdiger, M. Gellert, M. Schultz, R. Hollerbach, and F. Stefani, Mon. Not. R. Astron. Soc. **438**, 271 (2014).

[13] G. Ruediger, M. Gellert, M. Schultz, R. Hollerbach, F. Stefani, Mon. Not. R. Astron. Soc. **438**, 271 (2014)

[14] R. Hollerbach, and G. Rüdiger, Phys. Rev. Lett. **95**, 124501 (2005).

[15] A. Balbus, and J. F. Hawley, Astrophys. J. **400**, 610 (1992).

[16] L. Rayleigh, Proc. R. Soc. Lond. A **93**, 148 (1917)

[17] G. I. Taylor, Proc. R. Soc. Lond. A **223**, 289 (1923)

[18] S. A. Balbus, and J. F. Hawley, Rev. Mod. Phys. **70**, 1 (1998)

[19] J. Z. Wu, H. Y. Ma, and M. D. Zhou, *Vorticity and Vortex Dynamics* (Springer-Verlag, 2006)

[20] V. A. Vladimirov, and H. K. Moffatt, J. Fluid Mech. **283**, 125 (1995)

[21] V. A. Vladimirov, H. K. Moffatt, and K. I. ILIN, J. Fluid Mech. **390**, 127 (1999)

[22] A. Balbus, and J. F. Hawley, Astrophys. J. **392**, 662 (1992).

[23] R. Zou, and Y. Fukumoto, MI-preprint **MI 2014-8** (2014).

[24] R. J. Tayler, Mon. Not. R. Astron. Soc. **191**, 151 (1980).

[25] O. N. Kirillov, F. Stefani, and Y. Fukumoto, Astrophys. J. **712**, 52 (2012).

[26] O. N. Kirillov, F. Stefani, and Y. Fukumoto, Fluid Dyn. Res.,*to appear* (2014).

[27] S. J. Desch, Astrophys. J. **608**, 509 (2004).

[28] A. BRANDENBURG, A. NORDLUND, R.F. STEIN, and U. TORKELSSON, Astrophys. J. **446**, 741 (1995).

[29] J. C. B. Papaloizou, and C. Terquem, Mon. Not. R. Astron. Soc. **287**, 771 (1997).

[30] C. Terquem, and J. C. B. Papaloizou, Mon. Not. R. Astron. Soc. **279**, 767 (1996).

[31] G. I. Ogilvie1, and J. E. Pringlel, Mon. Not. R. Astron. Soc. **279**, 152 (1996).

[32] O. N. Kirillov, and F. Stefani Phys. Rev. Lett. **111**, 061103 (2013).

[33] C. Curry, and R. E. Pudritz Mon. Not. R. Astron. Soc. **281**, 119 (1996).

[34] F. Stefani, Th. Gundrum, G. Gerbeth, G. Rüdiger, M. Schultz, J. Szklarski, and R. Hollerbach, Phys. Rev. Lett. **97**, 184502 (2006).

[35] J. P. Goedbloed, and S. Poedts, *Principles of Magnetohydrodynamics* (Cambridge University Press. Cambridge, 2004).

[36] W. Liu, J. Goodman, I. Herron, H. Ji, Phys. Rev. E **74**, 056302 (2006)

[37] J. P. Goedbloed, R. Keppens, and S. Poedts, *Advanced Magnetohydrodynamics* (Cambridge University Press. Cambridge, 2010).

[38] D. H. Michael, Mathematika **1**, 45 (1954).

[39] E. Knobloch, Mon. Not. R. Astron. Soc. **255**, 25 (1992).

[40] A. B. Mikhailovskii, J. G. Lominadze, R. M. O. Galvao, A. P. Churikov, N. N. Erokhin, A. I. Smolyakov, and V. S. Tsypin, Phys. Plasmas **15**, 0521038.

[41] Y. Fukumoto, J. Fluid Mech. **493**, 287 (2003).

[42] P. G. Saffman, *Vortex Dynamics* (Cambridge University Press. Cambridge, 1992).

[43] V. I. Arnold, *Mathematical Methods of Classical Mechanics*, 2nd Ed., (New York: Springer, 1980).

[44] E. Hameiri, Phys. Plasmas **5**, 3270 (1998)

[45] E. Hameiri, Phys. Plasmas **10**, 2643 (2003)

[46] M. B. Isichenko. Phys. Rev. Lett. **80**, 972 (1998)

[47] R. S. MacKay, *in* Nonlinear Phenomena and Chaos *(ed. S. Sarkar), Adam Hilger. Bristol*, 254 (1986).

[48] Y. Fukumoto, M. Hirota, and Y. Mie, Phys. Scr. **2010**, 014049 (2010).